Measurement and modelling of catchment erosion dynamics under different land cover types, Jonkershoek Catchment, Western Cape.

Student: Ebrahiem Abrahams (3173595)

Submitted in partial fulfilment of the requirements for the degree of

MAGISTER SCIENTIAE

Department of Earth Sciences, Faculty of Natural Sciences, University of the Western Cape

Supervisor: Dr M.C. Grenfell

Co-supervisor: Dr J. Glenday

2019.

DECLARATION

I, Ebrahiem Abrahams declare that "Measurement and modelling of catchment erosion dynamics under different land cover types, Jonkershoek Catchment, Western Cape." is my own work, that it has not been submitted for any degree or examination in any other university, and that all the sources I have used or quoted have been indicated and acknowledged by complete references.

Full name: Ebrahiem Abrahams

Date……2019/.....

Signed……

ABSTRACT

Several attempts have been made to assess the impact of post-fire soil erosion; however, erosion occurs as a result of the complex interplay between many factors, such as climate, land cover, soil and topography, making precise estimation difficult. Additionally, these factors are far from constant in space and time, and often interact with one another. To assess the impact of wildfire on soil erosion and factors influencing its variability, the post-fire soil erosion response of two mountainous headwater sub-catchments namely Langrivier and Tierkloof, with different vegetation cover in the Jonkershoek Valley was examined using a systematic approach that combines efforts in field and laboratory work, spatial analysis and process-based numerical modelling. Geospatial modelling shows high spatial variability in erosion risk, with 56 % to 67 % of surfaces being highly susceptible excluding rock cover. The model highlights the importance of terrain and vegetation indices, with predicted erosion being more severe on steep slopes with lower vegetation cover. This was consistent with field estimates showing that within catchment differences in soil loss were related to topographic characteristics such as slope and soil properties, while between catchment differences were mainly related to vegetation cover. Field estimates showed that Tierkloof received less rain during 2016, had a higher run-off, plot scale erosion, sediment exported and higher sediment concentration in the storm event on Saturday, 26 July 2016 (11 am to 3 pm) during the study period. Plot erosion estimates for the duration of the study were ~8.20 *mm* (100.15 *tons/ha/one rainy season*) on average in the Tierkloof catchment, used for pine plantations, while the Langrivier catchment, dominated by indigenous fynbos vegetation, experienced average losses of ~5.6 *mm* (68.32 *tons/ha/one rainy season*) over the sampling period. Suspended sediment samplers at stream outlets caught 56 g and 52 g, over the 6-month sampling period from Tierkloof and Langrivier respectively, equivalent to 0.62 g/ha and 0.36 g/ha of surface erosion from the catchment surfaces. Peak suspended sediment concentration estimated from field data was 0.026 *g/l* in Tierkloof and 0.012 *g/l* in Langrivier. These differences in post-fire erosion estimates between the two catchments may be due to vegetation characteristics, management and fire severity. Although the model and field estimates show contrasting results, simulations using CAESAR-Lisflood under the current conditions indicates the importance of vegetation cover in regulating surface hydrological processes and sediment movement. The study shows that a simple geospatial and numerical model, once calibrated, can be used to assess similar mountain catchments where data remains limited. This study provides a comprehensive spatio-temporal

assessment of post-fire soil erosion in two small headwater catchments of the Jonkershoek valley. Such an approach may provide the potential for full explanation of catchment dynamics and enables decision makers to work towards sustainable soil remediation and river restoration in the catchment.

Key words: Mediterranean, fire, pine plantations, fynbos, land cover and management, Mountain catchments, Cape fold, erosion pins, erosion risk, suspended sediment samplers, cellular automaton, numerical modelling, landscape evolution, geospatial modelling.

ACKNOWLEDGMENTS

I would like to express my sincere gratitude firstly to the University of the Western Cape for allowing me the opportunity to fulfil my dream of attaining a higher education. In addition, I would also like to thank the Department of Earth Sciences for accepting me into the master's program. Being part of this intellectually stimulating environment and erudite faculty has made my academic experience extraordinary.

Moreover, I would like to express my appreciation to SAEON Fynbos node for funding me; this award has assisted me tremendously. In addition, I would like to take this opportunity to thank Dr Julia Glenday for her valuable advice and feedback. Her expert advice played a significant role in the completion of this thesis. Similarly, I would like to thank Dr Flugel for his valuable GIS and remote sensing skills as well as Mr Blake for expert advice on the geological setting of the study area. This has certainly contributed significantly to the content in this thesis. I acknowledge and submit my heartiest gratitude to my respected supervisor, Dr Michael Grenfell, whom has played a pivotal role in this entire project. I would like to thank him and extend my deepest appreciation for giving me the opportunity to work and be a part of this research project. Having to work under the supervision of an expert in the field has equipped me with invaluable skills, knowledge and expertise. Of particular importance and most admirable quality that has been embedded in me throughout was his professionalism in its entirety. It is this quality that will be cherished and implemented in the near future. I am extremely grateful for his guidance, advice and reviewing this thesis to completion despite his busy schedule. He has made several important suggestions, which enhanced this thesis. Without his valuable assistance, this work would not have been completed.

To my parents and family, thank you for your support. You sacrificed the world so that I can educate myself and always pushed me to pursue a better future. I am truly grateful for everything that you have done for me. Lastly, I would like to express my sincere appreciation to my wife Nurunesa Ebrahim. Thank you for your support and patience. I know it was a major challenge for you, but you remained steadfast and gave me the opportunity to complete this thesis. Your support will always be cherished.

DEDICATION

TO MY WIFE AND PARENTS,

THANK YOU.

TABLE OF CONTENTS

CHAPTER 1: GENERAL OVERVIEW 1
1.1. Introduction 1
1.2. Research design summary 3
1.3. Research questions 4
1.4. Research aim 5
1.5. Research objectives 5
1.5. Research outline 6
CHAPTER 2: LITERATURE REVIEW 8
2.1. Introduction 8
2.2. Soil erosion overview 8
2.3. Factor affecting surface water erosion 9
2.4. Influence of rainfall erosivity 10
2.5. Influence of soil erodibility 11
2.6. Influence of vegetation 12
2.6.1. Influence of stem density 13
2.7. Influence of rock cover 14
2.8. Influence of slope 15
2.9. Influence of aspect 18
2.10. Influence of wildfire 18
2.11. Spatial and temporal variability in surface water erosion 20
2.12. Water and sediment regime in river basins 21
2.13. Methods used to estimate surface water erosion 23
2.14. Conclusion 24
CHAPTER 3: STUDY AREA AND RESEARCH CATCHMENTS 25
3.1. Introduction 25
3.2. Description of study area 25

3.3. Historical overview, land use and current management practices.....**Error! Bookmark not defined.**

3.4. Climate 4

3.5. Geological setting 5

3.6. Soils 7

3.7. Vegetation 9

3.8. Description of research catchments 11

3.8.1. Langrivier 11

3.8.2. Tierkloof 13

CHAPTER 4: GEOSPATIAL MODELLING OF EROSION RISK BASED ON TERRAIN AND VEGETATION INDICES IN THE TWO CATCHMENTS. 16

4.1. Erosion risk assessment based on terrain and vegetation indices 16

4.2. Methods 17

4.2.1. Source data and data processing 17

4.2.2. Data processing 20

4.2. Results 26

4.2.1. Spatial distribution of slope 26

4.2.2. Spatial distribution of the LS factor in the USPED model 28

4.2.3. Spatial distribution of vegetation cover estimated from NDVI 30

4.2.3. Spatial distribution of erosion risk based on LS and NDVI 34

4.3. Erosion risk (ER) assessment discussion 36

CHAPTER 5: ASSESSING SURFACE EROSION AND THE RELATIVE DIFFERENCES IN SEDIMENT EXPORT BETWEEN THE TWO CATCHMENTS. 40

5.1. Introduction. 40

5.2. Materials and methods. 43

5.3. Rainfall and streamflow 43

5.4. Erosion and deposition measurements. 44

5.5. Particle size distribution. 47

5.6. Vegetation and stem density. 48

5.7. River sediment export and suspended sediment concentration. 50

5.8. Analysis and statistical procedures. 53

5.7. Results 54

5.7.1. Assessing rainfall and streamflow characteristics of the two catchments. 54
5.7.2. Relationship between average soil loss from erosion pins and factors affecting its variability 63
5.7.3. Exported sediment and suspended sediment concentration. 73
5.8. Discussion 78
5.8.1. Impact of rainfall. 78
5.8.2. Influence of streamflow characteristics. 79
5.8.3. Factors influencing sediment flux in the two catchments. 81
5.8.4. Influence of river sediment flux and storm-based event on suspended sediment concentration. 83
CHAPTER 6: NUMERICAL MODELLING ON SOIL EROSION UNDER CURRENT CATCHMENT CHARACTERISITICS IN THE TWO CATCHMENTS. 86
6.1. Introduction 86
6.2. Methods 87
6.2.1. CAESAR-Lisflood landscape evolution model 87
6.2.3. Hydrological and hydraulic modelling 88
6.2.4. Sediment layers and sediment transport 91
6.2.5. Representation of sediment layers 94
6.2.6. Hillslope processes 97
6.2.2. Model input parameters 97
6.2.7. Model calibration 98
6.2.8. Model performance and evaluation 99
6.2.9. Uncertainty analysis and model limitations 101
6.3. Results 103
6.4. Discussion 117
CHAPTER 7: UNDERSTANDING POST-FIRE EROSION DYNAMICS IN THE TWO CATCHMENTS 121
CHAPTER 8: CONCLUSIONS AND RECOMMENDATIONS 126
8.1. Conclusion 126
8.2. Limitations and recommendations 128
8.2.1. Field-based limitations 128
8.2.2. Model based limitations 128

List of Tables

TABLE 3.1. PHYSICAL FEATURES OF THE STUDY AREA AND EXPERIMENTAL CATCHMENTS 2

TABLE 3.2.BROAD SOIL PATTERN OF THE JONKERSHOEK NATURE RESERVE MAPPED AT A SCALE OF 1:250 000 BY ICSW, ARC (2007). 7

TABLE 3.3. BROAD TERRAIN AND MORPHOLOGY OF THE JONKERSHOEK NATURE RESERVE MAPPED AT A SCALE OF 1:250 000 BY LAND TYPE SURVEY STAFF 1972-2002. 12

TABLE 3.4.SOIL STRUCTURAL CHARACTERISTICS OF LAND TYPE INVENTORY CLASS. 13

TABLE 4.1.SPATIAL VARIABLE OF SLOPE (DEGREES) AND TOTAL PERCENTAGE AREA COVERED PER CATCHMENT. 26

TABLE 4.2. SPATIAL VARIABLE OF NDVI) AND TOTAL PERCENTAGE AREA COVERED PER CATCHMENT. 30

TABLE 4.3.SPATIAL VARIABLE OF CLASSIFICATION OF NDVI GROUPINGS AND TOTAL PERCENTAGE AREA COVERED PER CATCHMENT. 33

TABLE 4.4. SPATIAL VARIABLE OF CLASSIFICATION OF EROSION RISK AND TOTAL PERCENTAGE AREA COVERED PER CATCHMENT..... 34

TABLE 5.1. SUMMARY STATISTICS OF DAILY RAINFALL (MM) AND RUN-OFF (MM) MEASUREMENTS IN LANGRIVIER AND TIERKLOOF FOR THE STUDY PERIOD JANUARY TO DECEMBER 2016.. 76

TABLE 5.2. DAILY FREQUENCY DISTRIBUTION OF RAINFALL (MM) AND RUN (MM) IN LANGRIVIER AND TIERKLOOF DURING THE STUDY PERIOD BETWEEN JANUARY TO DECEMBER 2016... 82

TABLE 5.3. SUMMARY STATISTICS OF SOIL LOSS (MM PER PLOT) DURING SAMPLE PERIOD AND FACTORS INFLUENCING ITS VARIABILITY FOR SAMPLED PLOTS IN LANGRIVIER..... 85

TABLE 5.4. SUMMARY STATISTICS OF SOIL LOSS (MM PER PLOT) DURING SAMPLE PERIOD AND FACTORS INFLUENCING ITS VARIABILITY FOR SAMPLED PLOTS IN LANGRIVIER..... 86

TABLE 5.5. SUMMARY OF OUTCOME OF CORRELATION ANALYSIS ON VARIABLES MEASURED. 101

TABLE 5.6. SUMMARY OF OUTCOME OF CORRELATION ANALYSIS ON VARIABLES MEASURED. 101

TABLE 6.1. CAESAR-LISFLOOD PARAMETERS USED IN LANGRIVIER AND TIERKLOOF TO SIMULATE HOW CHANGES IN LAND COVER INFLUENCES BASIN HYDROLOGY AND SEDIMENT YIELDS 103

TABLE 6.2. SUMMARY STATISTICS OF DAILY OBSERVED AND MODELLED STREAM DISCHARGE IN THE LANGRIVIER AND TIERKLOOF CATCHMENTS. QD REPRESENTS OBSERVED DISCHARGE, QM REPRESENTS MODELLED DISCHARGE, WHILE 1 AND 2 INDICATES NON-VEGETATED AND VEGETATED CATCHMENT RESPECTIVELY 104

TABLE 6.3. SHOW THE EVALUATION CRITERIA USED TO ASSESS OBSERVED AND PREDICTED STREAMFLOW. 111

TABLE 6.4.SUMMARY STATISTICS OF THE RELATIVE SOIL (SOIL LOSS $m3$ PER PLOT) FROM MODEL GRID CELLS MATCHING THE LOCATIONS OF SURFACE EROSION PLOTS IN THE FIELD. PLOTS ARE L1, L2, T1 AND T2. 112

TABLE 6.4.SUMMARY STATISTICS OF THE RELATIVE NORMALIZED SOIL LOSS ($m3/ha$) FROM MODEL GRID CELLS MATCHING THE LOCATIONS OF SURFACE EROSION PLOTS IN THE FIELD. PLOTS ARE L1, L2, T1 AND T2. 114

List of Figures

FIGURE 2.1. ILLUSTRATES RUN-OFF AND EROSION GENERATION PROCESSES AT THE HILLSLOPE SCALE (MICHAEL ET AL., 2006). 15

FIGURE 2.2. BASIN WIDE CONFIGURATION SHOWING THE SPATIAL AND TEMPORAL DISTRIBUTION OF THE SEDIMENT REGIME AND FACTORS CONTROLLING ITS VARIABILITY. ADJACENT UPLANDS MAY CONTRIBUTE TO UPSTREAM (US) AND LATERAL (LA) INPUT (I), WHILE MATERIAL INTRODUCED TO THE CHANNEL. 22

FIGURE 3.1. LOCATION OF STUDY AREA; DAM, TRIBUTARIES, RAIN GAUGES AND HYDRAULIC STRUCTURES. ..... **ERROR! BOOKMARK NOT DEFINED.**

FIGURE 3.2. GEOLOGY AND STRUCTURAL CONTACTS OF THE JONKERSHOEK NATURE RESERVE.6

FIGURE 3.3. LAND TYPE (SOIL AND TERRAIN) OF THE JONKERSHOEK NATURE RESERVE. THE DOMINANT LAND IN THE STUDY AREA IS FA. THE LAND TYPES OF THE TWO EXPERIMENTAL CATCHMENTS ARE IC AND FA, WHERE IC DOMINATES, WHILE FA OCCURS ONLY IN THE LOWER PART OF TIERKLOOF. 8

FIGURE 3.4. VEGETATION TYPES OF THE JONKERSHOEK NATURE RESERVE. ILLUSTRATES THE DIVERSITY AND DISTRIBUTION OF VEGETATION IN THE STUDY AREA. THE DOMINANT TYPES ARE BOLAND GRANITE FYNBOS AND KOEGELBERG SANDSTONE FYNBOS. 10

FIGURE 3.5. TERRAIN PROFILE OF LAND TYPE IC 118 (ARC, 2002). 11

FIGURE 3.6. TERRAIN PROFILE OF LAND TYPE FA 145 (ARC, 2002). 14

FIGURE 3.7. THE LANGRIVIER AND TIERKLOOF EXPERIMENTAL CATCHMENTS, EROSION PLOTS, WEIRS AND RAIN GAUGES. THESE CATCHMENTS ARE IN PROXIMITY, BUT WITH CONTRASTING LAND COVER TYPES. THEY ALSO HYDROLOGICALLY DIFFERENT AS WELL AS IN SIZE. THE LANGRIVIER CATCHMENT IS 257 HA, WHILE TIERKLOOF IS 155 HA. 15

FIGURE 4.1. CONCEPTUAL MODEL DETAILING THE STEPS FOLLOWED TO PRODUCE THE FINAL EROSION RISK MAP. 18

FIGURE 4.2. CONCEPTUAL MODEL DETAILING THE STEPS FOLLOWED TO PRODUCE THE FINAL EROSION RISK MAP. 21

FIGURE 4.3. SLOPE GRADIENT LANGRIVIER (RIGHT) AND TIERKLOOF (LEFT) CATCHMENTS SHOW AN INCREASE IN STEEPNESS TOWARDS IN THE NORTHEAST DIRECTION..... 27

FIGURE 4.4. LS AS ESTIMATED FROM USPED TERRAIN MODEL. THE LANGRIVIER (RIGHT) HAS A MAXIMUM VALUE OF 71, WHILE TIERKLOOF HAS A MAXIMUM OF THE LANGRIVIER (RIGHT) HAS A MAXIMUM VALUE OF 71, WHILE TIERKLOOF HAS A MAXIMUM OF 52. 29

FIGURE 4.5. NDVI MAPPED FOR LANGRIVIER (RIGHT) AND TIERKLOOF (LEFT) SHOWING INCREASED VEGETATION DENSITY OCCUR ALONG THE NATURAL DRAINAGE LINES. THE MAXIMUM VALUES OF THE CATCHMENTS ARE 0.71 AND 0.69 FOR LANGRIVIER AND TIERKLOOF RESPECTIVELY. 31

FIGURE 4.6.CLASSIFICATION MAP OF NDVI GROUPINGS. THE DOMINANT CLASS IN LANGRIVIER (RIGHT) IS LOW DENSITY VEGETATION COVER, WHILE BARE SURFACES DOMINATE TIERKLOOF. 32

FIGURE 4.7. EROSION RISK (ER) INDEX MAP PRODUCED USING MULTIVARIATE ANALYSIS OF USPED AND NDVI. THE LANGRIVIER (RIGHT) AND TIERKLOOF (LEFT) CATCHMENTS ARE DOMINATED BY LOW TO MEDIUM EROSION RISK CLASSES..... 35

FIGURE 5.1. SHOWS THE EXPERIMENTAL DESIGN OF FIELD SET-UP, CONSISTING OF RAIN GAUGES (TOP), EROSION PLOTS AND PINS (MIDDLE & BOTTOM), AND SUSPENDED SEDIMENT SAMPLERS (LEFT, ALSO WEIR LOCATION). 42

FIGURE 5.2. GRID USED DURING INSTALLATION OF EROSION PINS (BLACK DOT) I.E. WHERE THE HORIZONTAL AND VERTICAL LINE INTERSECT (N=25). SOIL SAMPLES (RED CIRCLES) WERE COLLECTED AT THE TOP, MIDDLE AND BOTTOM IN EACH PLOT (N=9). 45

FIGURE 5.3. MEASUREMENT (LEFT) TO QUANTIFY LAND-SURFACE (RIGHT) CHANGE FROM A KNOWN LENGTH (200 MM) OVER THE MONITORED PERIOD USING AN ENGINEERING RULER WITH A 0.1 MM ACCURACY. 46

FIGURE 5.4. ESTIMATING VEGETATION COVER FROM DIGITAL IMAGES. THE ORIGINAL SCALE IMAGE (TOP LEFT) WAS SCANNED FOR GREEN PIXEL VALUES (TOP RIGHT). PIXELS THAT

WERE NOT IN THE GREEN VALUE CLASS WAS REMOVED (BOTTOM). THE PERCENTAGE WAS DETERMINED FROM THE TOTAL PIXEL AND TOTAL GREEN PIXEL COUNT..... 49

FIGURE 5.5. INSTALLATION OF SUSPENDED SEDIMENT SAMPLERS. SAMPLERS WERE PLACED WERE MOST OF THE SEDIMENT TRANSPORTED BY THE RIVER ACCUMULATED IN THE WEIR. THE DEVICE WAS SECURED TO UPRIGHTS WITH CABLE TIES..... 51

FIGURE 5.6. LANGRIVIER DAILY RAINFALL AND STREAMFLOW IN 2016. MAXIMUM RAINFALL AND STREAMFLOW WERE 52.7 MM/DAY AND 42.09 MM/DAY AT AN AVERAGE RATE OF 2.66 MM/DAY AND 2.39 MM/DAY RESPECTIVELY..... 55

FIGURE 5.7. TIERKLOOF HOURLY RAINFALL AND STREAMFLOW IN 2016. MAXIMUM RAINFALL AND STREAMFLOW WERE 41 MM/DAY AND 69.79 MM/DAY AT AN AVERAGE RATE OF 1.94 MM/DAY AND 3.96 MM/DAY RESPECTIVELY..... 56

FIGURE 6.1. CAESAR-LISFLOOD BASIC MODEL STRUCTURE (ADAPTED FROM VAN DE WIEL ET AL., 2007). THE CATCHMENT OF INTEREST IS DEFINED (I.E. INITIAL CONDITION) AND SUBJECTED TO SOME FORCING (I.E. RAINFALL), WHICH ALTERS (I.E. EROSION AND DEPOSITION) THE OUTPUT STATE OF THE LANDSCAPE. 88

FIGURE 6.2. SHOWS THE SEDIMENT LAYERS IN CAESAR-LISFLOOD (VAN DE WIEL ET AL., 2007). 95

FIGURE 6.3. EVOLUTION OF THE ACTIVE LAYER DURING EROSION (A) AND DEPOSITION (B) ITERATION, WHERE $\boldsymbol{n}$ DENOTES THE INITIAL NUMBER OF STRATA. $n*\ and\ n''$ SHOWS THE NEW NUMBER OF LAYERS THAT ARE BURIED, EITHER AS EROSION OR DEPOSITION: $n*= n$-1 AND n''+1 (VAN DE WIEL ET AL., 2007). 96

FIGURE 6.4. ACTUAL STREAMFLOW (MM/DAY) BLUE AND MODELLED DISCHARGE (MM/DAY) FOR LANGRIVIER 2016. AVERAGE OBSERVED DISCHARGE WAS 2.39 MM/DAY AND MODELLED OBSERVED DISCHARGE WAS 2.41 MM/DAY IN L1 SIMULATION..... 106

FIGURE 6.5. ACTUAL STREAMFLOW (MM/DAY) BLUE AND MODELLED DISCHARGE (MM/DAY) FOR TIERKLOOF 2016. AVERAGE OBSERVED DISCHARGE WAS 3.96 MM/DAY AND MODELLED OBSERVED DISCHARGE WAS 1.48 MM/DAY IN T1 SIMULATION..... 107

FIGURE 6.6. COMPARISON OF OBSERVED AND SIMULATED SEDIMENT FROM EROSION PLOTS IN THE LANGRIVIER. THE OBSERVED AVERAGE SEDIMENT FLUX WAS 4.2 $m3$ PER PLOT AND THE SIMULATED SOIL LOSS 1.49 $m3$ PER PLOT. 113

FIGURE 6.7. COMPARISON OF OBSERVED AND SIMULATED SEDIMENT FROM EROSION PLOTS IN THE TIERKLOOF. THE OBSERVED AVERAGE SOIL LOSS WAS 6.2 $m3/m2$ AND THE SIMULATED SEDIMENT FLUX 4.87 $m3/m2$..... 114

FIGURE 6.8. COMPARISON OF THE RELATIVE DIFFERENCE IN SEDIMENT OUTPUT FROM SIMULATIONS, SHOWING THE INFLUENCE OF VEGETATION ON SEDIMENT OUTPUT. 115

LIST OF ABBREVIATIONS

L1: Langrivier simulation 1 (current conditions)

L2: Langrivier simulation 2 (vegetation cover)

T1: Tierkloof simulation 1 (current conditions)

T2: Tierkloof simulation 2 (vegetation cover)

USPED: Unit Stream Power Erosion and Deposition index

NDVI: Normalized Difference Vegetation Index

RMSE: Root Mean Square Error

MSE: Mean Square Error

RB: Relative Bias

MAE: Mean Absolute Error

DEM: Digital Elevation Model

USLE: Universal Soil Loss Equation

LS: Length-Slope Factor

Us: upstream

la: lateral

I: input

ds: downstream

H_2CO_2: Hydrogen peroxide

HCL: Hydrochloric acid

km/yr : Squared kilometres per year

$t\ ha/yr$: tons per hectare per year

l/hr: litres per hour

mm/hr: millimetres per hour

ha: hectare

m^3*:* cubic meters

m^3/m^2: cubic meters per square meter

m^3/hr: cubic meters per hour

g/cm^3: grams per cubic centimetre

D_{50}: Median grainsize

μm: microns

m^2: Square meters

kg: Kilograms

g/l: grams per litre

g/ha: grams per hectare

CHAPTER 1: GENERAL OVERVIEW

1.1. Introduction

Soil erosion and associated land degradation is a major threat to the security of reservoir water supply, water quality (Le Roux et al., 2008, Yuksel et al., 2008), river and wetland ecology (Macfarlane et al., 2009, Nunes et al., 2011), and the sustainability of food production systems (Montgomery, 2007). Soil erosion has been recognized as a hazard in steep, well-dissected terrain (Ganasri et al., 2016, Montgomery, 2007), such as the mountainous areas of South Africa's Western Cape, which are also critical water source environments (Scott, 1993). Accelerated generation and routing of hillslope sediments through catchment drainage networks causes siltation of reservoirs, reducing their operational lifespan, and can lead to reservoir eutrophication (Le Roux et al., 2008, Wohl et al., 2015, Ganasri et al., 2016). This study aims to improve quantitative understanding of post-fire erosion and sediment transport rates and drivers in a case-study water-source catchment in the Western Cape.

Soil erosion is a process of detachment and transportation of earth material by an erosive force such as water, through raindrop impact and/or particle entrainment by surface water runoff (Shakesby, 2011, Fagbohun et al., 2016). While soil erosion is a naturally occurring process and normal geological phenomenon associated with surface and subsurface runoff processes, human activities such as clearing of vegetation, tillage of agricultural fields, and disturbances such as wildfire, have accelerated soil erosion at alarming rates (Montgomery, 2007, Le Roux et al., 2008, Nunes et al., 2011, Shakesby, 2011, Gelagay et al., 2016). In high mountain environments eroded material is often readily transferred to rivers, wetlands and reservoirs with consequent effects on ecosystem processes and water resource degradation. In many parts of the world, water shortages serve as the driving force to find alternative ways of increasing water yields in streams and rivers for socio-economic supply, whilst maintaining ecological reserves becomes a challenge (Huddle et al., 2010). Future plans should rethink the value of natural soil and sediment systems, and strategies should include better conservation of these systems. However, current river management plans tend to neglect the sediment regime (Poff, 1997, Wohl et al., 2015). To properly manage the system there is a need to better understand

the interactions between water and sediment (Wohl et al., 2015). This is locally important because of the dependence of the Western Cape on these inter-related resources (Scott, 1993).

Rivers are one of the most dynamic features of a landscape and are typically shaped by some level of sediment movement. The supply and transfer of sediment to and through rivers drives many aspects of river ecological condition such as their physico-chemistry and morphological diversity (Wohl et al., 2015). The magnitude and frequency of river sediment transfer processes are largely determined by basin wide configuration such as climate, geology and substrate, terrain and land-use activities (Poff, 1997, Wohl et al., 2015). For protection of these areas, it is important to understand the spatial extent of soil erosion and how disturbances both natural (e.g. wildfire) and anthropogenic (e.g. land management practices) influence erosion rates at the catchment level (Montgomery, 2007, Scott et al., 2008).

Sediment erosion, transport and exchange processes at the catchment scale may be influenced by numerous interacting factors such as rainfall erosivity, soil erodibility, slope steepness and slope length, and land cover and management practices (de Vente et al., 2007, Waghmare et al., 2017). These controls are typically difficult to disentangle, such that the process of determining the 'natural' sediment flux (and geomorphic health) for a river may be complex and contested. For example, the relationship between slope and surface water erosion has been investigated for decades but results differ greatly across locations due to the complexity of process interaction. A further complication occurs as a result of wildfire, which has the potential to synchronize source areas by consuming the soil protective layer (e.g. vegetation), causing an equal amount of sediment to enter streams (Shakesby, 2011, Florsheim et al., 2015, Perreault et al., 2016).

Sediment flux from steep hillslopes to stream channels typically increases following wildfires (Florsheim et al., 2015). Surface vegetation as canopy cover and ground cover protects the soil surface from the disintegrating effect of raindrops and provides root cohesion (hydraulic resistance) that reduces the shear stress of overland flow acting on soil particles (Istanbulluoglu et al., 2004). Fire denudes vegetation and alters soil structural and chemical properties that may alter hillslope erosion rates, thereby leading to high post-fire soil erosion risk (Florsheim et al.,

2015, Perreault et al., 2016). Garcia-Ruiz et al. (2010) reported on the severity of soil loss under dense shrubs post-fire. They show that the average soil loss was five times greater than pre-fire levels indicating that wildfires can have a dramatic impact, which may lead to larger parts of a catchment acting as run-off and sediment source areas (Scott et al., 2008). The response to such environmental forcing is usually spatially and temporally variable throughout a catchment, with process-interactions making precise estimation or prediction of soil loss difficult (Sharma, 2010).

Since most of the water being used by people originates from high-relief mountain environments, it is imperative that fires and the resultant earth surface responses such as soil erosion and in-stream sedimentation be assessed, to reduce adverse effects on water resources (Yuksel et al., 2008). Such measures can only be achieved through the implementation of effective pre-and post-fire management systems (Prasannakumar et al., 2012). To develop an effective management system, there is a need for predictive understanding of post-fire hillslope erosion rates and processes controlling their spatial and temporal variability at the catchment scale (Boardman et al., 2015, Jazouli et al., 2017).

Several tools and approaches for estimating surface erosion and sediment transport are currently available, involving direct measurement and/or geospatial or numerical modelling (Lamb et al., 2011, Coulthard et al., 2016). The main problem with direct measurements is one of underdetermination (Kleinhans, 2010); how to ensure representative sampling of spatially and temporally variable processes, and whether erosion plot and sediment sampler data can be upscaled to an entire landscape (Pasculli et al., 2014). However, computational models provide an alternative approach to address some of the shortcomings and can complement field-based studies to partly alleviate these problems (Hancock, 2009, Kleinhans, 2010).

1.2. Research design summary

Delineation of degraded areas and estimation of soil loss is essential for the development of adequate erosion prevention measures for sustainable management of land and water resources. However, erosion occurs as a result of the complex interplay between many factors such as

climate, land cover, soil and topography. Precise estimation or prediction is difficult because these factors are far from constant in space and time, and often interact with one another. Thus, the current study applies a systematic approach that combines efforts in field and laboratory work, spatial analysis and process-based numerical modelling. Such an approach provides the greatest potential for full explanation of catchment dynamics (Kleinhans, 2010, Grenfell, 2015). The approach adopted was sequential, and involved the following steps;

a) GIS technology and remote sensing techniques were used to assist in geospatial model formulation i.e. development of an index-based model illustrating the spatial variation in water erosion potential.

b) Field measurements involved hillslope and river sediment flux along with soil texture, vegetation measurements. Hillslope erosion was measured using erosion pins and river sediment flux was estimated using time-integrated sediment samplers. Soil samples were analysed for particle size distribution using a mechanical sieve machine.

c) The CAESAR-Lisflood model (Coulthard et al., 2016) was calibrated using gauged precipitation and river flow data collected within the research catchments and used to investigate the hydrological and geomorphological impact of land cover changes.

d) Insights from different research approaches were integrated to advance understanding of erosion processes in the research catchments.

1.3. Research questions

In this thesis, an effort is made to address the following questions with reference to the Langrivier, a fynbos dominated catchment area and Tierkloof, a catchment dominated by pine plantation, both within the Jonkershoek Nature Reserve, Stellenbosch.

1. Does a mountain headwater catchment dominated by pine plantations have a greater post-fire suspended sediment export than a comparable catchment dominated by fynbos vegetation?
2. Is land cover a dominant driver of post-fire sediment movement at the plot scale in steep headwater catchments with Table Mountain Group lithology?

3. Does the CAESAR-Lisflood landscape evolution model predict similar patterns in erosion and sediment yields as indicated by the field data?

4. How will land use change affect surface erosion and catchment sediment yield?

1.4. Research aim

In response to the critical need to better understand sediment supply, transfer and storage, this study aimed to increase understanding of erosion, deposition and sediment yields at the scale of a headwater stream catchment (100-300 ha), using Langrivier and Tierkloof catchments in the Jonkershoek Nature Reserve as comparative case studies. An attempt was made to understand the dominant processes controlling hillslope erosion rates and sediment fluxes in these catchments, which have different land management practices, fire histories, and associated vegetation cover.

1.5. Research objectives

1. To evaluate spatial variation in hillslope erosion over the period of one wet season in the Langrivier and Tierkloof catchments.

2. To measure suspended sediment flux at catchment outlets through the wet season.

3. To investigate the relationship between erosion and environmental factors such as slope gradient, vegetation cover and soil texture.

4. To conduct numerical modelling experiments, using CAESAR-Lisflood, to evaluate how changes in land cover influence streamflow, erosion and sediment yields in the Langrivier and Tierkloof catchments.

1.5. Research outline

This thesis is divided into eight chapters as follows:

- **Chapter 1** provides the general introduction of the study and demonstrates the need for improved evaluation of soil erosion processes, especially in high mountain environments, which are vital in supplying the study region with water.

- **Chapter 2** presents a critical review of literature on controls on erosion from plot to catchment scales, and methods used to quantify and assess soil erosion.

- **Chapter 3** describes the study area and research catchments. Information is presented on climate, topography, soil and land management practices. It also includes a description of the stream channels and the necessary devices used to capture rainfall and measure streamflow characteristics.

- **Chapter 4** presents a geospatial assessment used to identify erosion risk and discuss the results of areas susceptible to soil erosion based on terrain and vegetation indices.

- **Chapter 5** presents the fieldwork approach used to quantify spatial and temporal variation in surface erosion and river sediment flux. Thereafter the results are presented and discussed.

- **Chapter 6** describes the model used and details its operation, how it was calibrated and its intended use. The results of numerical experiments are then presented and discussed.

- **Chapter 7** provides a concise synthesis/overarching discussion that draws together the findings of all results chapters and situates key knowledge contributions in the context of the review presented in Chapter 2.

- **Chapter 8** provides a brief conclusion and recommendations based on the findings of the study.

CHAPTER 2: LITERATURE REVIEW

"Mankind has learned painfully that the system is highly complex, involving many variables- dependent as well as independent- and that ignorant tampering with the system can have a jack-straw effect leading to undesirable results, Sharp, 1982".

2.1. Introduction

Soil erosion is a geomorphic process that persistently occurs at the landscape scale. This process occurs naturally and operates over geological time scales contributing to landscape evolution (Montgomery, 2007). However, when viewed over shorter time scales, erosion and deposition can be regarded as instantaneous processes that are highly dynamic and may be governed by one or more catalytic factors such as variation in climate, terrain, soil type, vegetation cover and wildfire. Due to the complexity in ascribing cause and effect, quantifying erosion and sediment yields at the catchment scale can be problematic, making it difficult to manage catchment systems. An approach comprising extensive field measurements, laboratory and numerical modelling provides the greatest potential for full explanation of natural river dynamics by alleviating weaknesses of individual methods (Kleinhans, 2010, Grenfell, 2015). This chapter presents the reviewed literature in an analytical and systematic manner to provide what is known and unknown regarding earth surface sediment dynamics in high mountain environments. Mechanisms controlling these processes from plot to catchment scale are synthesized, and the methodological approaches and techniques (in situ assessments versus computational models) to quantify soil erosion, will be analysed.

2.2. Soil erosion overview

Soil erosion is recognized as a significant form of land degradation impacting both land and water resources management across the globe (Ganasri et al., 2016, Garcia-Ruiz et al., 2013, Diaz et al., 2010, Sharma, 2010, Le Roux et al., 2008, Yuksel et al., 2008). Land degradation has been of concern for more than a hundred years in South Africa, with the focus of concern

being the loss of fertile topsoil and reduced soil productivity as a result of overgrazing (Boardman et al., 2012, Boardman et al., 2015). Compton et al. (2010) indicated that by the 20th century, surface erosion and the subsequent deposition of material in the Upper Orange River catchment had increased due to surrounding landscapes being intensely cultivated, while large masses of land were being grazed (Boardman et al., 2015).

In addition to human pressures, several studies around the world show the importance of other environmental factors including climate, terrain, soil properties, wildfire and land cover (Perreault et al. 2016, Defersha et al. 2011, Vásquez-Méndez et al. 2010, Nearing et al. 2005, Istanbulluoglu et al., 2004). Studies from the Mediterranean point towards the combined interaction of climate variation and extreme weather events, while topography, soil type and wildfires are other key factors, which have collectively created ideal conditions for high soil erosion rates in the region (Zhou et al., 2008, Garcia-Ruiz et al., 2013, Feng et al., 2016). This results in greater volumes of sediment being introduced from adjacent upland areas (Florsheim et al., 2015, Lamb et al., 2015). Garcia-Ruiz et al. (2013) suggest that, as a result of increased catchment erosion, rivers in the Mediterranean region have higher sediment yields than the rest of Europe.

2.3. Factor affecting surface water erosion

Surface water erosion is defined by two processes, the detachment of particles by rain splash or scour from overland flow, and its subsequent transport from surfaces by water (Madi et al., 2013, Shakesby, 2011, Le Roux et al., 2008). The potential for detachment depends on the balance between the erosive forces of water i.e. in the form of raindrops or overland flow, and the inherent susceptibility of a soil to detachment and entrainment i.e. a soil's resistance to being moved (Madi et al., 2013). This balance between erosive force and soil resistance is influenced by many environmental factors, including slope characteristics, wildfire frequency and severity, and land use/cover changes (Defersha et al., 2011, Shakesby, 2011).

2.4. Influence of rainfall erosivity

Rainfall erosivity can be defined as the potential ability for rainfall to erode and transport sediment (Moussaoui et al., 2014). It refers to the total sum of kinetic energy of falling raindrops, which according to Moussaoui et al. (2014) is the most appropriate measure of erosivity. The capacity of rain to detach and transport material depends on the mechanics of rainfall characteristics including drop size distribution and its terminal velocity i.e. speed of fall (Arnaez et al., 2007, Van dijk et al., 2002, Romkens et al., 2001). Drop size distribution is related to rainfall intensity and the type of shower experienced (e.g. convection or frontal storm systems). Moussaoui et al. (2014) assessed the influence of rainfall intensity on drop size distribution under laboratory conditions. In this study the relationship between intensity (I) and drop size (D_r) was expressed by a power law function ($D_{r50} = 0.945\, I^{0.245}$). They found that when rainfall intensity was increased from 12 mm/hr to 103 mm/hr, the median drop size changed from 1.75 mm to 3.07 mm. Rain drops fall at a speed proportional to the root of their drop diameter such that larger drops (more mass) fall faster, according to the polynomial function $V = -0.718D^2 + 4.01D + 0.018$ (Moussaoui et al., 2014). These factors all contribute to the kinetic energy of fall and thus to rainfall erosivity (Moussaoui et al., 2014). This agrees with several other studies (e.g. Martins et al., 2010).

Field and laboratory studies have explored the relationship between rainfall intensity and soil erosion rates. Arnaez et al. (2007) assessed soil loss using a rainfall simulator that produced 22 storm events, which varied in intensity from 30 mm h^{-1} to 117.5 mm h^{-1}. Results from their research indicated a linear relationship between intensity, surface run-off and soil loss. For example, soil loss increased from 18.2 g m^{-2} h^{-1} for storms of 30 mm h^{-1} to 93.2 g m^{-2} h^{-1} for storms of 104 mm h^{-1}. Romkens et al. (2001) evaluated soil loss from plots under different rainfall intensities. In their study intensities increased from 15 mm h^{-1} to 60 mm h^{-1} (at 15 mm h^{-1} sequences) and produced sediment yields of 0.01 kg m^{-2} to 0.40 kg m^{-2} respectively. However, under natural conditions the direct disintegrating effect of rainfall may be influenced by other environmental variables. The ability of soils to resist detachment and transport by rain depends on the soil's physical characteristics. For example, infiltration speed and infiltration capacity are determined by soil type such that coarse textured

soils allow more infiltration, thus reducing overland flow and subsequent erosion (Defersha et al., 2011).

2.5. Influence of soil erodibility

The inherent susceptibility of soil to erosion as determined by its internal properties has been termed "erodibility" (Defersha et al., 2011) A soil's erodibility is influenced by its properties including texture, organic matter, aggregate stability and bulk density. For example, greater organic matter improves soil physical conditions, reduces bulk densities and improves aggregate stability, thereby promoting infiltration and thus reducing run-off (Vásquez-Méndez et al. 2010). Defersha et al. (2011) showed that the highest erosion rates occurred in soils with the lowest organic matter content. Water uptake also increases with increasing surface soil macroporosity and is highly governed by soil texture (Peterson, 2005).

There are two main effects soil texture has on erosion: Firstly, porous material allows water to infiltrate the system with ease. Coarse particles have larger and typically better-connected spaces between pores than fine textured soils, and consequently have higher infiltration capacities through preferential flow paths. These soils are assigned a low erodibility i.e. soil cohesiveness and resistance to dislodging and transport) value because they readily infiltrate water. Therefore, the rainfall to run-off response on fine textured soils tends to be greater than that on sandy soils. Sandy textured soils are thus assigned higher erodibility values because they produce more run-off thereby increasing the chance of soil erosion.

Defersha et al. (2011) investigated erosion mechanisms on different types of soil under laboratory conditions. They observed that infiltration rates were more rapid on coarse textured material. Secondly, soil texture increases (or decreases) the probability of particle detachment. Silty material is easily dislodged and transported as these soils lack a binding agent such as clay to form larger aggregates, which require greater forces to be detached and transported (Defersha et al., 2011). On top of its inherent erodibility, the susceptibility of soil to detachment and transport may be influenced by vegetation cover and rock fragment armouring (Nearing et

al., 2005). These factors protect the surface from direct impact and increase hydraulic roughness that reduces the speed of overland flow (Nearing et al., 2005).

2.6. Influence of vegetation

Many studies have assessed the relationship between cover versus the extent of bare soil surfaces, and soil loss (Zhou et al., 2008, Vásquez-Méndez et al. 2010). These studies show a clear correlation between cover and erosion. The general trend shows that overland flow and erosion increase with decreasing cover (Zhou et al., 2008). Zhou et al. (2008) indicated that disturbance of vegetation cover significantly increases overland flow and surface water erosion, especially in mountainous environments. Feng et al. (2016) and others suggest that the main effects of vegetation are interception, reduced infiltration and increased surface storage, addition of organic matter improving soil structure, and the cohesive strength of roots binding soil. In a burnt fynbos catchment, Scott (1993) indicated a slight post-fire increase in streamflow and attributed this to reduced transpiration.

However, there are conflicting views regarding the exact role of vegetation cover and soil loss (Perreault et al., 2016, Romero-Diaz et al., 2010). The structural characteristics of certain plant species have shown to play a role in increasing surface erosion (Vásquez-Méndez et al., 2010). For example, Pines and eucalyptus tend to exclude understory vegetation. While their canopies slow down rainfall hitting the surface, at the ground level there is less roughness and stem density to slow down runoff that is produced (some of which is perhaps produced elsewhere uphill in a catchment, on rocky cliffs for example) compared to fynbos, which is more likely to be thicker at ground level

Zhongming et al. (2010) demonstrated that natural vegetation is more effective at reducing soil erosion than plantations (e.g. eucalyptus, pines). However, in many parts of the world the natural vegetation is being replaced with commercial tree species such as pines for timber harvest for large scale production. In other countries areas are being afforested for soil and water conservation. For example, in southeast Spain afforestation has been carried out to protect soil and water resources (Romero-Diaz et al., 2010). Afforestation consisted of

establishing artificial forests in degraded areas. Romero-Diaz et al. (2010) indicated that 99% of afforestation schemes in Spain is completed using fast growing species such as *Eucalyptus sp* and *Pinus sp*. Replacement of natural species with exotic tree species to combat soil and water resource depletion was not always beneficial in regulating soil loss and was criticized that the type of species used was not achieving the desired outcome to reduce soil erosion. Scott (1993) similarly reported that an afforested (*Pines sp*) catchment produced greater sediment yields than a catchment still covered by indigenous vegetation.

Several other studies, including Zou et al. (2015), showed that the effect of cover on soil loss can vary depending on vegetation type, spatial spread and morphological characteristics. Nearing et al. (2005) compared erosion from a surface with grass to that of shrubs and showed that the shrub surfaces produced greater run-off and soil loss. This was due to the spaces between vegetation compared to the dense nature of grasses, which retards overland flow thus reducing soil erosion. Looking at various shrub species, Vásquez-Méndez et al. (2010) showed that *Opuntia sp* produced less run-off and less erosion than *O. imbricata*, with the latter sometimes producing similar results to that of bare surfaces. In the same study even under low rainfall erosivity, *O. imbricata* sites showed signs of erosion. From this it is evident that the species type and associated spatial patterns and morphological characteristics can have an important influence in regulating surface hydrological and erosional processes (Vásquez-Méndez et al., 2010)

2.6.1. Influence of stem density

In addition to overall surface cover, looked from above, several studies have shown that stem density at ground level specifically influences hydraulic roughness for overland flow and therefore reduces the detachment and entrainment of soil particles (Madi et al., 2013). Vegetation roughness at the ground surface increases the total flow roughness associated with surface irregularity and reduces the fraction of the flow's shear stress that is acting solely on soil particles (Istanbulluoglu et al., 2004, Busari and Li, 2014, Madi et al., 2013). Experimental studies show a connection between cover density and roughness, but limited information exists for natural landscapes (Istanbulluoglu et al., 2004). Istanbulluoglu et al. (2004) modelled the influence of stem density as a fraction of cover and showed that it exerts control on surface

roughness, which reduced flow velocity and thus surface erosion. A laboratory study by Madi et al. (2013) indicated a statistically significant correlation between stem density, flow velocity and soil loss; flow velocity was reduced by 14 % to 27 % for soil trays with stems, resulting in a reduction of sediment concentration in the water column.

Nearing et al. (2005) argued that while vegetation cover influences erosion, differences in geomorphological factors such as topography and rock cover are overriding drivers to which more of differences in erosion rates between locations can be attributed. Garcia-Ruiz et al. (2010) stated that these contradictory findings demonstrate the complexity and multi-scale nature of the interactions among controls and overland flow processes, soil erosion, sediment transport and fluvial dynamics, highlighting the need to adopt a multiscale approach when assessing sediment dynamics.

2.7. Influence of rock cover

Soil surface characteristics such as the spatial density and distribution of rock fragments have been shown to influence the intensity of soil erosion (Nearing et al., 2005). For example, they may increase the macroporosity of the soil and thereby increase infiltration capacities, resulting in reduced overland flow and soil erosion (von Bennewitz et al., 2017). When assessing the spatial pattern and rate of sediment yields between two catchments with different land cover types, Nearing et al. (2005) found that although vegetation may be the dominant factor explaining differences between the two, rock fragments explained within-catchment differences and was more important as a control on erosion than slope gradient and curvature.

Most studies examining the influence of rock cover have been experimental in nature, where surfaces of known cover are subjected to rainfall simulation. The influence of rock fragments across natural landscapes is still not well understood (Zavala et al., 2010, Jomaa et al., 2012). Rock fragments may play an important role in regulating erosional processes through protection against raindrop impact and flow detachment (armouring), reduction of physical degradation of underlying soil, and retardation of flow velocities caused by greater hydraulic roughness associated with rock fragments (Zavala et al., 2010, von Bennewitz et al., 2017).

2.8. Influence of slope

The physical processes involved in sediment movement, transport and deposition are fundamentally driven by catchment hydro-geomorphology. Topography directly determines run-off behaviour over the landscape, which is the component of the hydrological cycle most associated with surface water erosion (Oliveira et al., 2013). While many studies have demonstrated that soil erosion is highly sensitive to topographical factors, additional work is still needed to validate and test the influence of topography and how this affects soil loss in South African geomorphological contexts. Le Roux et al. (2008) has stated that the erodibility of parent material and resultant soils are the dominant factors influencing the variability of erosion rates across South Africa, rather than slope gradient. This is an important factor to consider as most erosion models assume a positive relationship between slope gradient and soil loss (Defersha et al., 2011). However, if soil properties dominate it doesn't mean there is no positive relationship with slope gradient. Instead, control for any variations in soil properties across your different slope gradient sample in order to be able to see this relationship should be taken into account.

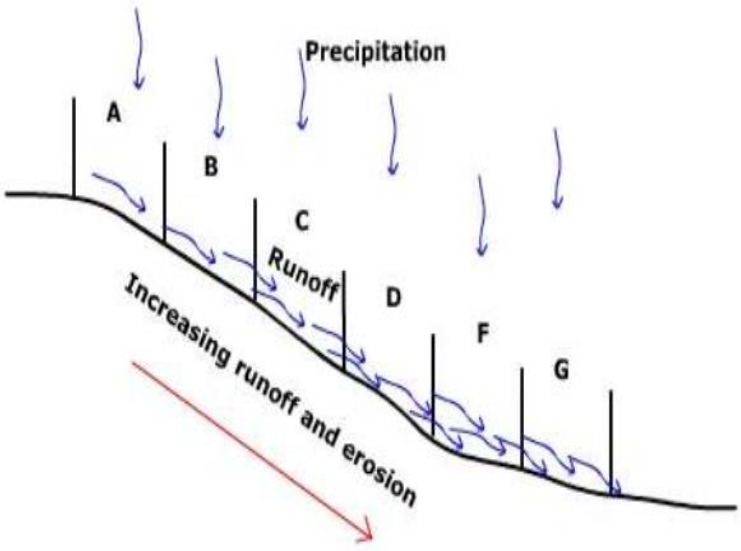

Figure 2.1. Illustrates run-off and erosion generation processes at the hillslope scale (Michael et al., 2006).

Slope characteristics influencing the mechanism of erosion are steepness, length, aspect and shape (Ganasri et al., 2016). It is the most important factors influence run-off generation and thus soil erosion as it maximizes flow velocity, transport capacities and surface flow erosion. As seen in Figure 2.1 that run-off increases towards the foot of the slope. In each section on the slope the lower part has a greater volume of water than sections above it as flow accumulates. The higher flow velocity and greater volume of water through the slope profiles result in increased erosion. Zingg (1940) and others developed an empirical relationship between erosion and gradient. Empirically, the relationship is represented by equation, which show that the amount of erosion increases with slope gradient i.e. proportional relationship (Liu Qing-quan et al., 2001).

$$\gamma = ax^b \tag{2.1}$$

Where x and y are the slope (degrees) and quantity of erosion, respectively. The a and b coefficients are empirical constants.

It is evident from the literature that under the same rainfall conditions, surface flow and erosion magnitude can be drastically different due to differences in slope gradient (Defersha et al., 2011, Quin-quan et al., 2001). Romkens et al. (2001) conducted laboratory experiments and showed that under the same rainfall intensity (45 mm/hr) sediment yields on slopes of 2 %, 8 % and 17 % were 0.19 kg m^{-2}, 0.24 kg m^{-2} and 1.89 kg m^{-2}. Several researchers reported the onset of a critical slope gradient above which soil erosion decreases (Renner, 1936, Quin-quan et al., 2001, Hortan, 1945). In their study, soil loss decreased when slopes approach a gradient of 20° to 25°, which was also reported by others. Defersha et al. (2011) assessed erosion mechanisms considering slope steepness and found that soil loss increases on slopes between 9° to 25°, and then decreases for slope > 20°. This was due to the nature of the material has an over-riding influence on erodibility.

Large efforts have been made to establish relationships between erosion and controlling factors (Bagio et al., 2017). However, contradictory evidence exists in the literature concerning the

role of slope gradient and erosion (Defersha et al., 2011). It is evident that the relationship between these factors is not that simple, and the influence of other slope properties may become more important. In fact, soil loss from hillslopes decreases above a slope gradient threshold because the amount of rainfall over the slope decreases (Defersha et al., 2011). However, this critical angle threshold varies among studies and sites for example, Chen fa yang (1985) found a threshold of 25°, Renner (1936) > 45° and Hortan (1935) found a value of 57°. Within these contradictory findings, the influence of slope length may also play a significant role (Qing-quan et al., 2001).

Slope length determines hydraulic properties such as velocity of the water layer on the surface and therefore the shear stress and transport capacity for detached soil particles. The length factor influences erosion by increasing the volume and speed of run-off, with increasing slope length, causing an increase in transport capacity to erosion and transportation. Weishmeir and Smith. (1978) indicated that when slope length was doubled, soil losses increased 1.5 times, while Resiman (2011) showed that when the length of the slope was doubled, soil erosion increased three-fold.

However, as with slope gradient, the influence of the length factor is not well understood. Some researchers indicate a linear relationship, while others indicate insignificant changes in soil loss with longer slope lengths (Bagio et al., 2017). For example, Silver et al. (2011) assessed soil loss on slope lengths of 25 m, 50m and 75 m. They found that there was an insignificant relationship between length and soil loss. In addition, may be due to slope form (concave or convex), which can accelerate or decelerate overland flow and resulting erosion and deposition (Mitsova, 1995). A seen in Figure 2.1, this would mean that the ridge of the slope would have reliable erosion, while the mid-section has active erosion and where flow accumulates at the foot slope deposition would be the dominant process. Yet, for the same slope, spatial variation in rainfall intensity or soil erodibility will produce different results. All these studies highlight the complex interaction between slope and soil loss. These contradictory results may be due to the conditions under which studies were carried out (e.g. natural rain or rainfall simulator), differences in land use/cover and soil characteristics, and / or the difficulty of controlling for the effects of different parameters and parameter interactions in determining erosion rates.

2.9. Influence of aspect

The direction hillslopes face relative to the sun, plays a role in creating local climates, which determine the vegetation species and densities that can colonize the slope (Akbari et al., 2014). Depending on the drivers of the local climate, aspect will also influence the amount and intensity of rainfall received – particularly in mountainous areas. Aspect is geomorphological property of a site that can impact multiple factors with direct influence on erosion rates. Both soil properties and vegetation characteristics may differ between north and south facing slopes. In mountainous regions, topography influences the amount of solar radiation received (Perreault et al., 2016). In the southern hemisphere, north facing hillslopes receive more sunlight and are therefore warmer, drier, have shallower soils and are more sparsely vegetated than south facing hillslopes. This may influence hydrological (e.g. run-off) and erosional processes. However, results of studies attempting to link erosion rates to aspect as an overarching variable are often inconsistent from each other especially in landscapes affected by natural disturbances such as wildfire (Akbari et al., 2014, Perreault et al., 2016).

2.10. Influence of wildfire

Vegetation provides root cohesion and surfaces that are resistant to surface erosion (Lamb et al., 2011). It also provides a protective cover and facilitates storage (e.g. stems, litter) trapping sediment by reducing flow velocity, causing sediment to settle. Wildfire reduces vegetation and burns the organic layer leaving surfaces susceptible to erosion (Shakesby, 2011). This leads to reduced infiltration capacities, and an increase in overland flow and soil erosion. Over time, depending on species, vegetation re-establishes and, in some circumstances, restores the landscape to conditions prior to burning (Scott & Prinsloo, 2008, Lamb et al., 2011, Florsheim et al., 2015).

Wildfires cause dynamic changes to landscapes, including the chemical and physical properties of the underlying soil system increasing its susceptibility to erosion (Bodí et al., 2012). One reason for observed increases in surface erosion is due to the development of soil water repellency (also called hydrophobicity) that forms parallel (but dis-continuously) to the soil

mineral surface (Shakesby et al., 2011). A water repellent layer forms when hydrophobic compounds coat soil particles preventing the movement of water through the soil profile (Mataix-Solera et al., 2007). This transformation of the soil system changes properties in the upper soil horizon that modifies infiltration capacities. Reduced infiltration and increased overland flow have been observed in many landscapes across the globe because of fire-induced water repellency (De Bano, 1981, Shakesby, 2011). Affected surfaces have been noted to increase sediment flux from hillslopes to channels by more than an order of magnitude post-fire (Lamb et al., 2011, Florsheim et al., 2015). It is evident that the formation of a water repellent layer has implications for the hydrological balance of affected soils, with consequent increases in run-off and erosion following a post fire rainfall event and therefore should be accounted for (Shakesby et al., 2011)

However, there are contradictory findings regarding the influence of fire on vegetation and soil characteristics. Several studies show a clear link between repellency and fire (Lamb et al., 2011), while others have shown that repellency occurs naturally and is dependent on the species of vegetation (Shakesby, 2011). Some studies have also indicated that coarse textured soils are more susceptible to repellency (e.g. Doerr et al., 2000). However, DeBano. (1991) and Malkinson et al. (2011) reported the presence of soil water repellency in soils with 10 to 40 % clay content. Showman (2012) indicated that repellency can occur in fine material as long as the structure is granular, so that the volatile organic compounds condense on particle or ped surfaces (De Bano, 1981).

In many environments, prescribed burning is used as a tool to manage landscapes for various purposes such as to control fire extent and timing, to promote grazing, to reduce invasive species, or to promote catchment water yields. In the past, prescribed burning as a management strategy has been practiced in the fynbos biome by both private and government land managers. The severity and intensity of fire plays a key role in determining the magnitude of soil erosion. Fires are generally more severe in catchments carrying species with abundant volatile organic compounds such as those produced by *Eucalyptus sp* and *Pinus sp*. Chamier et al. (2012) reviewed the impacts of invasive alien plants on water quality, with particular emphasis on South Africa. They indicated that many of these species are prominent in riparian ecosystems and their spread results in native species loss, increased biomass and fire intensity and

consequent erosion, as well as decreased river flows. In plots containing Eucalyptus sp and *Pinus sp* post-fire overland flow and soil erosion were 25 % higher when compared to control sites containing natural vegetation (Shakesby, 2011). Although, Versfeld (2010) studied relatively small overland plots (0.8ha) argued that treatments such as burning of fynbos and thinning of plantations had no significant impact on overland flow in a catchment, Scott (1993) showed that post-fire afforested catchments produced significantly higher sediment yields than natural fynbos catchments. The total annual yield produced by afforested catchments was 37 $\mathrm{t\ ha^{-1}}$, while in the natural catchment yields were approximately 7 $\mathrm{t\ ha^{-1}}$. The difference was attributed to vegetation-wildfire interactions and a range of other environmental factors including contrasting land use and cover. This serves as evidence of intensified soil erosion rates in afforested catchments. Because wildfire leads to significant changes in erosion rates, there is a need to include its effects in landscape evolution models to better predict landscape changes, especially in dryland environments where fire is a natural and necessary component of the ecology.

2.11. Spatial and temporal variability in surface water erosion

Whether burnt or unburnt, erosion of soil surfaces varies both spatially and temporally throughout a catchment. Soil loss can vary substantially when moving from point to catchment scale. For example, Shakesby (2011) reported values of 56 $\mathrm{t\ ha\ yr^{-1}}$ when estimated for a point, 8.8 $\mathrm{t\ ha\ yr^{-1}}$ for a 72 $\mathrm{m^2}$ plot and 0.005 $\mathrm{t\ ha\ yr^{-1}}$ for a 4-ha catchment. Catchment scale yield estimates were much lower than those based on point and plot measurements. Garcia-Ruiz et al. (2010) assessed the hydrologic and geomorphic response at the hillslope and catchment scale. At the hillslope scale, plots of 30 $\mathrm{m^2}$ were installed on 25° slopes. The distribution pattern of soil loss varied for different land uses. For example, for hillslopes with dense shrubs soil loss was 10 $\mathrm{t\ km^{-2}yr^{-1}}$, while burnt slopes and cultivated slopes produced losses of 11t $\mathrm{km^{-2}yr^{-1}}$ and 150 t $\mathrm{km^{-2}yr^{-1}}$ respectively. They also show that the former site when the same site was burnt a second time, soil loss increased to $55t$ $\mathrm{km^{-2}yr^{-1}}$. At the catchment scale total sediment flux was evaluated in a forest (San Salvador), abandoned (Arnas) and badlands (Aragua) (Garcia-Ruiz et al., 2010). The hydrological response was lower in the San Salvador forest compared to the Aragua badlands catchment recording 4 and 14 floods respectively. Sediment yields was 120 $\mathrm{km^{-2}yr^{-1}}$ for San Salvador, 160 $\mathrm{t\ km^{-2}yr^{-1}}$ for Arnas and Aragua

15 300 t $km^{-2}yr^{-1}$. The results of such studies are different and often contradictory due to the complexity of interacting environmental variables and processes operating at different spatial scales. Many studies including Garcia-Ruiz et al. (2010) show that vegetation cover and land use have significant impacts on the hydrological and geomorphic response at various scales. However, the vegetation factors may show a seasonal pattern, with higher rates of erosion during periods of exposed surfaces and large rainfall events (De Luis et al., 2010).

2.12. Water and sediment regime in river basins

River systems around the world are experiencing enormous change due to excessive supply of sediment originating from adjacent uplands (Wohl et al., 2015, Walling et al., 2013). Global estimates show evidence of clear changes in river sediment flux (Walling et al., 2013). Although sediment is present in all rivers, excessive supply of sediment has negative implications for aquatic habitat and in stream water quality (Syvitski, 2003). For example, it may result in loss of fish habitat whereas sediment carrying contamination from upland surfaces causes deterioration of water quality (Wohl et al., 2015). The increased mobilisation of sediment and its subsequent delivery to rivers is a major concern for local authorities in South Africa (Le Roux et al., 2008). Studies indicate that the current sediment loads in rivers have been significantly altered due to large scale human interventions, while other perturbations such as climate i.e. seasonality in precipitation, steep slopes and basin size make it difficult to disentangle the relative influence of land use/cover from other catchment characteristics (Syvitski, 2003, Chakrapani, 2005, Syvitski and Milliman 2007).

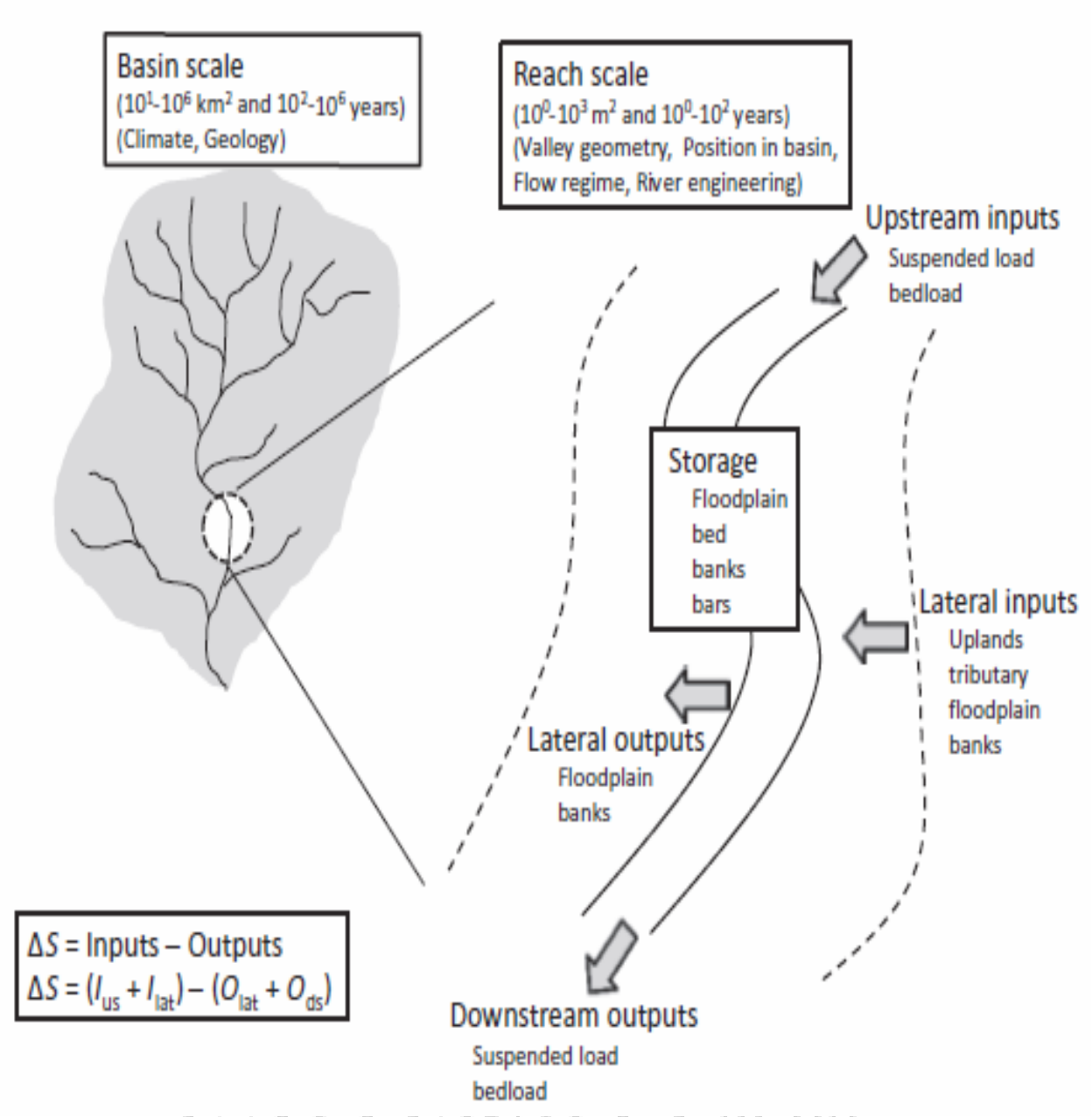

Figure 2.2. Basin wide configuration showing the spatial and temporal distribution of the sediment regime and factors controlling its variability. Adjacent uplands may contribute to upstream (us) and lateral (la) input (I), while material introduced to the channel.

Wohl et al. (2015) provides a conceptual framework with which sediment exchange processes at the catchment scale can be tracked. In this simplified framework, sediment is supplied to the river reach from both upstream and lateral inputs. Therefore, any changes occurring in the

upper level (basin) may impact processes in the lower (reach) levels. For example, under natural conditions the steady supply of sediment from adjacent areas can be transported by the river depending on the flow of the system. When the landscape is disturbed (e.g. removal of vegetation), excessive supply of material under the same flow regime may lead to sedimentation. While this provides an intuitive means of understanding and managing river catchments its validation requires extensive ground truthing.

2.13. Methods used to estimate surface water erosion

Quantifying sediment loads in an important step to improving river management. However, its estimation remains difficult due to current techniques used as well and spatial and temporal variability (Walling and Webb 1982, Syvitski, 2003, Syvitski and Milliman 2007). There are several methods available to quantify and assess land surface change (Boardman et al., 2016, Coulthard et al., 2016, Sharma, 2010). Methods can be classified as direct such as instantaneous grab and automated samplers, or indirect such as the use of satellite imagery for spatial analysis and numerical modelling. However, the choice of method depends on the complexity and the objectives of the study. For example, erosion pins can be used to determine actual amounts of material being eroded from a surface but capturing the spatial dynamics of soil erosion at the landscape level may prove difficult. The use of remote sensing techniques offers considerable advantages in this regard (Yuksel et al., 2008). By using image processing techniques e.g. raster manipulation, the relative spatial distribution of erosion can be predicted. For example, Sharma. (2010) investigated the role terrain and vegetation characteristic using remote sensing imagery to develop an erosion risk map. They found that with the simple application of remote sensing and spatial analysis can provide valuable information for assessing and managing affected landscapes.

One challenge with all these approaches is whether or not they are representative (i.e. both in spatial and temporal terms) and can take into account the influences of basin connectivity to properly account for physical processes such as flow and sediment routing across the landscape (Whole et al., 2015). Under natural conditions soil erosion may be highly episodic and dynamic in space and time. To address this, the spatial complexity of sediment exchange processes at

the catchment scale may be assessed using distributed and process-based computational models (Van De Wiel et al., 2010, Grenfell. 2015, Coulthard et al., 2016).

Models estimating soil loss can further be classified as empirical or conceptual (e.g. RUSLE), and physics-based (e.g. CAESAR-Lisflood) (Ganasri et al., 2016). Physics-based models aim to replicate processes that form the landscape by routing water across a mesh of cells (Digital Elevation Model- DEM), and adjust cell elevations according to particle flux-balance operating across hillslope and fluvial environments (Van De Wiel et al., 2011, Coulthard et al., 2016). Effective modelling can provide information of the current rates and trends of erosion and can test hypotheses and run what-if scenarios to assess the impact of various environmental changes such as those influencing land cover (Ganasri et al., 2016, Waghmare et al., 2017). Even so, these models are perhaps most useful when constrained by empirical field data, and the most mature explanations typically emerge from studies that combine approaches that make different simplifying assumptions about landscape processes (Kleinhans, 2010).

2.14. Conclusion

This review highlights the complex relationships between soil erosion and various environmental factors at all levels of catchment systems. A fundamental issue that surfaces is the challenge of spatial and temporal variability of occurrence. For example, processes that occur at the plot level may have little influence on overall sediment output. Therefore, in this study an approach like Garcia-Ruiz et al. (2010) is adopted. Garcia-Ruiz et al. (2010) indicated that to improve assessments of soil erosion there is a need to adopt a multi-scale approach that includes plot, hillslope and catchment scale evaluation. Each scale provides information on the nature of interactions among various environmental factors and process including run-off generation, sediment transport and fluvial dynamics.

CHAPTER 3: STUDY AREA

3.1. Introduction

Sediment erosion, dispersal and exchange processes at the catchment scale may be influenced by numerous controls, both natural (e.g. variation in burn severity, lithology and terrain), and anthropogenic (e.g. changes in land use due to agricultural development). These controls are typically difficult to disentangle, such that the process of determining the 'natural' sediment flux (and geomorphic health) for a river may be complex and contested. This makes it difficult to develop and implement management strategies that target the cause of any observed deterioration in river health. The gauged catchments in the Jonkershoek Nature Reserve provide an ideal outdoor laboratory to test ideas about key controls on erosion and deposition processes at the catchment scale. This section describes the broader research area and experimental sub-catchments including the climate, geology, topography, soils and land use/cover.

3.2. Description of study area

The research was carried out in the Jonkershoek mountain catchment- a quaternary catchment situated 10 km southeast of Stellenbosch in the Western Cape Province, South Africa. The Jonkershoek falls within the larger Hottentots Holland mountain complex, which is one of 5 reserves that make up the Boland Mountain Complex of the Cape Floral Region. The Hottentots Holland Nature reserve is important for the conservation of mountain fynbos with approximately 1 300 species occurring here, including several rare and endemic plant species (Dalwai, 2014).

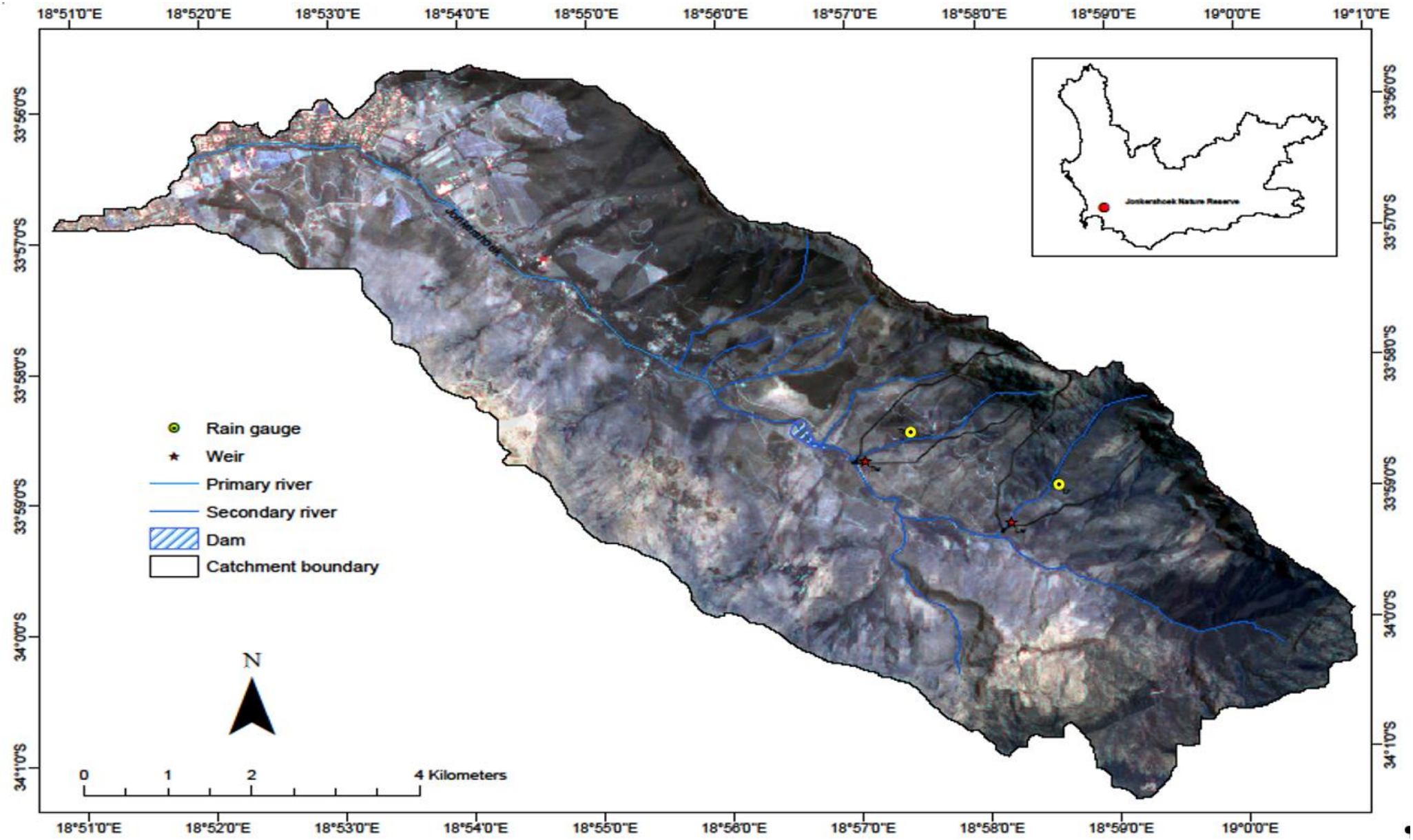

Figure 3.1. Location of study area; dam, tributaries, rain gauges and hydraulic structures.

The Jonkershoek catchment covers an area of approximately 6303 ha and comprises the end of a long narrow valley, which has been eroded along a line of faulting by the Eerste Rivier (Wicht, 1940). The valley, elongated in a northwest to northeast direction is enclosed on three sides by the Jonkershoek Mountain (north), Stellenbosch Mountain (south) and Dwarsberg Mountain (southeast) so that a 'cul de sac' is formed (Wicht, 1940, Wicht, 1941, Wicht et al., 1969, van Wyk, 1987, Scott, 2000). From valley bottom to ridge top the elevation ranges from 90 to 1507 m, with a mean elevation of 583 m. These mountains remain steep and rugged due to the quarzitic sandstone geology, having a maximum slope of 69° and a minimum slope of 0.003°, with a mean of 22° (Scott et al., 2008).

These high peaks and steep slopes along with small tributaries facilitate a quick streamflow response to rainfall events. The layout and the physical features of the study area is shown in Table 3.1 and Figure 3.1. The results shown in Table 3.1 are slightly improved from previous work of Scott. (1993) and others as a result of high spatial resolution a satellite imagery and advance remote sensing techniques. For example, terrain attributes such as slope, elevation and catchment delineation were extracted from a 10 m resolution terrain model. From a hydrological perspective, accurate terrain estimation on a cell by cell basis leads to better understand of complex terrain units, which ultimately enhances flow tracing capabilities for geomorphologic work.

Table 3.1. Physical features of the study area and experimental catchments

characteristics	Jonkershoek	Langrivier	Tierkloof
Location	33°57'S, 18°55'E	33°59'S, 18°58'E	33°58'S, 18°57'E
Area (ha)	6303	257	155
Maximum elevation (m)	1507	1481	1477
Minimum elevation (m)	90	367	290
Mean elevation (m)	583	854	725
Maximum slope (°)	69	65	62
Minimum slope (°)	0	0.4	0.5
Mean slope (°)	22	32.1	29.8
Aspect		SW	SW

The high mountainous environment and steep slopes give rise to several ravines that drain the valley through the Jonkershoek River, a major tributary of the Eerste Rivier (Wicht, 1940, van Wyk, 1987). The river flows downstream in a southeast (Dwarsberg) to northwest (i.e. the open side of the valley) direction. Drainage lines are deep, rocky and generally underlain by Table Mountain Group (TMG) quartzitic sandstone forming the steep peaks with shale and granite below in the toe-slope regions. Tributaries from sub-catchments on either side of the Jonkershoek valley naturally drain into the Eerste River (Moses, 2013). All sub-catchments of the area are mountainous type and situated near one another. However, they vary in size, rainfall pattern, land management, fire histories and resultant vegetation cover.

The Eerste Rivier flows through urban and rural developments of Stellenbosch and passes through mostly agricultural land before its mouth in False Bay (Moses, 2013). The valley supports a rich diversity of habitats on a local scale, fuelled by variable climatic and topographic conditions (Scott, 1993).

As with most mountainous environments, selected portions of the reserve have been extensively affected by land use changes at various stages of its history (van Wyk, 1987). These changes occurred since the 1850's where early European settlers were over-exploiting South Africa's indigenous forest resources to meet demands for timber (Chapman, 2007). In response, a program of afforestation (usually a fynbos conversion) completed by local authorities was performed using fast-growing species such as *Pinus sp, Eucalyptus sp* and some *Acacia sp* (Chapman, 2007, Scott & Prinsloo, 2008). By the 1900's concerns had been raised when experimental studies from around South Africa showed that these plantations were significantly affecting streamflow's (van Wyk, 1987, Scott & Prinsloo, 2008, Moses, 2013). These concerns formed the basis for the development of the Jonkershoek Forestry Research Station. The reserve was established in 1935 and construction of several hydraulic structures were set forth the following year with the aim of finding ways to safeguard, and if possible, improve water supplies (Wicht, 1939, Midgely et al., 1994).

The Jonkershoek valley has been used as a centre of research for more than 70 years, with a rich publication history. To this end, the area has a dense network of weather stations, hydraulic structures (i.e. weirs) and rain gauges as seen in Figure 3.1 (Moses 2013). It is exceedingly rare to have access to this type of data and thus offers tremendous opportunity to monitor and assess hydrological and geomorphological change at the catchment scale.

The main land management practices in the study area are nature conservation, which has included prescribed burning of fire breaks in the natural fire-prone fynbos vegetation as a strategy to reduce the movement of wildfire to surrounding areas, , and the use of land for the production of timber (Scott & Prinsloo, 2008, Scott, 1993). Management suffers from the contrasting perspectives and fragmented responsibility of agencies i.e. plantations are management by MTO, conservation of indigenous vegetation by Cape Nature, water resource development by the Department of Water and Sanitation and Stellenbosch Municipality, and various aspects of environmental monitoring by SAEON Such contexts can make it difficult to manage the entire river ecosystem (Poff, 1997). It has been argued that the species used in plantations tend to increase the risk of fires since they have a high content of resin and substances that fuel combustion and the spreading of fire (Romero-Diaz et al, 2010). The response to fire between these two contrasting land cover types may be different from one

another (Scott, 1993). However, of their associated environmental risk, the hydrological response of timber plantations has received the most attention (Wicht, 1940, van Wyk, 1987).

3.4. Climate

The climate of the study area is defined as Mediterranean mountain type and is characterized by marked seasonality i.e. cool wet winters (April to September), followed by hot, dry summers during October to March (van Wyk, 1986, Midgley and Scott 1994). The mean annual rainfall of 1390 mm has a high inter-annual variability and seasonal concentration with 85% occurring during the winter period when cold fronts move in a general south easterly direction off the Atlantic Ocean as long-duration, low intensity, frontal storms (Wicht et al., 1969, Scott, 1993). During this period strong north westerly winds (high pressure systems) enter the open side of the Jonkershoek (NW), which is forced through the valley over the Dwarsberg Mountains introducing a steep orographic rainfall gradient, which increases towards the southeast end of the catchment (Wicht et al., 1969). The marked difference in rainfall became evident when observing rain gauge data collected at an elevation of 1237 meters above mean sea level (mamsl) in Dwarsberg relative to valley bottoms 244 mamsl. Results indicated that rainfall amount decreased from 3874 mm/yr at the peak to 1180 mm/yr at the base of the valley (Wicht, 1969, Scott, 2000, Chapman, 2007). It is worth noting that the total rainfall of 3874 mm/yr was the highest rainfall recorded in the region (Wicht, 1969, Chapman, 2007).

Summers are usually extremely hot and dominated by strong south easterly winds that blow moist air from the warmer Indian Ocean up higher elevations where it precipitates as mist (Moses, 2013). The area has a mean annual temperature of 16.1°C, with a maximum and minimum of 38.1°C and 0.7 °C respectively (Chapman, 2007). The month of July is the coolest with a mean minimum temperature of 5.9°C while February is the hottest month with a mean maximum temperature of 27.9°C (Chapman, 2007). Wildfires are an inherent risk during the summer (Scott et al., 2000, Scott, 1993). Several wildfires as well as prescribed burning occurred in the valley, readers are referred to Scott. (1993) for further details.

3.5. Geological setting

Jonkershoek lies within the Cape Fold belt and is characterised by dramatic vertical sandstone cliffs, steep topography and valley bottoms associated with soils less resistant to weathering (New, 1999, Dye and Croke, 2003). The rocks involved are generally quartzitic sandstones and shales, with shales persisting in the valley floors and the erosion resistant sandstones forming the parallel ranges of the Cape Fold Mountains (van Wyk, 1987; Midgley and Scott, 1994; Scott & Prinsloo, 2008).

The rugged nature of the study area is associated with the underlying geology and structural deformation that shaped the steep mountain ranges over geological times. The layout of the geology and structural contacts can be seen in Figure 3.2. The Tygerberg Formation (Malmesbury Group) – Namibian (*~800-550 Ma)* – consists predominantly of shale and minor feldspathic sandstone (greywacke). Stellenbosch Batholith (Cape Granite Suite) – Namibian-Cambrian (*~555-540 Ma*) – consists of porphyritic, medium-coarse grained biotite granite that occur in the lower parts of the valley and can be found up to a depth of 10 m (Scott & Prinsloo, 2008). Peninsula Formation (Table Mountain Group) – Ordovician (*~480-460 Ma)* – makes up the thickly bedded quartzitic sandstones, with minor conglomerate and shale layers. This formation covers most of the upper half to two thirds of the catchment and outcrops as cliffs at higher elevations. Thin shale bands occur intermittently on steep slopes. These layers are topped by undifferentiated Quaternary sediment – Quaternary (*~2.5-0 Ma)* – consists of boulder – rich scree/talus, coarse quartzitic alluvial and fluvial gravels/sands, clayey gravelly loamy soils overlying basement rocks (Tygerberg Formation and Stellenbosch Batholith).

Faulting, fracturing and folding deformation events are linked to the Saldanian Orogeny (which formed the Saldania Belt *~800-500 Ma*, deformation affected the Malmesbury Group and Cape Granite Suite only), Cape Orogeny (which formed the Cape Fold Belt *~280-230 Ma* but still visible today; deformation affected basement rocks and Cape Supergroup, lower portions of the Karoo Supergroup in the vicinity of the Cape Fold Belt) and Gondwana breakup *(~180-110 Ma*, faulting of basement rocks, Cape Supergroup and Karoo Supergroup.

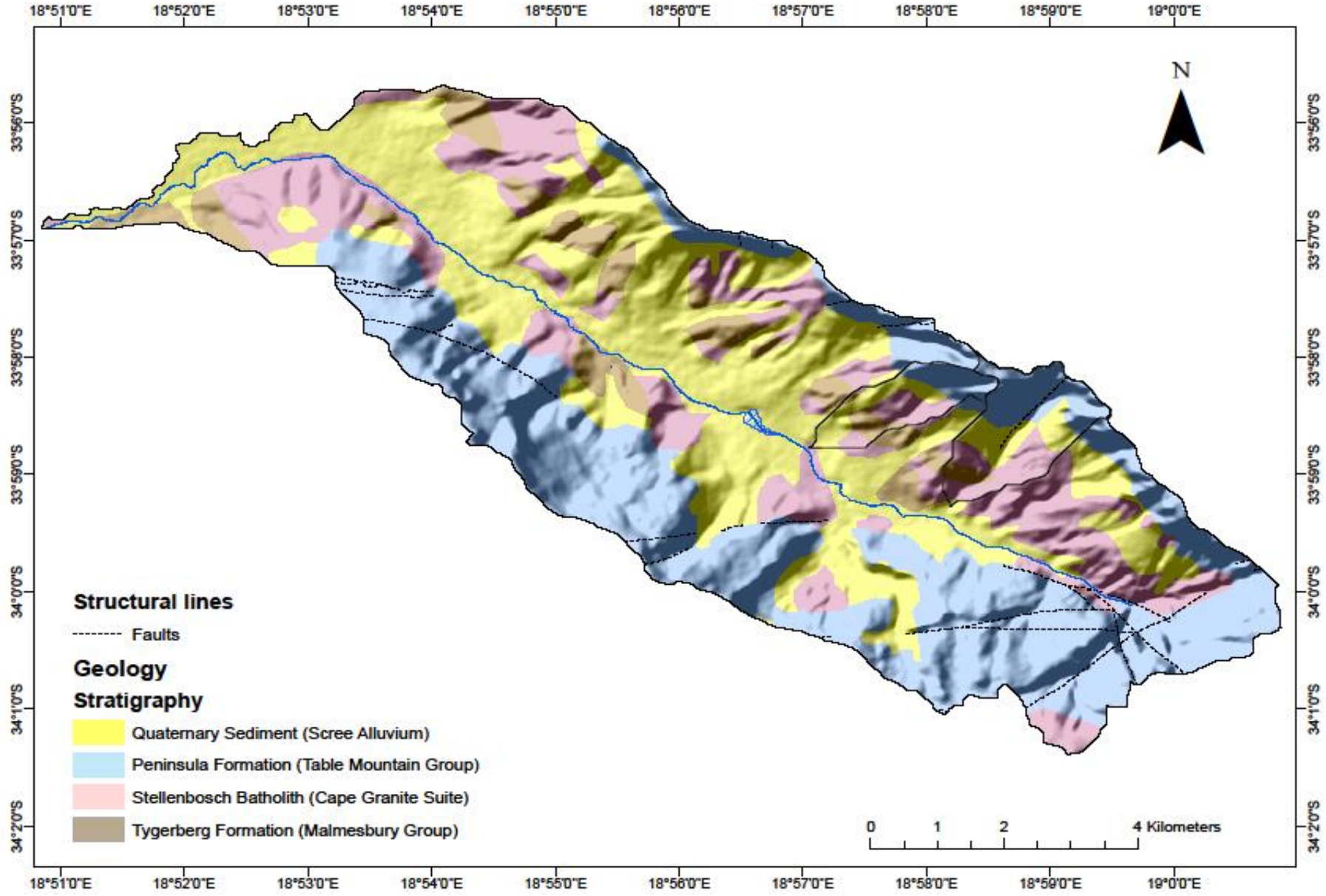

Figure 3.1. Geology and structural contacts of the Jonkershoek Nature Reserve.

3.6. Soils

Soils are derived from these geological layers through a combination of weathering, soil creep and colluviation (Scott, 1993). These processes have led to a complex and spatially distributed pattern of soil parent material on the valley floor, Figure 3.3 and description of each broad pattern in Table 3.2 and Figure 3.3 (Scott & Prinsloo, 2008). Accumulated sediments are characterized as being apedal or poorly developed soils (Garcia Quijano et al., 2007). These soils generally have a sandy loam texture, rich red-brown and yellow-brown colours, mostly low in organic matter content with a low bulk density (Scott & Prinsloo, 2008). The low bulk density hence high total pore volume facilitates infiltration.

These physical characteristics along with their high gravel and rock content favour the movement of water through the soil profile (Scott, 1993). Soils of the study area are deeper on the lower slopes, ranging from 1 to 2 m. Soil depths are key to understanding how much water can be stored in the soil column, as storage capacity increases as depth increase. However, in Jonkershoek the unconsolidated and decomposed material beneath the soil allows for free drainage of water (Scott, 1993). Despite high infiltration and low water holding capacity, surface run-off occurs in high rainfall intensity events likely as a combination of direct run-off from bare-rock cliff surfaces, saturation overland flow from thinner soil upper slopes and saturated hollows, or infiltration excess overland flow on high slopes.

Table 3.2.Broad soil pattern of the Jonkershoek Nature Reserve mapped at a scale of 1:250 000 by ICSW, ARC (Land Type Survey Staff 1972-2002).

Broad soil pattern	Description
Ac	Freely drained, red and yellow, apedal soils comprise >40% of the land type
Ba-Bd	Red (>33%) and yellow, apedal soils with plinthic subsoils (>10%)
Ca	Qualifies as Ba-Bd, but >10% occupied by upland duplex/margalitic soils
Fa	Shallow soils predominate this land type, with little to no lime
Ia	Deep alluvial soil comprise >60% of this land type
Ic	Rock outcrops comprises >80% of this land type

ICSW (2007.) ARC.

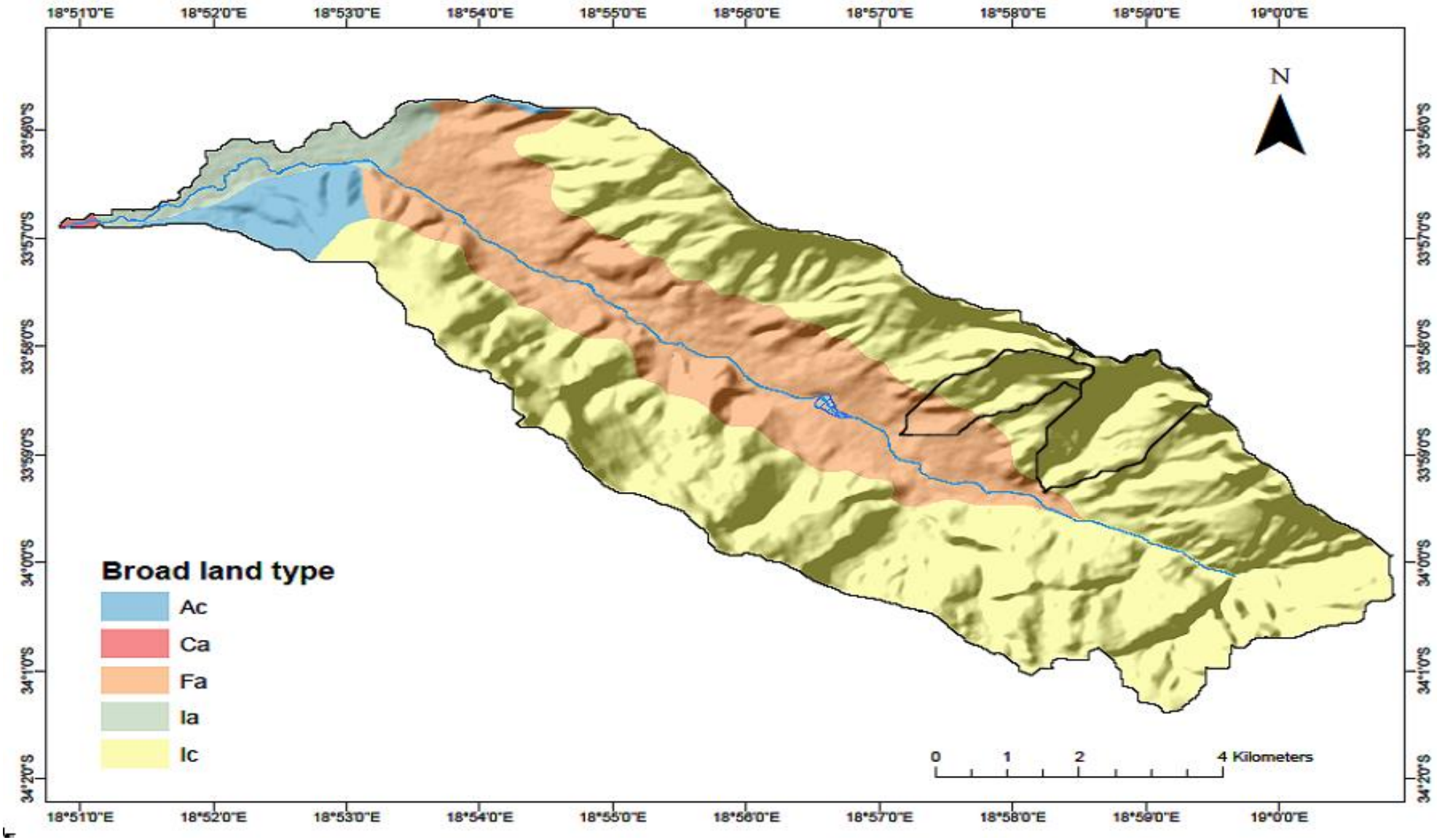

Figure 3.2. Land type (soil and terrain) of the Jonkershoek Nature Reserve. The dominant land in the Study area is Fa. The land types of the two experimental catchments are Ic and Fa, where Ic dominates, while Fa occurs only in the lower part of Tierkloof.

3.7. Vegetation

The Jonkershoek Nature Reserve supports a rich diversity of habitats on a local scale and forms a valuable conservation area (Dalwai, 2014). Located within the highly biodiverse Cape Floristic Region, the indigenous vegetation of the area is mountain fynbos, a sclerophyllous scrub between 2 to 3 meters tall found in the Mediterranean climate of the Western Cape Province (Scott & Prinsloo, 2008). According to the latest vegetation map by the South African National Biodiversity Institute (SANBI), the predominant vegetation types are Boland Granite Fynbos (54.3%), Koegelberg Sandstone Fynbos (36.8%) and Cape Winelands Shale Fynbos (5.9%), see Figure 3.4. The main species are *Protea neriifolia, Protea repens, Brunia nodiflora* and *Widdringtonia nodiflora* (van Wyk, 1987).

Confined to stream courses there are naturally occurring belts of native riparian forest (Van Wilgen, 2012, Scott, 1993). Natural forests occur sporadically throughout the catchment and includes Swartland Shale Resnosterveld (2.2%), Western Coastal band vegetation (0.3%), Afrotemperate forest (0.3%) and Swartland Granite Resnosterveld (0.1%). Although making up a relatively small proportion, these small patches of evergreen forest (>10m tall) dominated by *Ilex mitis* and *Cunonia capensis* are mainly found on suitable sites along permanent streams and scree slopes (Figure 3.4). Apart from the natural vegetation, in certain locations in the valley, the wetter south facing slopes have been afforested with pine plantations, particularly *Pinus pinaster* initially, *Pinus radiata* some acacias (*A. mearnsii*) and eucalypts (Chapman, 2007). These plantations are grown for timber and wood harvesting

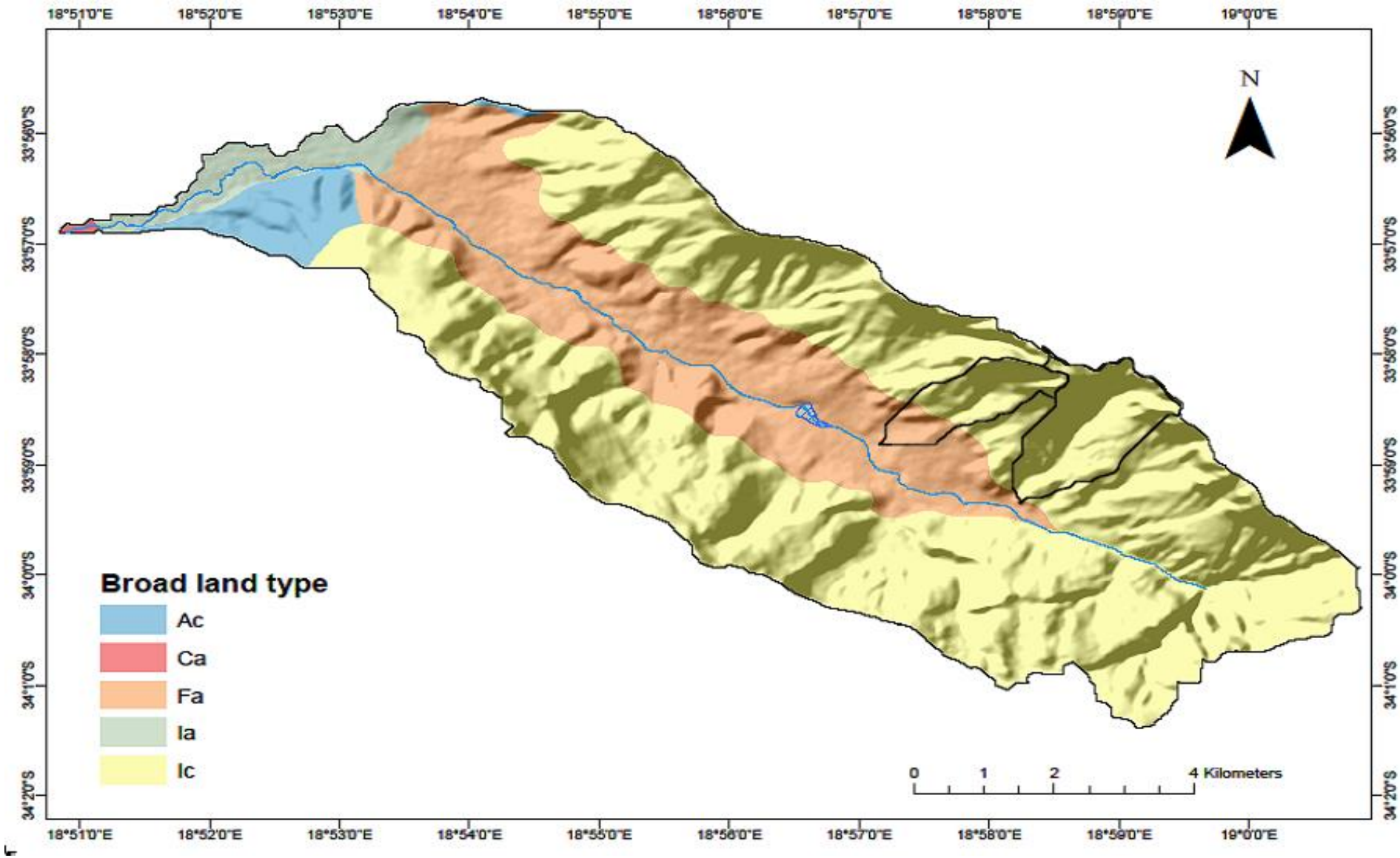

Figure 3.3. Vegetation types of the Jonkershoek Nature Reserve. Illustrates the diversity and distribution of vegetation in the study area. The dominant types are Boland Granite Fynbos and Koegelerg Sandstone Fynbos.

3.8. Description of research catchments

The two experimental catchments considered in this study are located in the upper Jonkershoek valley as seen in Figure 3.3 supplement Figure 3.7. Although these catchments are located in close proximity, they are hydrologically different from each other. They also differ in terms of size, land management, vegetation cover and fire regimes. It should be noted that both catchments had recently (2015) burned due to wildfire prior to sampling.

3.8.1. Langrivier

Langrivier is located in the northeast at an elevation of 367 to 1481 m in the valley and covers an area of approximately 257 ha, the physical features can be seen in Figure 3.1, Table 3.1 and broad soil and slope characteristic in Table 3.2 and Table 3.3 respectively. The catchment is protected and still carries the indigenous mountain fynbos, a sclerophyllous shrub ranging in height between 2-3 m tall when mature. The dominant species are *Protea nerifolia*, *Protea repens*, *Brunia nodiflora* and *Widdringtonia nodiflora* (van Wilgen, 1982, Van Wyk, 1987). However, shorter ericoid scrubs occur in the headwaters.

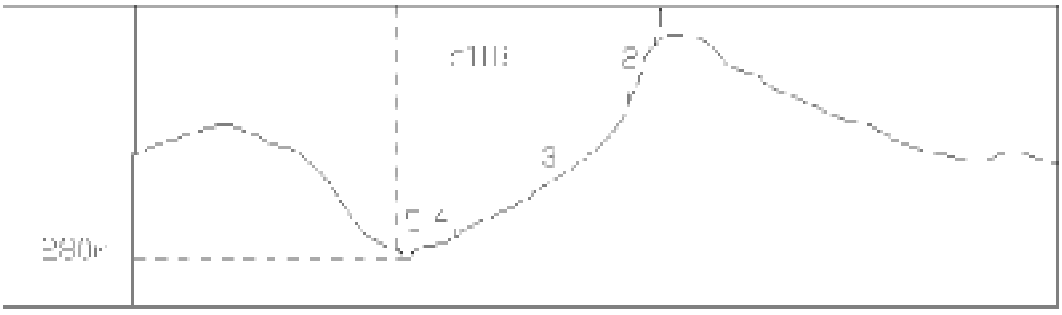

Figure 3.4. Terrain profile of land type Ic 118 (Land Type Survey Staff 1972-2002).

The catchment is characterized by steep hilly topography with a maximum and minimum slope of 65 to 0.41 respectively. A regional terrain/soil map of South Africa was produced at a scale

of 1:250 000 by the Agricultural Research Council (ARC), Land Type Survey Staff 1972-2002. Accordingly, Langrivier falls within terrain unit Ic 118 as seen in Figure 3.3 (supplement Table 3.2).

This land type consists of 5% crest, 30% scarp, 45% midslopes, 15%-foot slopes and 5% valley bottoms. Slope become more gentle towards the base, where slope percentages range from 0-20% at the crest, >100% scarps, 20-80% in the midsection, 5-15% for the foot slopes and 0-5% at the base. Slope lengths range from 10-200m at the crest, 200-400m scarps, 400-1500m midslopes, 100-1400m for the foot slopes and 10-40m at the base. Slope shape is convex at the crest, concave-straight for the scarps, straight midslopes and concave for both the foot slopes and valley bottoms seen in (Table 3.3 and Figure 3.5).

Table 3.3. Broad terrain and morphology of the Jonkershoek Nature Reserve mapped at a scale of 1:250 000 by Land Type Survey Staff 1972-2002.

Land type	Fa 145			Ic 118				
Terrain unit	3	4	5	1	2	3	4	5
% of land type	90	5	5	5	30	45	15	5
Slope (%)	15 to 40+	0 to 6	0 to 4	0 to 20	>100	20 to 80	5 to 15	0 to 5
Slope length	200 to 1000	50 to 450	20 to 50	100 to 200	20 to 400	400 to 1500	100 to 1400	10 to 40
Slope shape	Y-X	X-Z	X	Y	Y-Z	Z	X	X

x- concave
y- convex
z- straght
Land Type Survey Staff. 1972 – 2005(ICSW)

Rock outcrops dominate this land type (79%) and cover 90% of the crest, 100% of the scarp, 85% of the midslopes, 20% of the foot slopes and 65% of the valley bottoms. The remaining portion is covered by a varying distribution of soil classes. Soil depth are generally shallow with an average thickness of approximately 0.2 to 0.3 m. The structural characteristics of soils in Langrivier can be seen in Table 3.4. Along the slope profile, soil texture varies from medium-coarse to sandy loam in the upper areas, whereas fine medium sand occurs towards the valley bottom. The average topsoil clay content (A-horizon) for slopes are 6 to 15%.

Table 3.4.Soil structural characteristics of land type inventory class.

Ic118	Fa145
Freely drained structureless soil cover	Soils with pedocutanic (block structured) horizons
Excessively drained soils	Shallow soils on hard weathered rock (lithosols)
Imperfectly drained soils, often shallow with plinthic horizon cover	
Rock outcrop dominates	

The north-south orientation of the stream results in an asymmetrical shape between slopes on the west and east sides of the catchments. The stream is a first order tributary, which flows for 2 km before entering the Jonkershoek River. In the headwater region, although stable, the stream channel shows signs of deep vertical incision in bedrock. At the mouth of the catchment, the channel becomes shallower and narrower. Conditions of the riverbed mainly comprise of boulders, gravel and solid rock deposits. Along the stream, banks are confined and stabilized by evergreen forest with heights of 10 m or more and is dominated by *Ilex mitis* and *Cunonia capensis* (Scott & Prinsloo, 2008).

3.8.2. Tierkloof

Tierkloof is located in the northwest at an elevation of 290 m to 1447 m in the valley and covers an area of approximately 155 ha (Table 3.1 and Figure 3.5). This area has been significantly affected by land use changes. The catchment is afforested with exotic tree species, particularly, *Pinus radiata* to produce timber. At the time of this study, the landscape was being prepared for plantations after having recently burned. The production process and management are carried out by MTO and the methods used are described in Scott & Prinsloo (2008). In summary, the land was cleared, and plots or compartments of 3 m x 3 m were demarcated through the catchment, except the natural riparian zones along each side of the stream channel. These compartments were then tilled and planted. The process occurred over a long period of time; therefore, the surface was left bare during erosion plot set-up.

The slopes of the catchment are like that of Langrivier, having a maximum and minimum slope of 62° and 0.50° respectively. Although a large portion of the landscape falls within the Ic 118 land type, the lower portion of the catchment falls within the Fa145 land type class (Figure 3.3). The terrain unit consists of 90% midslopes, 5%-foot slopes and 5% valley bottoms. Slopes are steepest through the midsection and phases out towards the valley bottom. For example, slope percentage for midslopes range from 15 to 40% compared to 0 to 4% valley bottoms. Slope lengths show the same pattern ranging from 200 to 1000 m midslopes, 50 to 450 m foot slopes and 20 to 50 m in the valley bottoms. Slope shapes for midslopes are convex-concave, foot slopes concave-convex and straight towards the bottom valley (Figure 3.6).

Rock outcrops covers a small proportion of midslopes (10%) and foot slopes (2%) relatively to the Ic 118 land type. The unit has a greater distribution of soil textural classes, with and average topsoil clay content of 15.1 to 25 %. The unit is dominated by shallow soils and have an average depth ranging from 0.3 m to 0.6 m. The broader soil structural characteristics as described in the land type inventory map can Table 3.4.

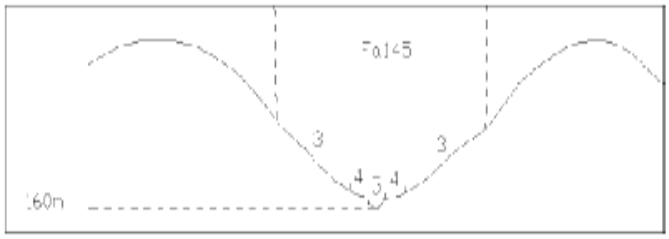

Figure 3.5. Terrain profile of land type Fa 145 (ARC, 2002).

Drainage lines of the catchment are more complex than Langrivier, with the main channel orientated in a north-west direction (Figure 3.7**).** The stream flows laterally for approximately 2 km, becoming narrow and shallow as it joins the Jonkershoek River. The streambed naturally comprises soil rock, gravel and boulder deposits. Along the stream course natural belts of riparian vegetation confines the channel, which is untouched from plantation. Although the two catchments are in close proximity, the chapters highlight the differences between Langrivier and Tierkloof.

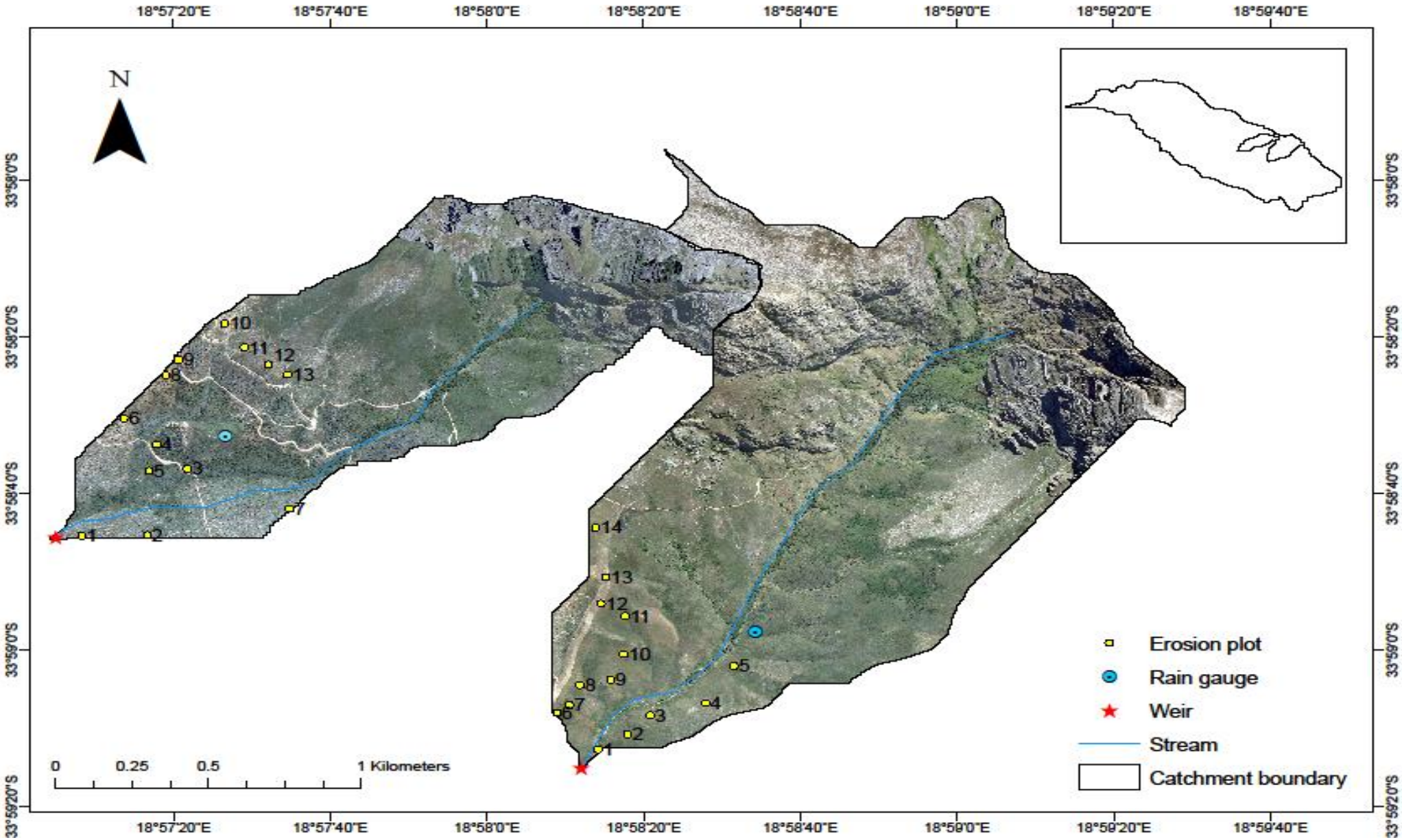

Figure 3.6. The Langrivier and Tierkloof experimental catchments, erosion plots, weirs and rain gauges.

CHAPTER 4: GEOSPATIAL MODELLING OF EROSION RISK BASED ON TERRAIN AND VEGETATION INDICES IN THE TWO CATCHMENTS.

4.1. Erosion risk assessment based on terrain and vegetation indices

Before prevention or remediation of soil erosion can be undertaken, the spatial distribution of the problem should be assessed (Le Roux et al., 2007). Soil erosion monitoring requires evaluation of the driving forces at the catchment scale. The requirement for identifying spatial distributions of soil erosion has led to the development of several empirical models with controlling factors that can be expressed spatially, and integrated within a GIS environment (Ganasri et al., 2016).

A wide range of spatial models with varying degrees of complexity have been developed for soil erosion studies (Yuksel et al., 2008, Ganasri et al., 2016, Bagio et al., 2016). The most commonly used is the Universal Soil Loss Equation (USLE) and its modified version the Revised Universal Soil Loss Equation (RUSLE), due to its simplicity, robustness and the availability of required input data (Wischmeier & Smith 1965). The model was originally developed by Wischmeier and Smith (1965) for agricultural fields with gentle sloping surfaces in the United States (Fagbohun et al., 2016). USLE estimates annual soil loss per unit area based on the relationship between various erosion factors, including rainfall erosivity, soil erodibility, topography (length and slope), vegetation cover, and agricultural support practices. For more insight into the factors represented in these empirical models, see (Wischmeier & Smith 1965, Yuksel et al., 2008, Ganasri et al., 2016, Bagio et al., 2016)

A common approach to modelling soil erosion in GIS is to develop raster layers that represent each of the components in the RUSLE, and to combine layers to illustrate the spatial variation of water erosion potential (Le Roux et al., 2008, Yuksel et al., 2008). Although widely applied across the globe, the use of RUSLE outside the conditions for which the model was derived has been questioned due to differences in erosion controlling factors (Defersha et al., 2011). For example, the model was developed for fields with slopes <30%. In the high mountains of

Jonkershoek much steeper slopes occur and therefore applying such a model may return contradictory or erroneous results. In addition, they do not account for deposition of sediment.

In this study, an approach based in principle on the RUSLE model was developed that incorporates raster layers that better describe the physical processes controlling sediment generation, dispersal, and deposition in topographically complex environments. The probability of erosion occurring in these environments is largely dictated by variation in topographic features and vegetation characteristics (Sharma, 2010). Topography represents an energy factor that influences the velocity and transport capacity of surface run-off, which in turn influences the potential for erosion. In contrast, vegetation represents a resistance factor, providing a surface layer that protects against detachment, stem mesh that retards overland flow, thereby reducing its velocity and sediment transport capacity. It should be noted that a severe wildfire occurred one year prior to when this study was conducted (2015) and at the time of field set up i.e. March 2016, the landscape of Tierkloof was being prepared for the plantation of pines, which left areas of the landscape completely bare.

The potential for erosion and deposition in the two catchments was modelled considering the above factors. Layers of spatial data were integrated in GIS to conduct cell by cell calculations to identify and map susceptible areas. Topographic controls were evaluated using the Length-Slope factors as represented on the Unit Stream Power Erosion and Deposition (USPED) algorithm developed by Mitsova (1995), while land cover controls were evaluated using the Normalized Difference Vegetation Index (NDVI). The final product was applied to assess the probable relative magnitude of erosion across the landscape to inform and compliment field data collection and analysis, and the morphodynamic modelling exercise

4.2. Methods

4.2.1. Source data and data processing

The main factors taken into account during geospatial model formulation were terrain attributes and vegetation cover of the landscape. To prepare maps of individual factors for this study,

various source data were compiled. These sources include the 5 m resolution Stellenbosch University Digital Elevation Model to extract topographic indices, 1:250 000 geological map to manually digitize rock outcropping and 10 m resolution Sentinel-2 satellite imagery to extract vegetation indices. Individual raster layers are stacked using a multiplicative approach to derive a final output map of potential water erosion risk in the two catchments. Preparation of raster layers used to develop an erosion potential map was executed in ArcGIS 10.3. Terrain and vegetation parameters were fed through equation to produce raster layers describing each of these components, which were then stacked to form a final erosion potential risk map. A conception model is presented in Figure 4.1 detailing the steps taken and the processes involved during map development

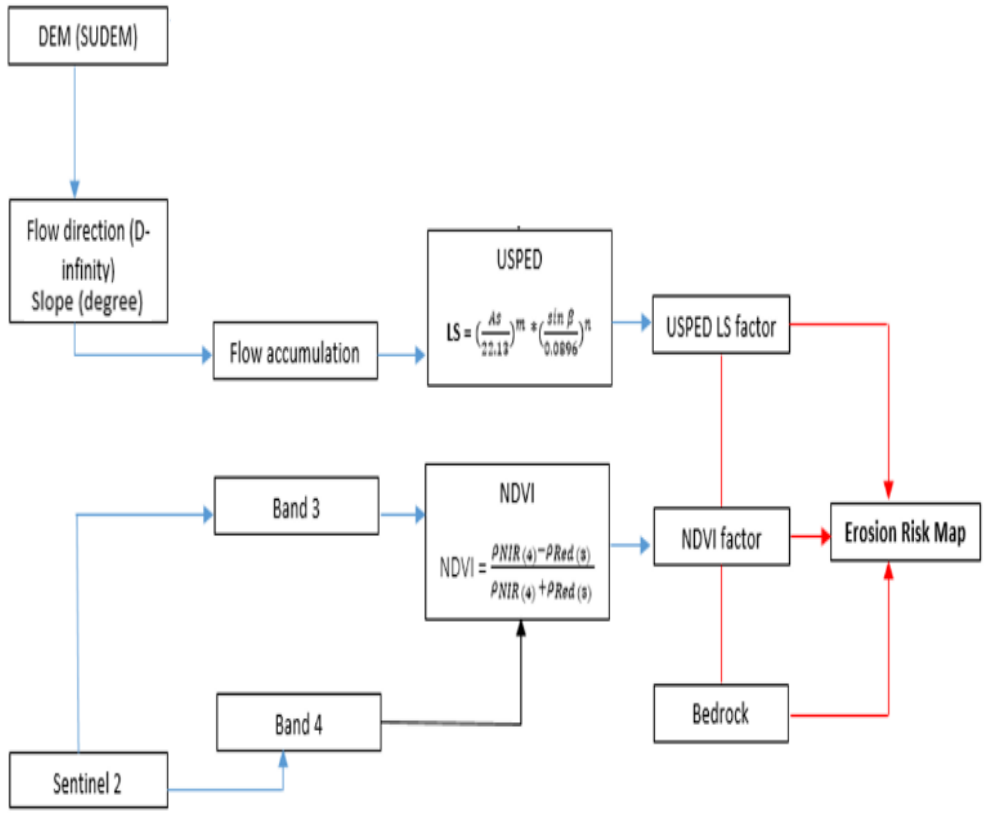

Figure 4.1. Conceptual model detailing the steps followed to produce the final erosion risk map.

4.2.1.1. Extraction of terrain indices

The Stellenbosch University Digital Elevation Model (SUDEM) of 5 m resolution was acquired from the Centre for Geographical Analysis (CGA) on October 3, 2017. SUDEM is a 5 m resolution DEM that includes four products with various level of processing. In the first step a generalized DEM at 5 m resolution was interpolated using spot heights and contours (level 1 product). The generalizations mainly occur in valley bottoms and corrected in subsequent steps. To overcome this, a 30 m STRM DEM was then corrected and up scaled to 5 m resolution, which was then fused with the output of the previous step to produce a 5 m DTM providing better detail in valley bottoms (level 2 product). In the next step, accurate elevations were extracting from 0.5 m stereographic aerial photographs to produce a detailed DSM (level 3 product). Surface objects were identified and subtracted from the DSM to produce a DTM (level 4 product), resampled to 5 m resolution and incorporated into the original level 2 product (van Niekerk, 2016). SUDEM was used to extract various topographic parameters such as slope steepness, slope form (concave/convex), and flow accumulation maxima. These parameters served as input for regression analysis and model formulation, and parameterisation for the geospatial erosion risk mapping.

4.2.3. Digitization of geological layers

Bedrock outcrops (i.e. essentially no soil) in the headwaters of the catchments were manually digitized from a geological map (1:250 000 Cape Town, map tile 3318), verified using a 0.5 m resolution orthorectified colour aerial photograph, and structural features were digitised from 1: 50 000 field sheets from the Council for Geosciences (CGS). The digitized layer was used as input to ensure that areas with no soil were effectively masked.

4.2.4. Estimation of vegetation cover

Sentinel 2 satellite imagery of 10 m resolution dated January 17, 2016 was accessed from the Copernicus website in 2017. These scenes were used to extract the presence and extent of vegetation cover for the Langrivier and Tierkloof catchments. Sentinel 2 contains a Multi-Spectral Instrument (MSI) with 13 spectral bands ranging from the visible to shortwave infrared (SWIR), and is suitable to assess vegetation characteristics and wildfire (Arellano-

Perez et al., 2018). The available higher resolution SPOT 6/7 imagery for the study period were greatly affected by shadows and were therefore not used in the study.

4.2.2. Data processing

Data received from satellites often needs some sort of correction e.g. atmospheric correction, as a result of artefacts caused by sensors (data acquisition) or arising during the interpolation (processing) methods used to generate imagery. For this purpose, hydrological conditioning in the form of filling of sinks is necessary to maintain continuity of flow routing, which breaks down if there are areas of internal drainage. It should be noted that sinks in a DEM can be real topographic features on the ground, they aren't always artefacts caused by data collection methods. It is filled for some hydrological applications because some are errors and for real ones, we may not want to go into the detail of considering them explicitly (i.e. model them filling up with water before the water can move on)

The initial terrain analysis using the sink-free SUDEM 5 m data produced drainage lines that did not match field and image observation. This was not simply a case of a small spatial offset that could be attributed to georeferencing. Rather, the 5 m SUDEM produced a drainage path in part of the catchment that was not observed in the field or 0.5 m imagery. The match improved when the 5 m data were smoothed (resampled) to 10 m resolution using a cubic convolution interpolation. This had the added advantage of consistency with the spatial resolution of the multispectral data used for vegetation cover mapping.

No corrections were applied to the Sentinel images as this was received in high-processing-level corrected form. Upon closer observation, shadows were present in the headwater regions of the catchments. However, these shadows largely fell within the digitized bedrock layer, which it was reasoned would not contribute any erosion of surface soil material during the study period.

4.2.2.1. Catchment delineation.

The initial step was to delineate each surface flow accumulation catchment from the raw data provided (e.g. the sub-catchments of Langrivier and Tierkloof). A schematic illustrating process of catchment delineation is given in Figure 4.2. Based on the definition of drainage area, the first step requires the creation of a depressionless DEM for which the hydrology of the landscape can be correctly determined. Within a geographical systems environment (GIS), watersheds are generally extracted using the D8 algorithm. To determine how flow pathways and delineate catchments in this study, the multiple flow routing algorithm (D-infinity) was used for flow tracing. D-Infinity is superior in determining flow directions for flow accumulation modelling, since D-8 produces stripy linear paths of flow accumulation. The advantages of D-Infinity flow routing are only realised when running operations like flow direction for flow accumulation, slope over area ratios, topographic wetness indices, etc. The advantages of this technique is realised when calculating your LS factor, as slope length would be given by the D-Infinity flow accumulation raster, while slope steepness is provided as an output during the D-Infinity flow direction step, and is useful because it is the slope steepness in the direction of flow accumulation (normal to the path of the triangular facet used to apportion flow to downslope neighbouring cells in D-Infinity). D-infinity was used to overcome the shortfall of the D8 algorithm improving model output accuracy.

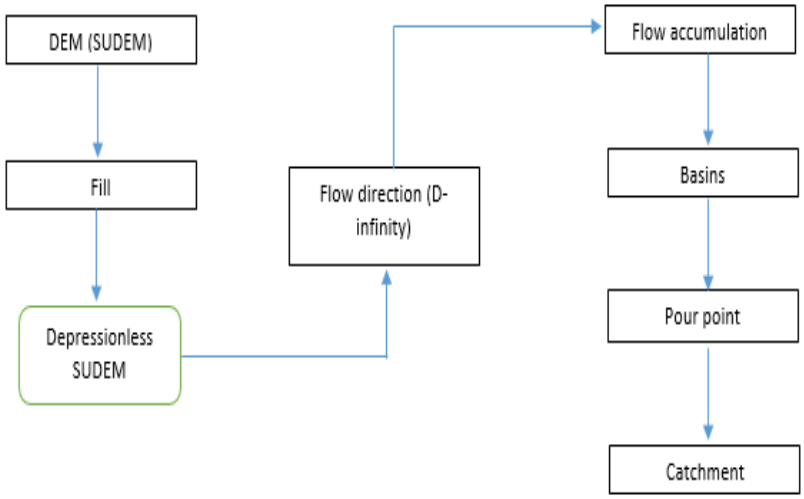

Figure 4.2. Conceptual model detailing the steps followed to produce the final erosion risk map.

Before delineation of catchments (basins), the flow accumulation raster was determined, which shows areas where water on the landscape is likely to concentrate and generally follows the drainage network. Water between ridge lines (high point boundary) usually drains to a single or outlet point in the catchment. The pour point tool was used and placed at the outlet or pixel that accumulates all the water in the study area. The tool delineates all the surface area contributing water to that pixel when running the watershed tool. Once the catchment areas of Langrivier and Tierkloof were delineated, the raster layers were converted to polygon shapefiles for further use.

4.2.2.2. Estimating the LS factors based on USPED

Most surface water erosion models combine some form of climate, topography (slope length and steepness factors), land cover and geotechnical information for predictive modelling. Of these factors, slope length (L) and steepness (S), combined to form the LS factor, consider the influence of terrain, and have a greater relative influence on model output than other parameters used for soil loss prediction (Hrabalikova et al., 2015, Gelagay et al., 2016). From a hydrological and geomorphological perspective, to improve erosion estimates it is important for models to incorporate surface flow, relief and slope curvature which influence erosion and deposition processes in complex terrain structures (Sharma, 2010, Oliveira et al., 2014).

The Unit Stream Power Erosion and Deposition (USPED) algorithm was developed due to perceived limitations of existing empirical models (Mitsova, 1995, Junakova et al., 2014). These models were based on standardized plots with slopes up to 9° making their application within complex mountainous terrain problematic. For example, D8 does not accurately calculate flow (and thus erosion) convergence and divergence, total contributing area, because of sending all the flow to only one neighbour so missing the development of a stream in certain directions losing some subtleties in the terrain (Zhang et al., 2017). Therefore, it cannot be applied where depositional processes occur. To overcome this problem, the LS factor as calculated in the USPED accounts for both convergent and divergent flow by incorporating upslope contributing area, which integrates surface water pathways and flow accumulation and therefore erosion and deposition patterns (Oliveira et al., 2014). It predicts net erosion in areas of profile convexity and tangential concavity (flow acceleration and convergence zones) and

net deposition in areas of profile concavity (zones of decreasing flow velocity). Including complex terrain geometry and contributing area aids in a better understanding of the spatial distribution of soil erosion and deposition processes (Gelagay et al., 2016).

USPED is a strongly physics based model that incorporates a spatial component (upslope contributing area or flow accumulation). The incorporation of contributing area allows for the influence of complex terrain structures and therefore is considered more suitable in high-relief mountainous environments (Mitsova, 1995). The computation of the length-slope factor in the USPED model is:

$$LS = \left(\frac{As}{22.13}\right)^{m} * \left(\frac{\sin \beta}{0.0896}\right)^{n} \quad (5.1)$$

Where *As* is the specific catchment area i.e. upslope contributing area per unit width of contour draining to a specific cell (flow accumulation x cell size), *Sin β* is the local cell slope angle (degrees) and the *m* an *n* are constants that can be adjusted according to slope and the soils susceptibility to erosion (Mitsova, 1995).

The model is highly sensitive to changes in m and n and many researchers have used different values for these constants based on the catchment characteristics (Datta et al., 2010, Prasannakumar et al., 2012, Oliveira et al., 2014, Gelagay et al., 2016, Zhang et al., 2017). The m and n parameters used here are 0.2 and 1.2 respectively. These values were used by Junakova et al (2014) under conditions similar to the field data collected for the two catchments in terms of sandy soil textures and steep slopes greater than 9°.

4.2.2.3. Normalized Difference Vegetation Index (NDVI)

The extent and density of surface vegetation cover was estimated using the Normalized Difference Vegetation Index (NDVI) (Barati et al., 2011). NDVI algorithm uses the visible

and near-infrared bands for identifying healthy green vegetation, where increasingly positive values indicate more photosynthetically active vegetation (Equation 2).

A simple linear regression analysis using field data was performed to determine the relation between ground cover and pixel values. There exists a positive correlation between pixel values and in-situ cover estimates. As a result, estimates of cover derived from pixel values using Sentinel were used as a proxy to describe the density and extent of vegetation cover during 2016. High resolution multispectral bands such as Sentinel imagery are commonly used to assess vegetation cover in erosion risk mapping, Le Roux et al (2008). NDVI is calculated using the following algorithm:

$$\text{NDVI} = \frac{\rho_{NIR\,(4)} - \rho_{Red\,(3)}}{\rho_{NIR\,(4)} + \rho_{Red\,(3)}} \tag{5.2}$$

Where ρ_{NIR} and ρ_{Red} are the reflectance of the near-infrared (i.e. band 4) and visible red (i.e. band 3) bands, respectively.

In addition, the extent and density of ground cover as presented by NDVI values serve as an indirect measure of the long-term effects of wildfire, which occurred a year prior to this study (2015). Although no direct measurements of water repellency were taken, Istanbulluoglu et al (2004) considers this phenomenon in their model indicating that repellency occurs in areas where vegetation was removed. Scott (1997) examined the hydrological and erosional response to fire and found reduced infiltration capacities as a result of water repellency. Based on these findings, soil water repellency was considered to occur in de-vegetated areas and would be representative of the long-term effects of fire (Istanbulluoglu et al., 2004).

NDVI values range value from −1 to 1, where extreme negative values represent water, values around zero represent bare soil and values over 0.5 represent dense green vegetation (Sharma, 2010, Chuai et al., 2013). Therefore, the NDVI (landcover) layer distinguishes erodible surfaces i.e. areas covered by grasses and fynbos prior to the fire, and bare following the fire)

from non-erodible surfaces i.e. areas covered by exposed bedrock, and dense vegetation largely intact following the fire.

4.2.2.4. Estimating the Length and Slope factor based on USPED and inversely assigned NDVI.

The original values obtained from LS and NDVI were normalized by re-scaling between minima and maxima of 0 and 1, where values around zero indicates non-erodible surfaces and values closest to 1 indict erodible surfaces. This was done to maintain consistent probability-type scale for all input data, output does not predict actual amounts but rather the probability of erosion, which is within the constraints of available data and the terrain setting. The bedrock outcrops in the headwaters of the catchment show high erosion potential. In reality these areas would not have contributed to erosion during the study period. It is included here however due to its influence of run-off generation.

Additional steps were implemented during NDVI transformation, as values closer to 1 reflect dense vegetation and therefore areas less likely to erode. The raster layer was thus inversely assigned so that values approaching zero reflect densely vegetated (low erosion risk) zones. Once normalized, high values are associated with areas of low vegetation cover and geochemical transformation of the soil surface following fire, which are associated with high erosion potential. Although the NDVI landcover layer ensures that non-erodible surfaces are effectively masked, the mapped bedrock outcrop layer was assigned a value of zero before the multiplication procedure.

Band multiplication and manipulation procedures were carried out like Sharma (2010). Normalized layers were stacked to produce a single multi band grid, which was run through a multivariate analysis to identify erosion probability classes. To achieve this, the unsupervised classification method was performed to determine the natural characteristics (jenks) of the cell value distributions in the multiband layer. The output signature file produced was then used in the maximum likelihood classifier to obtain four groupings that correspond to erosion potential categories i.e. very high, high, medium and low.

4.2. Results

4.2.1. Spatial distribution of slope

Table 4.1.Spatial variable of slope (degrees) and total percentage area covered per catchment.

	Langrivier		Tierkloof	
Slope	Area (ha)	Percentage (%)	Area (ha)	Percentage (%)
< 11	11	4	15	10
12 to 22	59	23	37	24
23 to 32	73	28	50	32
33 to 43	50	19	18	11
44 to 54	40	16	20	13
> 55	24	9	17	11

Langrivier: total area 257 ha, with a min slope of 0.41 and maximum slope of 64

Tierkloof: total area 157 ha, with a min slope of 0.50 and maximum slope of 62

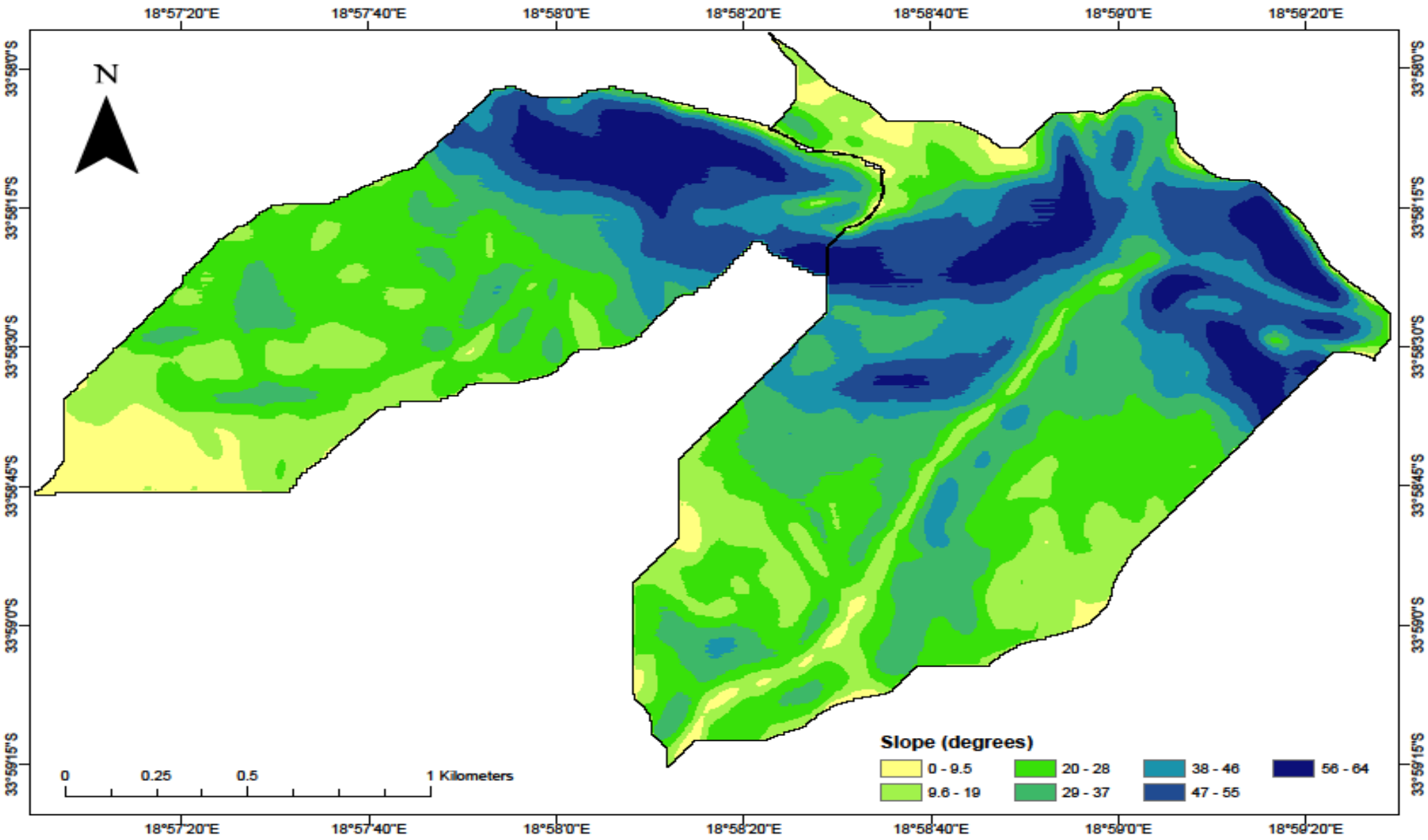

Figure 4.3. Slope gradient Langrivier (right) and Tierkloof (left) catchments show an increase in steepness towards in the northeast direction.

Topography plays an important role in driving rainfall through the catchment. The average slope in Tierkloof is 62°, while being slightly higher in Langrivier with an average slope of 69°. The spatial distribution of slope can be seen in Figure 4.3, which illustrates the two catchments are characterised by accentuated and very steep topography. Slopes in the catchments are steepest in the headwaters (north) and reduces downstream (south). The steepest slope occurs in the upper regions of the catchment, which have the maximum slope and reduces towards the low-lying areas. In these lower are slope reaches a minimum of 0.41° in Langrivier and 0.50° in Tierkloof. Table 4.1 shows the percentage area covered by various slope degrees. It is evident that 95% and 91% of slope surfaces are greater than 11° in Langrivier and Tierkloof respectively. It is reasoned that the drainage network and catchment morphology may be responsible for the observed differences in rainfall, stream flow response vegetation and soils as influenced by vegetation. Catchment morphology and slope morphology (e.g. concave and convex slopes) may influence run-off processes and thus sediment movement. It is important that these factors are considered when assessing the hydrological and erosion response of a catchment

4.2.2. Spatial distribution of the LS factor in the USPED model

The spatial variation of LS factor as calculated in USPED terrain model can be seen in Figure 4.4, which gives an indication of the topographic potential of areas susceptible to erosion and deposition. It is evident that areas with higher potential for erosion are located where slopes are steepest and have relatively long slope lengths. The maximum value estimated from this model for Langrivier and Tierkloof were 71 and 52. Highest values occur in the headwaters where slope characteristics are steepest but were masked using a bedrock layer. The Langrivier has greater potential to erosion due to steeper slopes and slope lengths. The mean LS USPED values for the catchments were 21.2 for Langrivier and 20.42 for Tierkloof, with a standard deviation of 9.85 and 10.25 respectively. The lowest values are found where slopes are relatively less steep, which occurs in the lower northwest parts of Tierkloof and distributed in the flatter areas in the Langrivier. In Langrivier these areas are mostly found on high ridges and plateaus at the boundaries of the catchment.

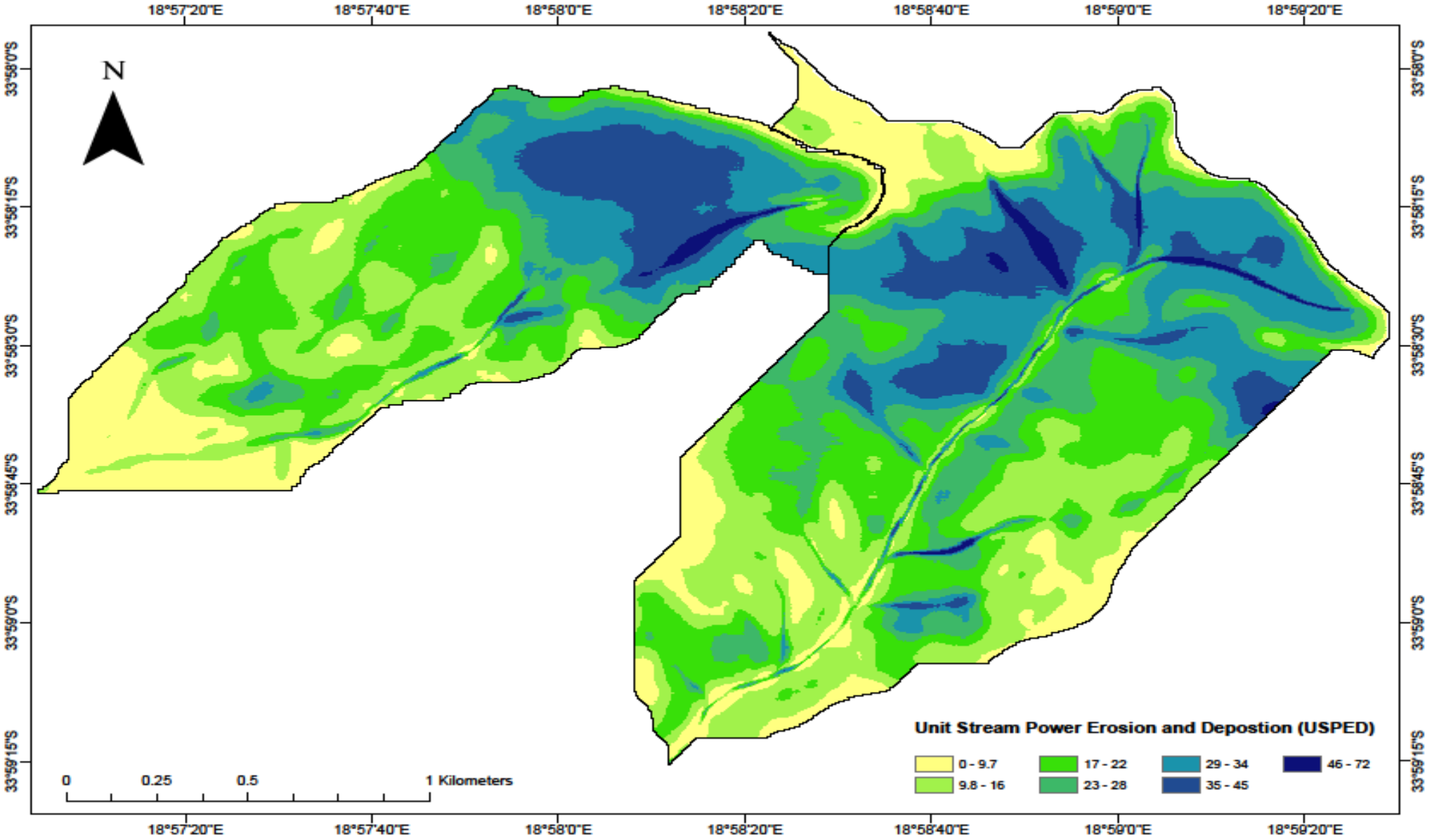

Figure 4.4. LS as estimated from USPED terrain model The Langrivier (right) has a maximum value of 71, while Tierkloof has a maximum of 52.

4.2.3. Spatial distribution of vegetation cover estimated from NDVI

Table 4.2. Spatial variable of NDVI and total percentage area covered per catchment.

	Langrivier		Tierkloof	
NDVI range	Area (ha)	Percentage (%)	Area (ha)	Percentage (%)
0	94	37	45	29
0 - 0.24	30	12	16	10
0.25 - 0.32	41	16	30	19
0.33 - 0.38	36	14	23	15
0.39 - 0.46	30	12	20	13
0.47 - 0.55	16	6	14	9
0.56 - 0.69	10	4	7	4

Classification based on NDVI of sentinel 2 scenes

The extent and density of vegetation cover was estimated using NDVI calculated from high resolution multispectral satellite imagery. The highest pixel values found were 0.71 and 0.69 with a mean of 0.22 and 0.23 for Langrivier and Tierkloof respectively. The range of NDVI values can be seen in Table 4.2. When validating outputs, it was found that values less than 0.32 represents barren/bare surfaces. The spatial spread of NDVI estimates can be seen in Figure 4.6. From this it is evident that the two catchments show a greater proportion of area with lower NDVI values i.e. <32. In Langrivier, 65% of the catchment was considered relatively bare, while 58% of the area in Tierkloof showed similar estimates. The spatial distribution of NDVI in terms of percentage area covered relative to catchment size show the same trend peaking in the bare to low and reducing towards the dense cover range.

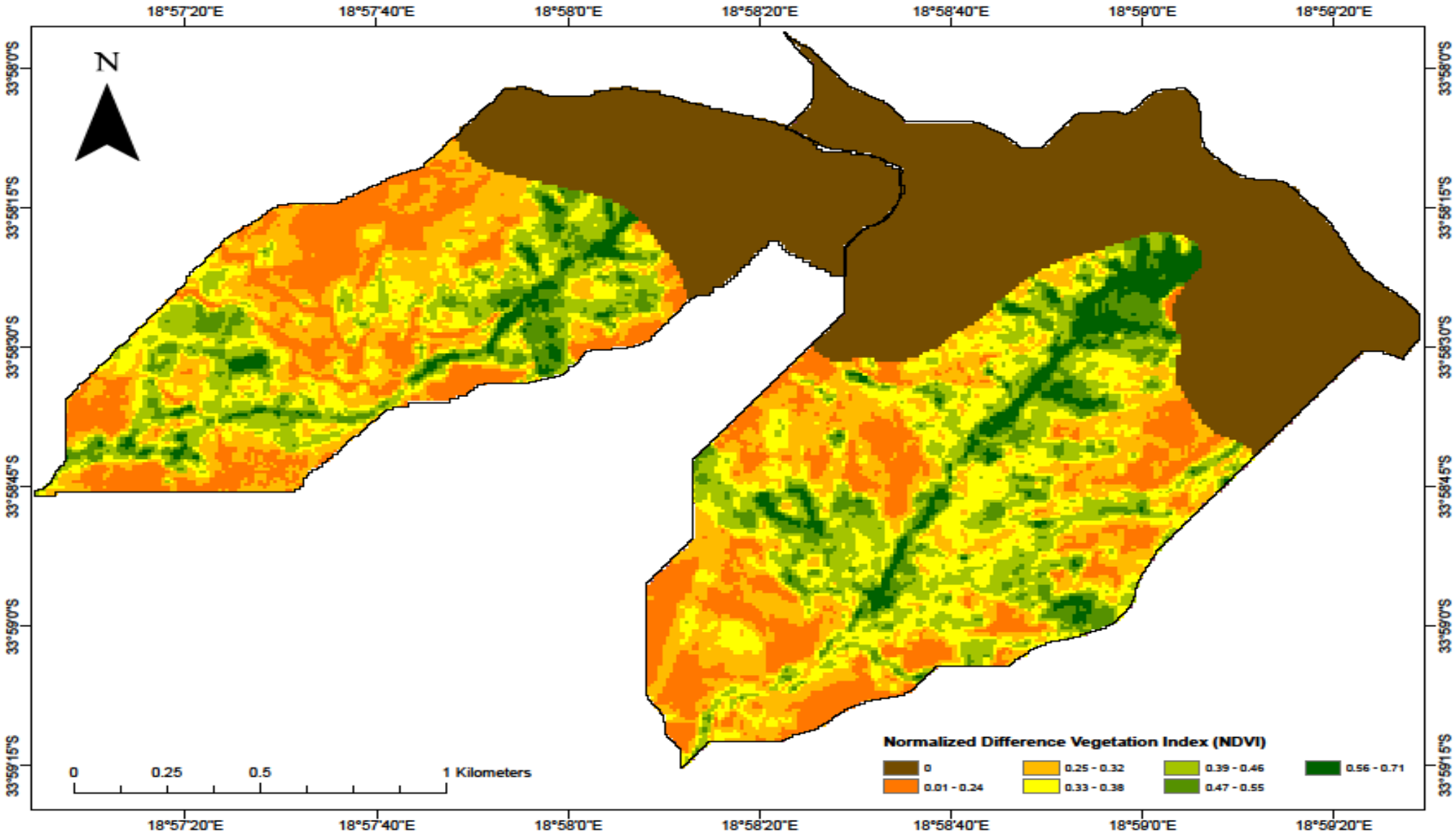

Figure 4.5. NDVI mapped for Langrivier (right) and Tierkloof (left) showing increased vegetation density occur along the natural drainage lines. The maximum values of the catchments are 0.71 and 0.69 for Langrivier and Tierkloof respectively.

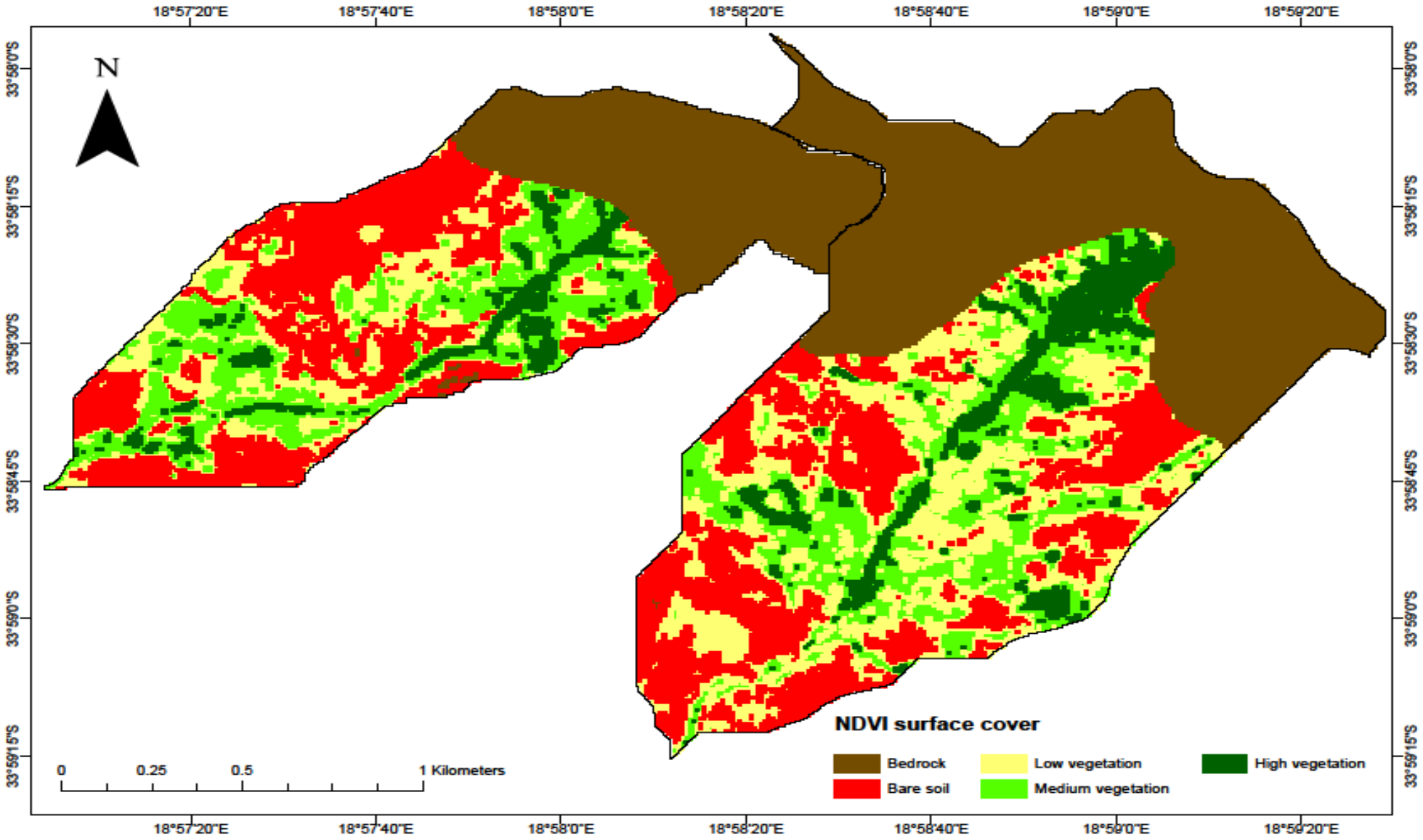

Figure 4.6.Classification map of NDVI groupings. The dominant class in Langrivier (right) is low density vegetation cover, while bare surfaces dominate Tierkloof.

Table 4.3.Spatial variable of classification of NDVI groupings and total percentage area covered per catchment.

NDVI	Langrivier		Tierkloof	
Characteristics	Area (ha)	Percentage (%)	Area (ha)	Percentage (%)
Bedrock	94	37	46	30
Bare soil	49	19	43	28
Low cover	53	21	32	21
Medium cover	42	16	25	16
High cover	19	8	9	6

The NDVI output file was grouped into four classes i.e. bare soil, low, medium and high-density vegetation cover (Figure 4.6). The Langrivier catchment is dominated by low density cover (53 ha) followed by bare surfaces (49 ha), while Tierkloof is dominated by bare surfaces (43 h) followed by low density cover classes (32 ha) (Table 4.3). Bare and low cover classes are distributed throughout the catchment particularly on steep slopes. In Langrivier, these surfaces occur in the bottom of the valley (south, either side of channel) and the steeper mid-section area. Closely scattered between bare surfaces are areas with low density vegetation cover. Relative to its size Tierkloof shows a greater area of bare surfaces with a lower area covered by low density vegetation cover.

4.2.3. Spatial distribution of erosion risk based on LS and NDVI

Table 4.4. Spatial variable of classification of erosion risk and total percentage area covered per catchment.

	Langrivier		Tierkloof	
Erosion risk class	Area (ha)	Percentage (%)	Area (ha)	Percentage (%)
Bedrock	114	44	52	33
Low	48	19	36	23
Medium	46	18	34	22
High	39	15	29	19
Very high	10	4	5	3

Classification based on terrain (USPED) and vegetation (NDVI) algorithms

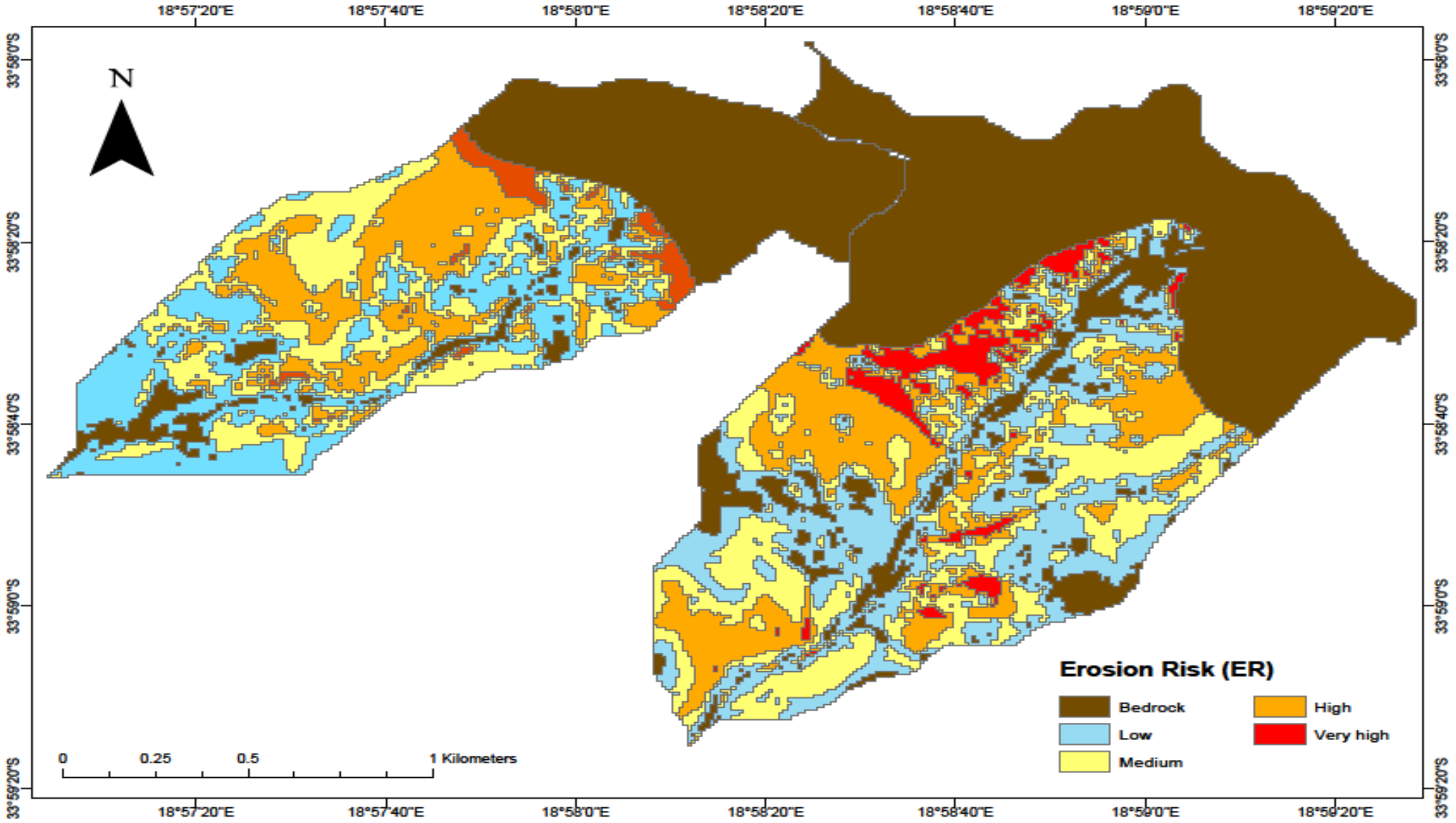

Figure 4.7. Erosion risk (ER) index map produced using multivariate analysis of USPED and NDVI. The Langrivier (right) and Tierkloof (left) catchments are dominated by low to medium erosion risk classes.

The results obtained from the erosion risk map produced from NDVI and the LS factor of the USPED can be seen in Table 4.5 and Figure 4.6. In Figure 4.7 it is evident that each catchment is susceptible to varying intensities of erosion risk. In Langrivier 19% of the catchment has low risk of erosion, which covers an area of approximately 48 ha. In Tierkloof this class covers an area of approximately 36 ha (23%). This was generally located in areas of lower slope but higher cover. The proportion of area showing erosion potential was larger in Langrivier compared relative to Tierkloof. The total area showing potential erosion risk in Langrivier was 95 ha, while in Tierkloof the total area was 68 ha. However relative to catchment size, this made up 37% in Langrivier and 44% in Tierkloof. These areas occurred on steep slopes with little to no vegetation cover.

4.3. Erosion risk (ER) assessment discussion

A simple risk map to assess the spatial variation in erosion in the two catchments was produced. The two main erosion controlling factors, namely topography and vegetation cover, were used as they represent the underlying physics of natural processes i.e. surface run-off, velocity, flow roughness and transport capacity, having important hydrological and geomorphological consequences for the landscape (Sharma, 2010).

The results obtained broadly indicate heterogenous patterns of erosion risk in both. Areas that fall within the very high-risk category cover the smallest area. In Langrivier, areas with greatest risk of erosion are found in the northern parts of the catchment and towards the southeast. Areas with high erosion potential can be seen mainly in the middle parts of the catchments, as well as in the bottom section of the Langrivier catchment. Based on terrain and vegetation, very high- and high-risk areas indicate areas on the landscape with low vegetation cover, steep slopes, long slope lengths and therefore likely receive greater surface runoff volumes per unit area. Although slopes of the catchments are relatively similar, the catchments differ in terms of size, extent and density of vegetation and morphology. These factors contribute to the relative difference in erosion risk potential.

Langrivier has a v-shaped character with a relatively straight, central, single main channel, while Tierkloof has a greater number of smaller channels. In Langrivier, the valley is deeply incised with some asymmetry between the east and west sides of the catchment. Slope not only decreases downstream (south), but also from the catchment perimeter (ridges) down to the stream channel. In the mid-section, slope from the boundary starts at 32° downstream towards the channel. The steep topography causes a quick response between precipitation and streamflow. Thus, the nature of terrain in Langrivier results in a high hillslope-channel connectivity and is evident when observing the relationship between precipitation and stream discharge.

In contrast, the drainage network in Tierkloof is much more complex than the linear nature of the channel in Langrivier. Here slopes increase from the valley bottom towards the headwaters as a result, the different response between precipitation and streamflow when compared to Langrivier, which may be in part due to lower hillslope-channel connectivity in Tierkloof. Large efforts have been made to establish relationship between erosion and controlling factors with slope being one of the main drivers (Bagio et al., 2017). However, using a model based on slope alone may not provide accurate results. To overcome this problem, model that incorporate a spatial component of upslope contributing area such as the USPED algorithm.

The impact of wildfire has played an important role in shaping the conditions of the current landscape. Although no hydrophobicity and run-off measurements were taken during assessment, the impact of fire is widely recognized as one of the main factors affecting the natural hydrologic and geomorphologic characteristics of fire prone landscapes (Shakesby, 2011). Istanbulluoglu et al (2004) developed a modelling experiment to compare the impact of harvest (anthropogenic) and wildfire (natural) on erosion in forest vegetation om a small watershed in the Idaho batholith. In their study they found that although harvest increases the frequency of sediment delivery, the delivery of material after fire is more severe. Removal of vegetation has a major hydrological and erosional consequences of affected areas. Vegetation provides root cohesion and surfaces resistant to erosion. Wildfire reduces vegetation leaving surfaces susceptible to erosion until vegetation re-establishes over-time (Lamb et al., 2011, Florsheim et al., 2011).

The density of vegetation cover generally increases towards the stream channel and follows the pattern of the drainage lines being denser along the riparian zone where water and sediment would generally accumulate. These areas are associated with minimal erosion and a shift towards depositional processes. Riparian zones play an important role in regulating or trapping sediment from the catchment. For example, the amount of sediment produces from hillslopes may be drastically different from the total coming out of the catchment.

Hillslope erosion and sediment movement into river channels increases dramatically post-fire (Florsheim et al., 2015). The sampling of this study was done a year post-fire. Many studies that report the effects of repellency years post-fire (Lamb et al., 2011, Florsheim et al., 2015). Although no direct measurements of water repellency were taken, Istanbulluoglu et al (2004) considers this phenomenon in their model indicating that repellency occurs in areas where vegetation was removed. Observed increase in overland flow and surface erosion as a result of water repellency have been observed in many landscapes across the globe as a consequence of fire-induced water repellency and therefore should be taken into account (Shakesby, 2011). Scott (1997) examined the hydrological and erosional response to fire and found reduced infiltration capacities as a result of water repellency. Based on these findings, soil water repellency was considered to occur in de-vegetated areas and would be representative of the long-term effects of fire (Istanbulluoglu et al., 2004).

In this study, bare areas are found on the steeper parts of the slope, which retain little moisture. When moving towards the channel, slopes reduces, and water starts to accumulate. This may remove the repellent layer, or reduce the potential for development of repellency initially, allowing vegetation to re-establish, which is evident by the increase in vegetation cover closer to the stream channel. Over time, depending on species, vegetation re-establishes and, in some circumstances, restores the landscape to conditions prior to burning (Scott & Prinsloo, 2008, Lamb et al., 2011, Florsheim et al., 2015).

Although there are numerous environmental factors that were not considered during the development of the present erosion risk such as rainfall erosivity, soil erodibility and land

management practices, Sharma (2010) presented that identification of areas with erosion potential based on indices used in this study prove valid as an initial step of assessment.

CHAPTER 5: ASSESSING SURFACE EROSION AND THE RELATIVE DIFFERENCES IN SEDIMENT EXPORT BETWEEN THE TWO CATCHMENTS.

5.1. Introduction.

Over the last decade numerous studies have been conducted to improve understanding of soil erosion at the catchment scale under a range of environmental settings (Boardman et al., 2016). In addition to the large variation of erosion rates reported, these studies show the variety of techniques employed to quantify soil loss and fine sediment transfer through fluvial systems (Boix-Fayos et al., 2006). These techniques can broadly be categorised into direct and indirect measurements.

Direct measurements include time integrated sediment samplers, automated samplers and erosion pins, and indirect measurements include assessment of erosion potential from satellite imagery (Phillips et al., 2000). While satellite imagery has been used successfully by several researchers, it does not provide estimates of actual soil loss or sediment exported at a catchment outlet (important for the design of effective management strategies). Furthermore, the results are often static i.e. carrying out calculations once, rather than producing dynamic time-series. For example, Jazouli et al. (2017) quantified soil erosion combining a range of satellite imagery representative of factors in the USLE within a geographical information system. In their study none of the factors considered were evolving over time. However, in reality the system changes with time, either due to external (e.g. rainfall) or internal forcing's (e.g. morpho-dynamic feedbacks).

Quantifying soil loss and movement, and how it changes over time is crucial for the development of effective management and restoration practices. In addition, field measurements can be used to calibrate numerical models used to understand the system aiding long-term forecasting. Common methods used to quantify actual soil loss and suspended sediments at river reach and catchment scales include erosion pins and suspended sediment samplers, respectively (Smith et al., 2014, Boardman et al., 2016). Smith et al. (2014) examined

the use of the time integrated sediment samplers developed by Phillips et al. (2000). Although the authors encouraged that further work be undertaken to examine the role of samplers in collecting sediment for contaminant and nutrient analyses, fieldwork indicated that the samplers were able to collect representative grainsize distribution information (Smith et al., 2014). Readers are referred to Phillips et al. (2000) and Smith et al. (2014) for detailed explanation on the mechanics and use cases of the sediment sampler.

The use of erosion pins to quantify land surface change as well as its strengths and weaknesses has been covered extensively by Boardman et al. (2016) and Boix-Fayos et al. (2006), and several researchers have made use of this simple and inexpensive technique. Ghamire et al. (2013) successfully incorporated erosion pins to monitor ground surface (sheet erosion), gullies, landslides and stream banks, while Hancock et al. (2015) showed that erosion pins can provide reliable information on hillslope erosion.

Surface water erosion is the main form of erosion considered in this study. The magnitude and extent of erosion is largely controlled by a group of factors that are loosely grouped under climate, topography, vegetation and surface conditions. The basic premise was to have plots set-up in a variety of different erosion risk classes and to estimate a total soil loss (Sum erosion (-) + Sum deposition (+)) from each plot. Additionally, suspended sediment concentrations were measured during a large storm event, and suspended sediment was sampled in time-integrated pipe samplers over a period of 6 months, to assess the relative differences in sediment export from the two catchments.

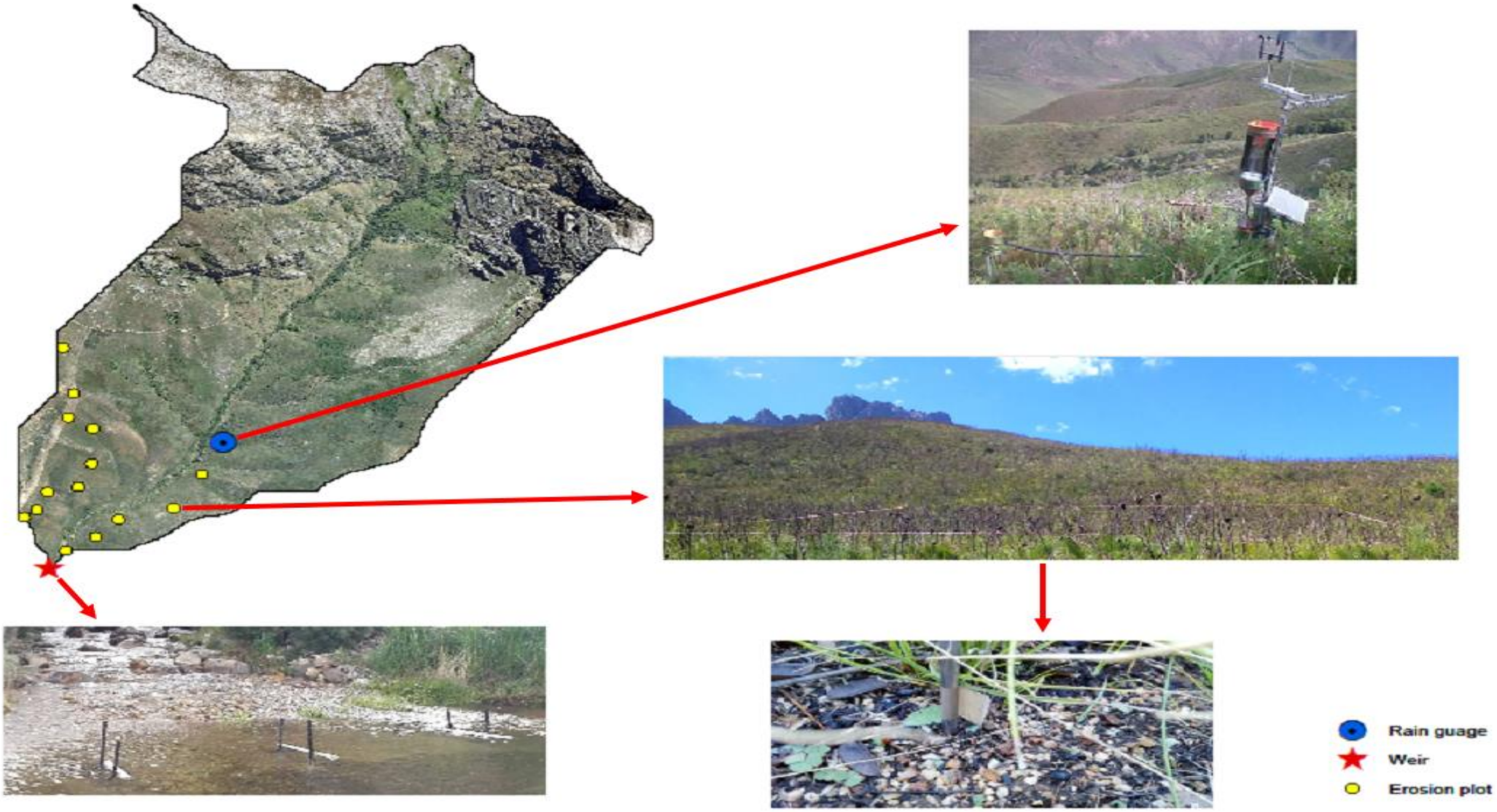

Figure 5.1. Shows the experimental design of field set-up, consisting of rain gauges (top), erosion plots and pins (middle & bottom), and suspended sediment samplers (left, also weir location).

5.2. Materials and methods.

5.2.1 Experimental design.

The approach followed is straight forward but provides comprehensive information on erosion/deposition and factors controlling its variability at the catchment scale. Figure 5.1 shows the experimental design used in the two catchments and workflow model followed to achieve accurate estimate of soil erosion and sediment exported from the two small mountainous headwater catchments in the Jonkershoek valley.

5.3. Rainfall and streamflow.

Rainfall and streamflow data for the two catchments was downloaded from the South African Environmental Observation Network database (SAEON fynbos node). Rainfall data contained missing values for the study period and required filling from nearby rain gauges. Full description of the filling technique used in this study can be found in Mbali. (2016) and Tennant et al. (2002). Mbali. (2016) used the same technique to fill in missing rainfall data in the Langrivier catchment.

5.3.1. Rainfall.

The rain gauges used for analysis were SAEON stations L14B and T13B in Langrivier and Tierkloof respectively. The gauges record rainfall in *mm/hr* at 0.25 mm accuracy. Hourly rainfall estimates were converted to daily estimates (*mm/day*). The selected gauges are located approximately midway of each catchment, at an elevation of 485 m in Langrivier and 438 m in Tierkloof. Each catchment contains a network of rain gauges, which was used to patch missing data. Additional rain gauges in the same catchment (T9B- Tierkloof and L8B- Langrivier) were used for filling based on the linear relationship relationships between the paired gauges. The process of imputing missing values using linear regression has been used successfully by others, including Tennant et al. (2002). It should be noted that the values from these single

gauges likely do not actually represent total rainfall over the entire sub catchment area, they were considered to be comparable indicators of the relative timing and magnitude of rainfall events between the two sub catchments

5.3.2. Streamflow.

V-notch weirs at the catchment outlet measure streamflow as the average flow in cubic meters per second (m^3/s). For comparison with rainfall, streamflow was converted to *mm* of runoff by dividing discharge by catchment area using Equation 5.1.

$$\text{Runoff } (mm/day) = \frac{discharge\ (m^3/s) * 1000 * 86\ 400}{Cathment\ Area\ (m^2)} \quad (5.1)$$

Where the discharge in cubic meters per second is converted to a volume of water over the area of the catchment to determine runoff in *mm/day* for comparison to rainfall estimates.

5.4. Erosion and deposition measurements.

During March 2016 erosion plots were demarcated at selected locations of the two catchments, based on an initial geospatial assessment of LS and vegetation cover, and ground surface conditions i.e. individual sites showing homogeneity in terms of local variation in surface roughness, slope and vegetation cover, and that were safely accessible within the time available to visit all plots during a round of monitoring. Each plot was marked using four wooden droppers and nylon string as seen in Figure 5.1 (middle) and covers an area of 900 m^2 (30 m x 30 m). A total of 27 erosion plots were installed, with 14 in Langrivier and 13 in Tierkloof. In each plot, 25 erosion pins were inserted using a 5 m x 5 m grid method (Figure 5.2).

According to Boix-Fayos et al (2006), potential errors and variation in erosion measurements are related to scale, inadequate representation of natural conditions (i.e. heterogeneity,

continuity and connectivity of factors and processes) and disturbances to natural conditions during installation (see also Ghamire et al., 2013). For example, insertion of pins may disturb the surface i.e. loosen sediment, which can produce excessive and misleading erosion estimates. To overcome these limitations, the plots set up in this study were open planned (i.e. not covered on any side) with a widely spaced array of thin pins that have minimal influence on surface water and sediment movement.

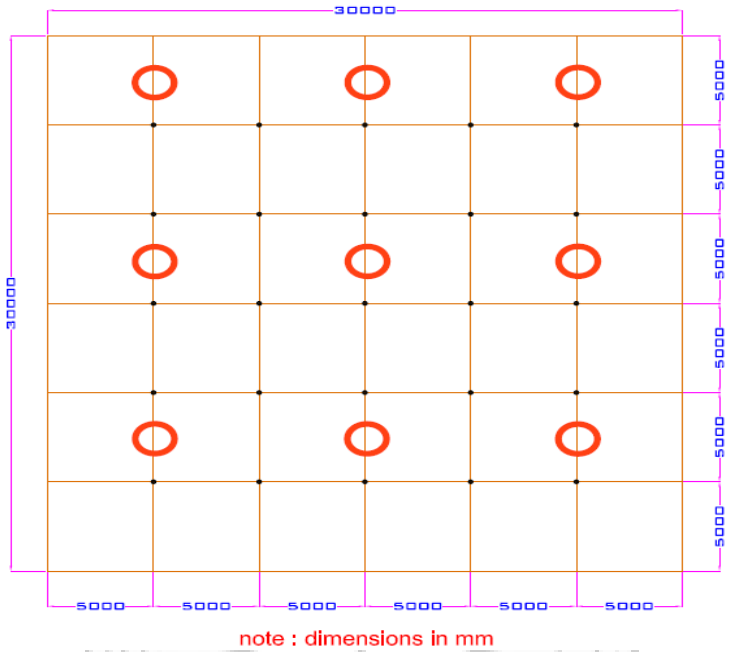

Figure 5.2. Grid used during installation of erosion pins (black dot) i.e. where the horizontal and vertical line intersect (n=25). Soil samples (red circles) were collected at the top, middle and bottom in each plot (n=9).

Erosion pins are a simple and inexpensive method to quantify land surface change (Boardman et al., 2016, Hancock et al., 2010). Pins were stratified in 5 m intervals by running across-slope and up-slope strings from end to end and inserting a pin at intersection points carefully to avoid any disturbance to the soil surface. For each plot, an array of 25 stainless steel pins, each 500 *mm* in length by 5 *mm* in diameter was inserted in the ground with 200 *mm* exposed above the surface (Figure 5.1: bottom). Each pin integrates over an area of 25 m^2 (5 m x 5 m), which means that the area assessed for soil loss was effectively 625 m^2 (25 m^2 x 25 pins). Plot soil

loss was estimated by assessing the change in pin exposure above the surface over a 6-month period (Apr to Oct 2016) using an engineering LBY double-sided stainless-steel ruler with an accuracy of 0.1 *mm* (Figure 5.3). A single measurement was taken at the end of October 2016 to estimate soil loss for the duration of the study period and to prevent any disturbance to plots from return measurements as a result of trampling.

Figure 5.3. Measurement (left) to quantify land-surface (right) change from a known length (200 *mm*) over the monitored period using an engineering ruler with a 0.1 *mm* accuracy.

The literature contains a wide variety of ways to estimate soil loss from erosion pins with no universal approach solidified in concrete. The most common approach is to determine net erosion (e.g. increased exposure) and net deposition (e.g. reduced exposure) using the arithmetic mean of measured values (Hancock et al 2010, Boardman et al, 2016). Values are then equated to tons using a known bulk density of the soil. Ghamire et al (2013) provide a way to determine a total soil loss (erosion minus deposition) by multiplying change in soil height and plot size. To derive a soil loss rate, the estimate is divided by the duration of the study period (e.g. estimate per month or year).

In this study soil erosion and deposition was determined using Equation 5.2 for each plot, which is a single metric that can be used as an outcome variable in a multiple regression (with predictor variables such as slope, or vegetation cover). The following calculation procedure

based in principle on Hancock et al. (2010) and Boardman et al. (2015) was carried out after data processing;

$$Sf\ (mm) = \frac{Sum\ erosion\ (-) + Sum\ depostion\ (+)}{number\ of\ pins} \quad (5.2)$$

Where *Sf* represent average soil loss per plot in mm over the sampling period, *erosion* is the sum of exposure lengths for pins showing increased (negative values = erosion) exposure per plot showing increased exposure (*mm*) i.e. *deposition* is the sum of pins per plot showing decreased (positive values = deposition) exposure (*mm*) i.e. deposition and number of pins equal 25 per plot, estimating the total average soil loss of each plot. To determine catchment averages a bulk density value of 1.22 g/cm^3 was used to convert the average soil loss in mm to *tons/ha/one rainy season*. The bulk density was estimated for the Langrivier catchment prior to the study by Hans (2015) and used here.

5.5. Particle size distribution.

Particle size distribution (PSD) is a fundamental and important physical property of a soil (Centeri et al., 2015). Permeability and erodibility are some of the factors that are strongly influenced by grain size distribution and interactions. For example, soils high in silt content produces greater run-off and are most erodible because they are easily detached compared to medium textured soils (Defersha et al., 2011). As a result of its influence on soil hydrology and thus initiation of erosion, soil samples were collected in each plot in order to capture the influence of grain size distribution on soil loss and serves as input into the modelling exercise.

Representative samples in each plot were collected using a grid method. Before excavation, the first 2 *cm* of burnt surface material (or wooden debris) was removed using a handheld shovel. Based on observation, these soils contained a large amount of small to medium rock fragments. Rock content also plays a role in protecting the surface from erosion and provides an additional roughness on surface flow reducing its velocity. An attempt was therefore made to roughly estimate the percentage rock cover of each plot. A disturbed sample to a depth of 5 cm was excavated, packaged, labelled and sealed. Samples were transported to the University of the

Western Cape Laboratory for further analysis. A total of 9 samples were collected per plot. For each plot, samples were placed into heavy duty bags and vigorously mixed so that one single representative sample per plot was used for assessment.

In this study, PSD was determined using both mechanical sieving and sedimentation as recommended by Ferro et al. (2009). Sample pre-treatment involved removal of organic matter and geochemical cementing agents using hydrogen peroxide and hydrochloric acid, respectively, and further dispersal in the case of sedimentation using a sodium hexametaphosphate solution. Approximately 1 *kg* of prepared sample was weighed and placed through a mechanical sieve shaker stacked with sieves with a mesh aperture of 2.00 (*mm*), 1.00 (*mm*), 500 (µm), 250 (µm) 125 (µm) and 63 (µm). The mass retained on each sieve was recorded and used to determine a soil D_{50}. Percentage sand, silt and clay was then determined using sedimentation by the pipette method.

5.6. Vegetation and stem density.

5.6.1. Vegetation.

In the study, a simple estimation of these characteristics was implemented, and estimates were used as predictor variables for erosion. In situ vegetation cover was estimated within a 0.8 *m* x 0.8 *m* square frame at a representative location selected based on field observation. Once the location was identified, the frame was placed firmly on the ground and a digital image was taken at a height of 1 *m* above the frame perpendicular to the soil surface (Vásquez-Méndez et al., 2010). Considerable effort was made to prevent and avoid any shadow effects. Images were pre-treated in Adobe photoshop CS5 extended, version 12.1 x 32, which included cropping so that each image has the same total number of pixels. The process of estimating cover from these pictures involved the amount of area covered with green pixels were determined as a percentage from the total number of image pixels (Figure 5.4).

$$\text{Vegetation cover} = \left(\frac{Total\ of green\ pixels}{Total\ count\ of\ pixels}\right) * 100 \quad (5.3)$$

In Equation 5.4, vegetation cover is given in %, green pixel represents those pixels covered by vegetation and total pixels represent to total pixel count of an image.

Figure 5.4. Estimating vegetation cover from digital images. The original scale image (top left) was scanned for green pixel values (top right). Pixels that were not in the green value class was removed (bottom). The percentage was determined from the total pixel and total green pixel count.

5.6.2 Stem density.

Stem density was determined by counting the number of plant stems within the 0.8 m x 0.8 m frame (0.64 m^2 plot area). Stem thickness was measured using a stainless-steel engineering ruler and averaged for the plot to obtain an average stem density estimate (Madi et al., 2013). The calculations using Equations 5.4 to 5.6.

$$\text{Total stem area} = (number\ of\ stems) * pi * ((average\ stem\ thickness/2)\text{^}2) \quad (5.4)$$

$$\text{Proportion of plot covered by stems} = (stem\ area)/(plot\ area) \quad (5.5)$$

$$\text{Plant stem density} = Proportion\ of\ plot\ covered\ by\ stems * 100 \quad (5.6)$$

5.7. River sediment export and suspended sediment concentration.

5.7.1. Suspended sediment.

The time-integrated sampler was originally developed to trap sediment based on the principle of sedimentation, which was used to assess the physical and geochemical properties of transported material in low lying rivers dominated by very-fine suspended sediment (Phillips et al., 2000). The sampler is inexpensive and can be operated unattended with no power requirements (Phillips et al., 2000). The mass collected by the sampler is also able to satisfy a wide range of data analysis and is used in this study to collect samples for the analysis of particle size distribution in the two catchments and the relative mass of sediment exported (Smith et al., 2014). Full instrument specification and principles of the sampling device can be found in Phillips et al. (2000), while its application and applications thereof can be found in (Smith et al., 2014). Samplers were installed in each weir using y-profile steel droppers and cable ties on the 12 May 2016. At the time, low flow conditions made it possible to observe where bulk of the sediment transported by the river was accumulating in the weir (Average flow rate was 0.603 m^3/day in Langrivier and 1.008 m^3/day in Tierkloof). As a result, a total

of three samplers were systematically installed in a transect across the channel as seen in Figure 5.5.

Figure 5.5. Installation of suspended sediment samplers. Samplers were placed were most of the sediment transported by the river accumulated in the weir. The device was secured to uprights with cable ties.

The velocity of flow tends to decrease with increasing depth and reaches a minimum velocity close to the bed of the river due to the influence of hydraulic roughness on flow. Therefore, the amount of material in suspension would be minimal. To determine a representative estimate, samples should be taken at an average depth of 0.6 *m* of the total flow depth. However, due to the extreme low flow conditions at the time of installation, the front and back inlets of the samplers were set approximately 5 *cm* below the water surface. An effort was made to ensure that sampling was carried out at a similar level in both weirs, so that trap amounts could be

compared. Samplers were left in for the duration of the study period and decanted at the end of September 2016. All the sediment and water obtained was transferred to 20 litre storage containers and transported to the University of the Western Cape for further analysis.

Samples were decanted by pouring the water-sediment mixture through 1 μm filter paper and funnel. The paper containing the sample was dried in an oven at 105°C. To determine the dry weight of samples, the mass of the filter paper was subtracted from the weight of the oven dried sample and normalized by catchment area (*ha*) using Equation 5.8, resulting in a relative indicator of the mass exported from each catchment in *grams/ha*. It is understood that this does not represent the total sediment export of the stream, the samplers only cover a small portion of the cross-section; however, it was assumed the outputs are indicators of the total sediment export that are comparable across the two sites.

$$\text{Relative sediment export indicator } (g/ha) = \frac{mass\ of\ sample - mass\ of\ filter\ paper}{Catchment\ area} \quad (5.7)$$

5.7.2. Storm event suspended sediment concentration.

The South African Weather Service advised the Disaster Risk Management Centre that a well-developed cold front was expected over the Cape on Friday evening, 26 July 2016, with pre-frontal rainfall from the morning throughout the day. Downpours of rainfall were expected with the passage of the frontal system that evening, which lead to significant rainfall amounts over the south-western parts (Cape Metropole, Overberg District and Cape) of the Western Cape with much of the rainfall over the mountainous areas.

Sediment concentration estimates were taken on Saturday, 26 July 2016 from 11 am to 3 pm, to capture as much of the sediment-discharge relationship for the storm event as possible. Samples were collected for each catchment every hour using 1 litre sample bottles. A series of samples were taken from the middle of the stream channel at each weir inlet. At every hour a sample bottle was submerged through the depth of the flow to capture an average sediment concentration for that time step. A total of 5 samples were collected in each catchment.

Sample bottles were decanted using a two-way suction pump and a handheld squeeze pump. The tanks were separated using 1 μm filter paper to extract the sediment from the water. The entire mixture was poured into the top of the device and the pressure pump was used to reduce the air pressure within the tank so that the water filters through to the second storage tank. Once all water was drained, the filter paper was removed gently and placed in an oven at approximately 105°C. At this temperature and due to the size of the filter paper all moisture from the film was evaporated within 5 hours. The dried sample filter paper was then weighed and used to estimate the average sediment concentration per sample using Equation 5.8;

$$\text{Sediment concentration } (Sc) = \frac{Weight\ of\ film - dried\ film\ weight}{litres\ of\ water\ in\ the\ sample} \quad (5.8)$$

Where *Sc* (*grams/litre*) represents the average sediment concentration and is determined by subtracting the actual filter paper weight before decanting sample by the weight of the filter paper and sediment in grams. *Sc* was determined by dividing the mass of sediment by the volume of water sample i.e. 1 litre, to estimate the relative sediment concentration per litre of water.

5.8. Analysis and statistical procedures.

Standard statistical analysis such as sum, mean, max, min was carried out on the result to illustrate differences in average sediment flux (i.e. soil loss) between plots and catchments. In addition to erosion/deposition measurements, in-situ soil samples and vegetation cover was estimated at each plot for further assessment as predictor variables. Statistical procedures such as correlation and regression analysis were used to better understand the relationships between the outcome variable (e.g. *TSe*) and predictor variables such as median grain size of soil samples, vegetation cover and slope (LS USPED). We refer to explanation of relationship found and provide details of significance of relationships in Table 5.3 and Figure 5.12. Furthermore, linear regression analysis was performed on the data. However, we only include visuals of results for those factors indicating some relationship with average sediment flux Table 5.3.

5.7. Results

5.7.1. Assessing rainfall and streamflow characteristics of the two catchments.

Rainfall totals for the study period show a significant difference in the amount of rainfall received in the two catchments. Results given are totals of 971.8 *mm* at Langrivier gauge and 708.3 *mm* at the Tierkloof gauge. The gauge at in Langrivier recorded 263 *mm* (37% more) more rainfall compared to the rain gauge in Tierkloof. It is evident that approximately 80% of the rainfall fell during the winter period between April and September, with totals ranging from 781.2 *mm* in Langrivier and 585.8 *mm* in Tierkloof.

Table 5.1. Summary statistics of daily rainfall (*mm*) and runoff (*mm*) measurements in Langrivier and Tierkloof for the study period January to December 2016.

Statistic	**Rainfall (mm)**		**Runoff (mm)**	
	Langrivier	**Tierkloof**	**Langrivier**	**Tierkloof**
mean	2.66	1.94	2.39	3.96
standard deviation	7.32	5.34	4.07	6.74
min	0	0	0.43	0.71
25%	0	0	0.64	1.05
50%	0	0	1	1.66
75%	0.6	0.4	2.4	3.98
max	52.7	41	42.09	69.79

Descriptive statistics of rainfall characteristics within Langrivier and Tierkloof during the study period are provided in Table 5.1. In the Langrivier catchment rainfall estimates varied from a minimum of 0 to a maximum of 52.7 mm/day with a mean rainfall of 2.66 mm/day, and a standard deviation of 7.32 *mm/day*. The maximum rainfall received for the same period in Tierkloof was 41 mm/day, with a mean of 1.94 mm/day and a standard deviation of 5.34 *mm/day*. Based on the standard deviation, it is evident that rainfall variability within each

catchment varies from the mean, being more widely spread in Langrivier than Tierkloof. However, correlation matrix indicated that there was a strong positive correlation (94%) between rainfalls in these two catchments. The general rainfall pattern found between these two catchments can be seen in Figure 5.6 and 5.7.

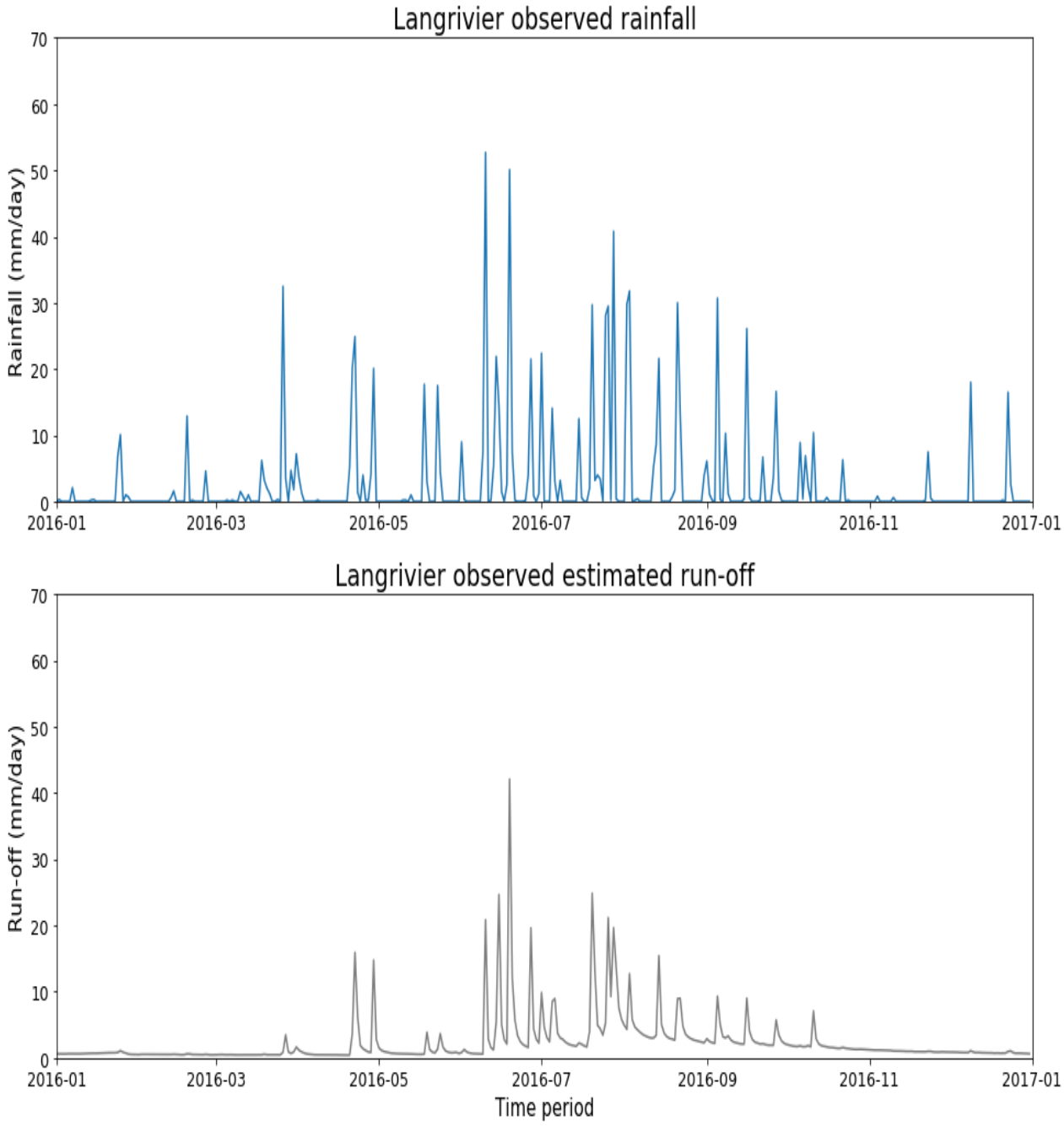

Figure 5.6. Langrivier daily rainfall and run-off in 2016. Maximum rainfall and runoff were 52.7 *mm/day* and 42.09 *mm/day*.

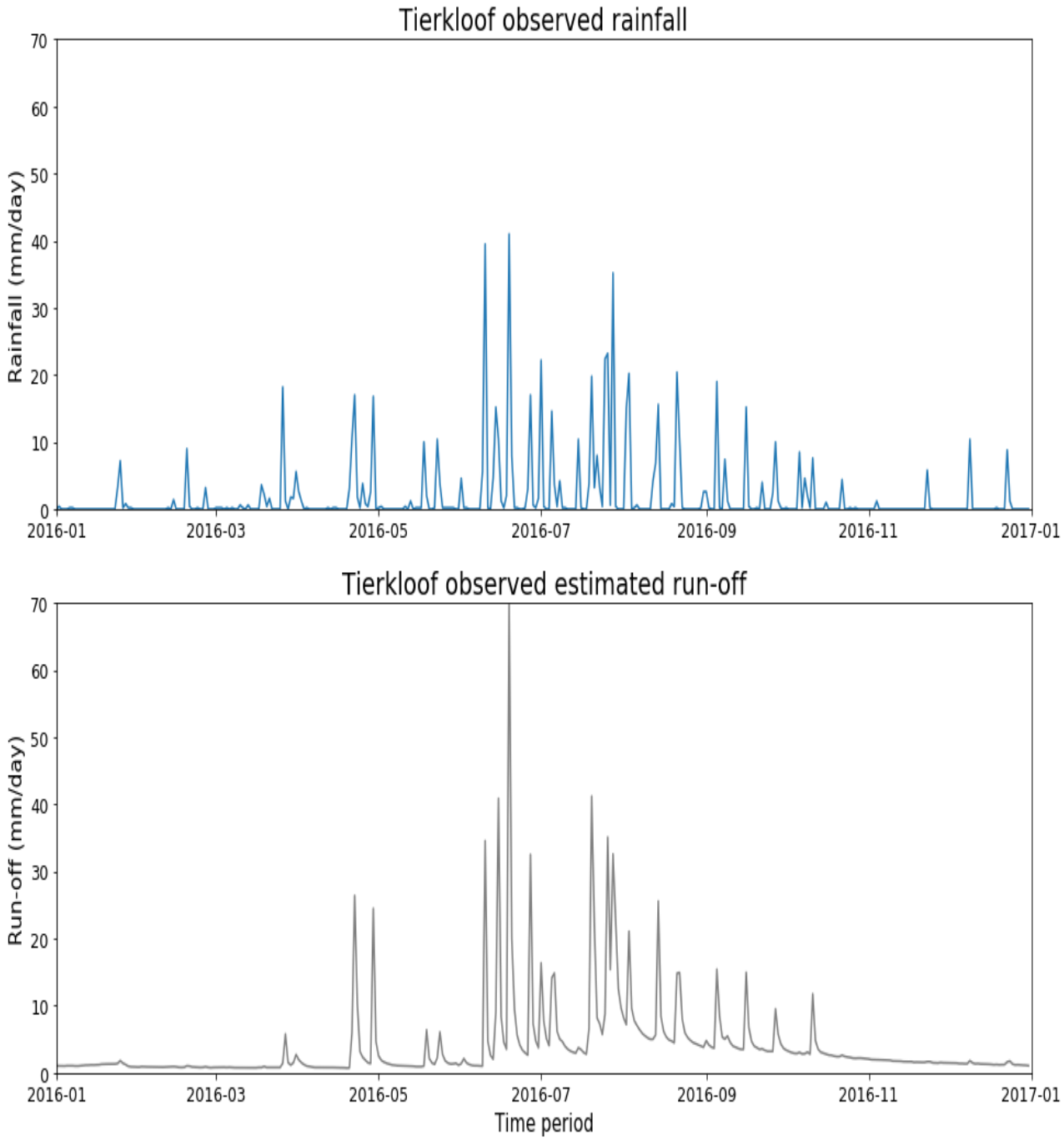

Figure 5.7. Tierkloof hourly rainfall and run-off in 2016. Maximum rainfall and runoff were 41 *mm/day* and 69.79 *mm/day*.

Table 5.2 shows the frequency and magnitude of daily rainfall in Langrivier and Tierkloof during the study period. It is evident from the results obtained these catchments remained dry for more than > 50 % of the year i.e. 249 days in Langrivier and 212 days in Tierkloof. The

total number of rainy days was slightly greater in Tierkloof catchment. Results for this catchment showed that a total of 154 rain days occurred, while in Langrivier only 126 rain days were evident.

Table 5.2. Daily frequency distribution of rainfall (*mm*) and runoff (*mm*) in Langrivier and Tierkloof during the study period between January-December 2016

Magnitude Rainfall (mm)	Occurrence frequency (days)		Magnitude Runoff (mm)	Occurrence frequency (days)	
	Langrivier	Tierkloof		Langrivier	Tierkloof
> 0.2 - 5	78	115	> 0 - 5	332	297
5 - 10	26	14	5 - 10	20	44
10 - 15	8	8	10 - 15	5	8
15 - 20	5	9	15 - 20	4	3
20 – 25	7	5	20 – 25	4	5
25 – 30	6	0	25 – 30	0	2
> 30	6	3	> 30	1	7
Dry	240	212			
Wet	126	154		366	366

Wet and dry relate to days with and without rain respectively. Rainfall occurs when 0.2 mm of rain falls in the catchment.

The frequency and magnitude of rainfall distribution are important to consider when assessing surface water erosion and sediment exported from river systems. From a general point of view, it is evident from the results that the catchments were dominated by low magnitude rainfall (< 5 *mm/day*), while higher magnitude (> 10 *mm/day*) rainfall was less frequent during the study period. The magnitude of rainfall between the two catchments were variable. The most frequent

daily rainfall readings recorded in 2016 were between 0.2 *mm/day* to 5 *mm/day* and 5 *mm/day* to 10 *mm/day*. In Langrivier, these daily values occurred 78 times and 26 times, while in Tierkloof it was 115 times and 14 times respectively. Rainfall magnitudes between 10 *mm/day* to 20 *mm/day*, was greater in Tierkloof occurring 18 times, while in Langrivier it occurred 13 times. Records between *20 mm/day* to 30 *mm/day* and those greater than 30 *mm/*day were more common in Langrivier, occurring 13 times and 6 times respectively. In Tierkloof, 20 *mm/day* to 30 *mm/day* events occurred 3 times, while greater than 30 *mm/day* events only occurred 3 times.

Streamflow totals show a significant difference in the amount of runoff produced per unit catchment area between the two catchments. Results given are totals of 873.9 *mm* at Langrivier weir and 1449.0 *mm* at the Tierkloof weir. Tierkloof had 575.1 *mm* more runoff than Langrivier, which is 65% more runoff. Table 5.1 provides descriptive statistics of run-off estimates during the study period for the two catchments. The runoff production derived from the v-notch weir in the Langrivier varied from 0.43 *mm/day* to a maximum of 42.09 *mm/da*y having a mean of 2.39 *mm/day* and a standard deviation of 4.07 *mm/day*. Tierkloof the minimum and maximum values were 0.71 *mm/day* and 69.79 *mm/day* respectively, with a mean of 3.96 *mm/day,* and a standard deviation of 6.74 *mm/day*. The correlation matrix performed of run-off indicated a strong positive correlation between the two catchments.

Table 5.2 shows the frequency and magnitude of run-off distribution for the Langrivier and Tierkloof catchments. It is evident from these results that both catchments were dominated by lower magnitude streamflow, while higher magnitude run-off was less common during the study period. The magnitude of run-off peaks between the two catchments was highly variable. The most frequent daily runoff estimates in 2016 were between 0.2 *mm/day* to 5 *mm/day* and 5 *mm/day* to 10 *mm/day*. In Langrivier, these daily values occurred 332 times and 20 times, while in Tierkloof it was 297 times and 44 times respectively. Runoff magnitudes between 10 *mm/day* to 20 *mm/day*, was greater in Tierkloof occurring 11 times, while in Langrivier it occurred 9 times. Records between 20 *mm/day* to 30 *mm/day* and those greater than 30 *mm/day* were more common in Tierkloof, occurring 7 times and 7 times respectively. In Langrivier, 20 *mm/da*y to 30 *mm/day* events occurred 4 times, while greater than 30 *mm/day* events only occurred 1 time.

Table 5.3. Summary statistics of soil loss (*mm* per plot) during sample period and factors influencing its variability for sampled plots in Langrivier.

Statistics	Vegetation			Soil	Topography					
	NDVI	Vegetation cover (%)	Stem density (%)	Median grain size (mm)	Elevation (m)	Slope (degrees)	Aspect	LS USPED	Flow accumulation (m^2)	Soil loss *(mm)*
count	14	14	14	14	14	14	14	14	14	14
mean	0.25	32.26	0.08	0.49	494.71	20.85	205.64	12.07	13.55	5.6
standard deviation	0.04	10.02	0.06	0.23	82.33	8.24	71.11	5.28	15.22	2.09
minimum	0.18	21.00	0.02	0.17	390.00	6.00	112.00	3.00	2.30	3.00
25%	0.23	25.25	0.04	0.30	456.25	15.75	144.00	8.50	5.55	4.13
50%	0.25	28.00	0.06	0.49	462.50	23.00	183.50	12.00	7.30	5.06
75%	0.29	39..75	0.10	0.60	563.00	25.50	277.50	14.75	14.75	6.81
maximum	0.32	53.00	0.23	0.97	635.00	36.00	313.00	20.00	50.20	10.08

Table 5.4. Summary statistics of soil loss (*mm* per plot) during sample period and factors influencing its variability for sampled plots in Tierkloof.

Statistics	Vegetation			Soil	Topography					
	NDVI	Vegetation cover (%)	Stem density (%)	Median grain size (mm)	Elevation (m)	Slope (degrees)	Aspect	LS USPED	Flow accumulation (m^2)	Soil loss *(mm)*
count	13	13	13	13	13	13	13	13	13	13
mean	0.24	30.23	0.24	0.59	442.69	16.38	236.23	10.15	26.75	8.21
std	0.05	17.84	0.25	0.10	103.86	7.12	35.88	4.08	23.06	4.72
min	0.13	4.00	0.01	0.47	302.00	6.00	180.00	3.00	3.00	2.64
25%	0.23	16.00	0.09	0.50	358.00	10.00	205.00	7.00	8.80	4.04
50%	0.24	25.00	0.10	0.58	447.00	18.00	244.00	11.00	16.70	9.00
75%	0.27	48.00	0.47	0.63	561.00	23.00	261.00	13.00	42.10	10.84
max	0.29	63.00	0.78	0.80	576.00	27.00	289.00	16.00	70.10	15.76

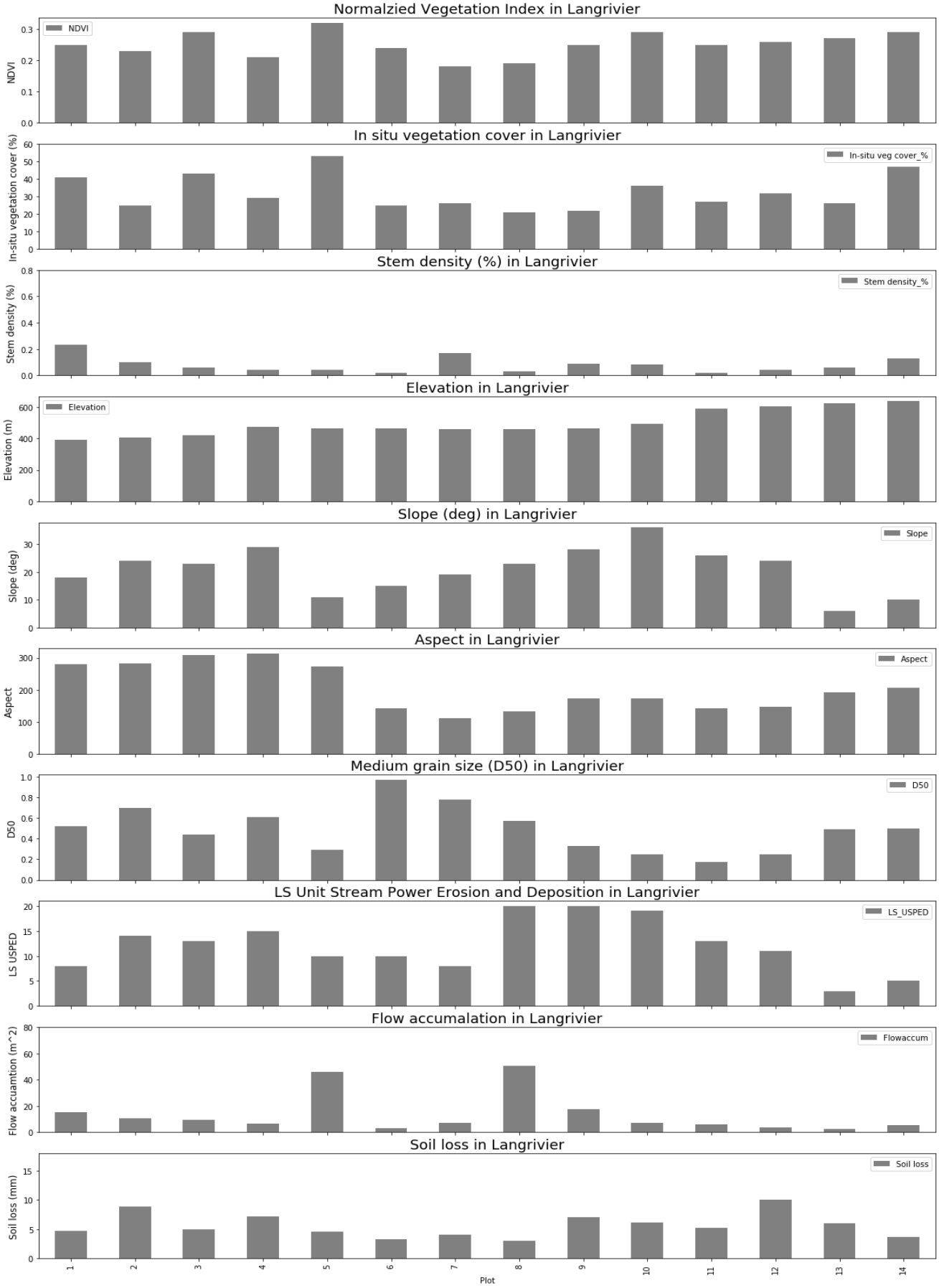

Figure 5.8. Soil loss and characteristics of sampled plots in Langrivier.

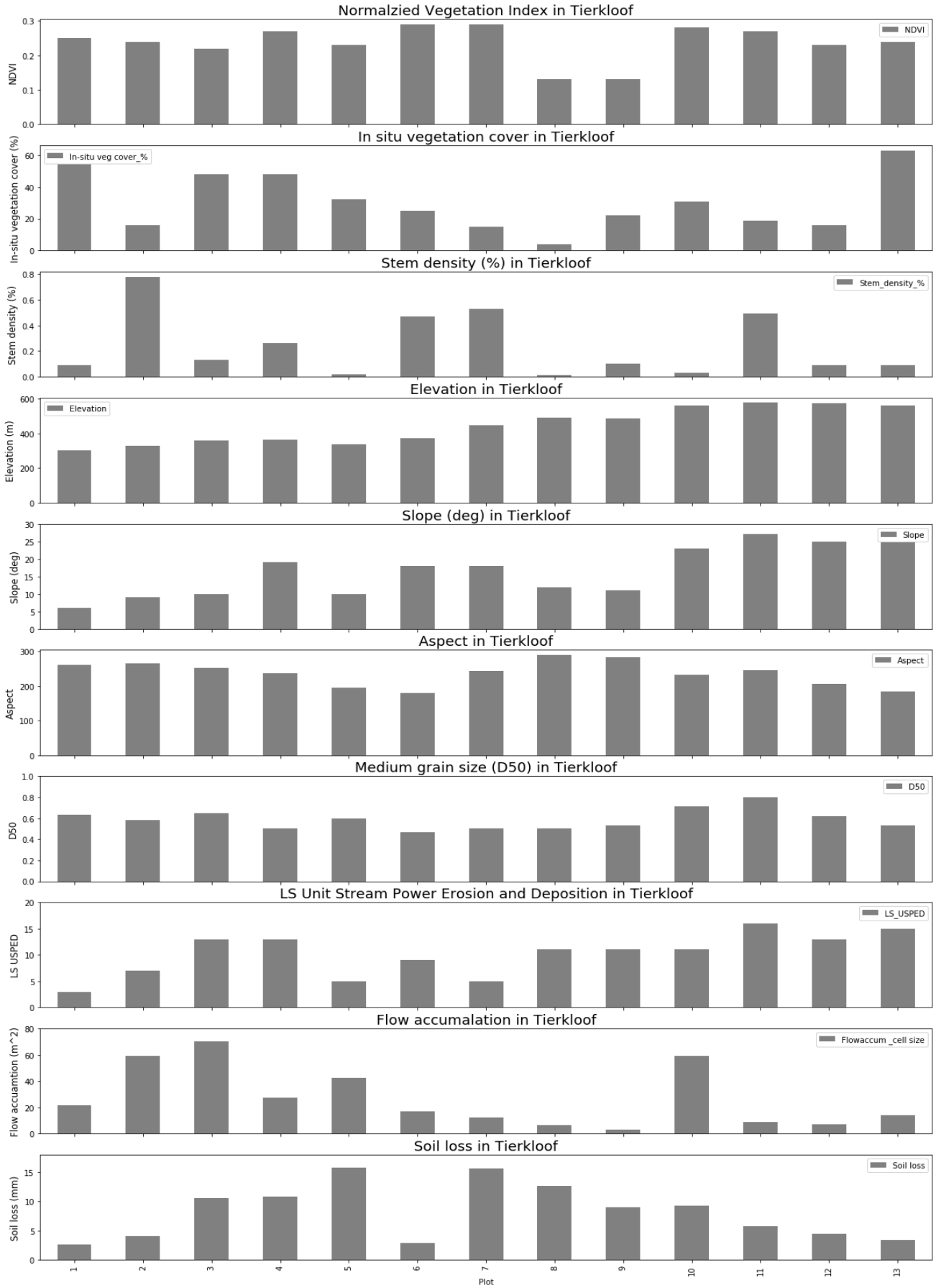

Figure 5.9. Soil loss and characteristics of sampled plots in Tierkloof.

5.7.2. Relationship between average soil loss from erosion pins and factors affecting its variability.

5.7.2.1. Average soil loss from erosion pin plots in Langrivier and Tierkloof.

The average soil loss from each plot within Langrivier and Tierkloof for the study period is shown in Figure 5.8, 5.9 and 5.10. It is evident that soil loss was highly variable across the two catchments. In Langrivier the maximum and minimum plot soil losses were 10.08 *mm* (120.96 *tons/ha*) and 3.00 *mm* (36 *tons/ha*) respectively. The plot with the highest soil loss occurred in the upper section of the catchment (plot 12), while the lowest loss came from plot 8, which is located approximately midway in the catchment. In Tierkloof, the maximum and minimum plot losses were 15.76 *mm* (189.12 *tons/ha*) and 2.64 *mm* (31.68 *tons/ha*) respectively. These plots are located at the bottom (plot 1, lowest) and midway in the catchment (plot 5, highest). The average plot soil loss from the Langrivier catchment was 5.6 *mm* (67.2 *tons/ha*), with a standard deviation of 2.09 *mm* (25.08 *tons/ha*), while Tierkloof had an average loss of 8.20 *mm* (98.4 *tons/ha*) and a standard deviation of 4.72 *mm* (56.64 *tons/ha*). Summary statistic is shown in Table 5.3 and Table 5.4 respectively.

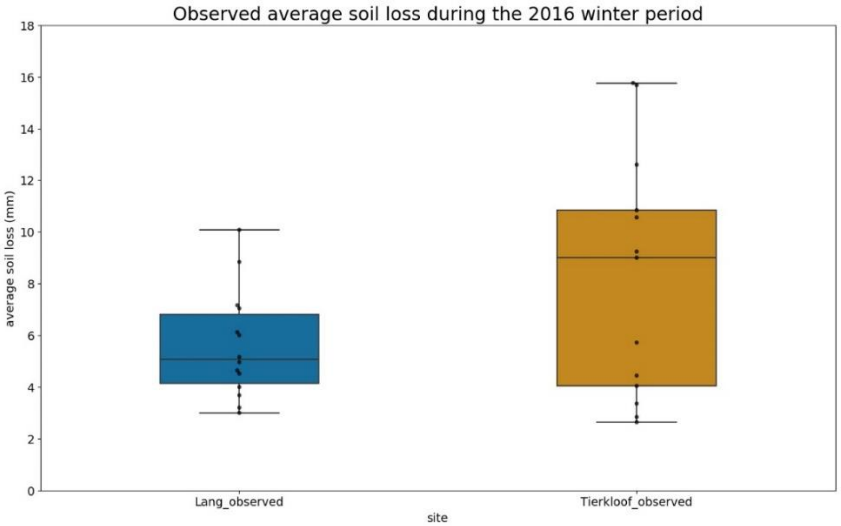

Figure 5.10. Average soil losses from each plot in the Langrivier and Tierkloof catchments over the study period. Maximum values were 15.76 *mm* and 10.08 *mm* for Tierkloof and Langrivier, while the minimum losses were 2.64 *mm* and 3.00 *mm* respectively.

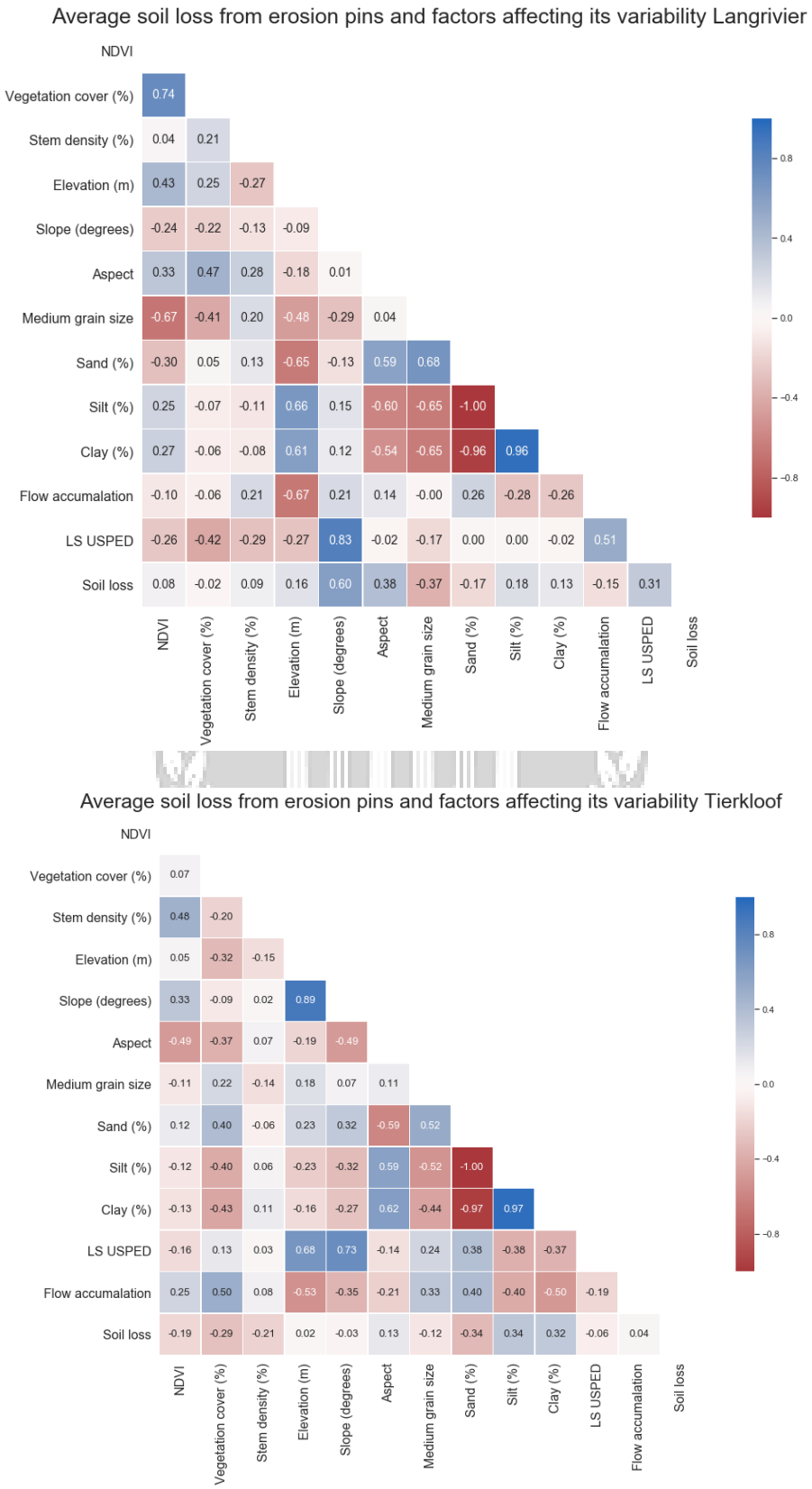

Figure 5.11. Correlation matrix of predictor variables and soil loss estimates from erosion pin plots.

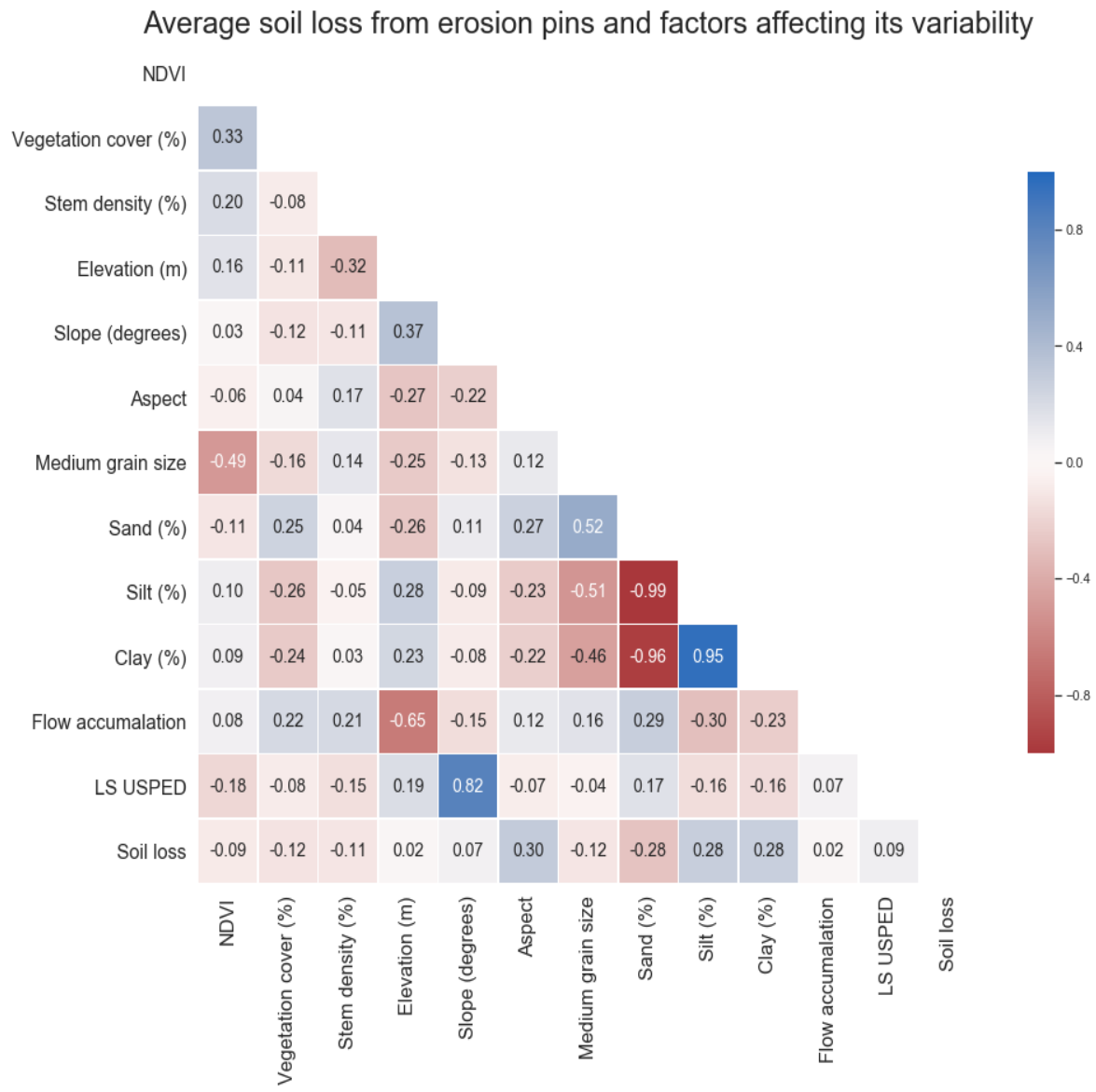

Figure 5.12. Lumped correlation matrix of predictor variables and soil loss estimates from erosion pin plots.

5.7.2.2. Vegetation characteristics and its influence on surface soil loss.

5.7.2.2.1. Estimates derived from the Normalized Vegetation Index (NDVI).

Summary statistics illustrate that the NDVI estimates derived from Sentinel 2 satellite imagery acquired 17 January 2016 for the Langrivier varied from 0.18 to 0.32, having a range of 0.14

with a mean of 0.25, standard error of 0.01 and a standard deviation of 0.04 (Table 5.3). The results obtained were slightly different in the Tierkloof catchment. Estimates in Tierkloof varied from 0.13 to 0.29 having a range of 0.16 with a mean, standard error and standard deviation of 0.24, 0.02 and 0.05 respectively (Table 5.4). These low values seem to be consistent with field observations at the time of plot set up. Based on visual inspection, surfaces of the two catchments were covered with tree stumps having no sprouts and regrowth of understory shrubs and grasses. In the early stages however, understory cover was heterogeneously spaced increased over the study period. From this, it is logical to think that initially surfaces had limited protection from raindrop impact and overtime gained some protection against the drag forces created by overland flow from the understory of grasses and shrubs. The relationship between NDVI and average soil loss from erosion plots show contrasting results. In Langrivier there was a 10 % (Rs = 0.1, p = 0.8) weak positive correlation, whereas there was a 20 % (Rs = -0.2, p = 0.5) weak negative relationship between NDVI and average soil loss in Tierkloof (Figure 5.11). When the results across the catchments were lumped together, the existed a 9% weak negative relationship across the catchment, Figure 5.12. The result obtained in Tierkloof is consistent to what has been reported by several others i.e. generally soil loss increases with decreasing vegetation cover.

5.7.2.2.2. In situ vegetation cover and stem density estimates.

To determine whether NDVI was able to represent in-situ vegetation density, the Spearman correlation was used (Figure 5.11, Table 5.5 and Table 5.6). The results showed a statistically significant relationship between in-situ cover and NDVI in Langrivier, Rs = 0.76, p = 0.05 with very weak positive relationship in Tierkloof, Rs = 0.27 p = 0.8. Lumped correlation results in Figure 5.12 indicate that there exists a moderately positive relationship between in-situ cover and NDVI (33%). Because of the statistically significant relationship between NDVI and in-situ estimates, NDVI can be used to capture estimates over a larger area. As a result, in-situ and NDVI measurements were used as predictor variables for soil loss. Results of in-situ vegetation cover derived from 0.8 m x 0.8 m plots in Langrivier varied from a low of 21 % to a density of 53 % having range of 31 % with a mean of 32 % and a standard deviation of 10%. In Tierkloof, the lowest cover was 4 % and the highest cover was 63 %. The mean and standard deviation for these plots were 30 % and 18 % respectively. The correlation matrix in Figure 5.11 and Table 5.5 shows a small weak negative correlation between in-situ vegetation cover

and soil loss. In Langrivier *Rs* = -0.02, *p* = 0.8, while *Rs* = -0.29, *p* = 0.5 was found in Tierkloof. This contrast in finding between in-situ cover and average sediment flux is similar to what was found with the NDVI estimates. When the results of the two catchments were lumped together, results indicate a smaller weak negative relationship between soil loss and in-situ cover (Figure 5.12).

Results on stem density show that Langrivier had a minimum stem density of 0.02 % and a maximum of 0.23 %, with a mean and standard deviation of 0.08 % and 0.06 respectively. The result varied from a low of 0 to a high of 1 %, with a mean and standard deviation of 0.24 % and 0.25 % in Tierkloof. Similar to in-situ cover, stem density showed a weak negation relationship with soil loss, *Rs* = -0.12, *p* = 0.8 in Langrivier and *Rs* = -0.22, *p* = 0.5 was found in Tierkloof. Lumped results show similar weak negative relationship between soil loss as stem density. With respect to the relationship between in-situ cover and stem density, there was weak positive correlation in Langrivier (*Rs* = 0.22, *p* = 0.8), while in Tierkloof there was a moderate positive correlation (*Rs* = 0.45, *p* = 0.5). Lumped results indicate a weak negative relationship between in-situ cover and stem density.

5.7.2.3. Soil properties and its influence on soil loss.

5.7.2.3.1. Influence of medium grainsize distribution.

The summary statistics illustrate that the median grainsize (D50) fraction from the particle size distribution analysis varied from 0.17 *mm* to 0.97 *mm* across the sample plots in Langrivier, having a range of 0.80 *mm* with a mean of 0.49 *mm*, standard error of 0.06 *mm* and a standard deviation of 0.04 *mm* (Table 5.3). For Tierkloof, Table 5.4 shows that the results obtained varied from 0.47 *mm* to 0.80 *mm*, having a range of 0.33 *mm*, and a mean and standard deviation of 0.59 *mm* and 0.10 *mm* respectively.

The distribution of soil types can be seen in Figure 5.13 for Langrivier and Tierkloof respectively. Results of soil texture analysis showed three main soil types; fine sand, loamy

fine sand and sandy loam, with the dominant type across both catchments being fine sand. Loamy fine sand was found more often in the Tierkloof plots compared to Langrivier.

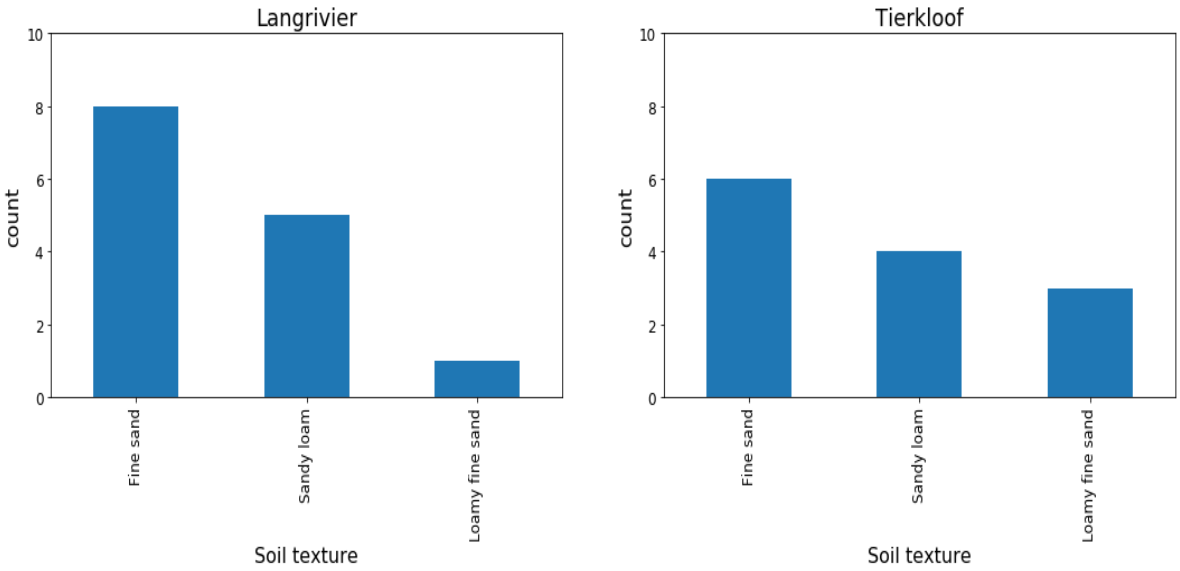

Figure 5.13. Shows the variation in soil type for the Langrivier and Tierkloof sample plots. The dominant texture class was fine sand.

The correlation matrix indicates that there exists a negative relationship between soil loss and median grainsize distribution (Figure 5.11 and Table 5.5). Median grainsize or D50 is used to characterise particle size, which is the particle diameter at 50% in the cumulative distribution. To describe the strength of association between soil loss and grain size, the Spearman correlation was used and indicates a moderate negative correlation, resulting correlation: Rs = -0.37, p = 0.2 in Langrivier and Rs = -0.2, p = .7 in Tierkloof. This means that soil loss reduces with increasing grain size in the two catchments. The relationship between soil loss and median grainsize distribution is in agreement with this weak negative relationship (Figure 5.12). To determine whether grainsize can be used as a predictor for soil loss in these catchments, a regression analysis was done. For Langrivier this indicated a weak negative relationship between grain size and soil loss (R^2 = 0.1, Figure 5.14), however not in Tierkloof (Table 5.6). From the regression results this means that for every unit of increase in grain size, soil loss would decrease by -2.3 m^3. However, only 10 % of the variance in sediment loss can be explained by grainsize distribution in this catchment. Correlation and regression analysis for

the Tierkloof catchment remained insignificant and are not reported however, results can be seen in Table 5.5 and Table 5.6.

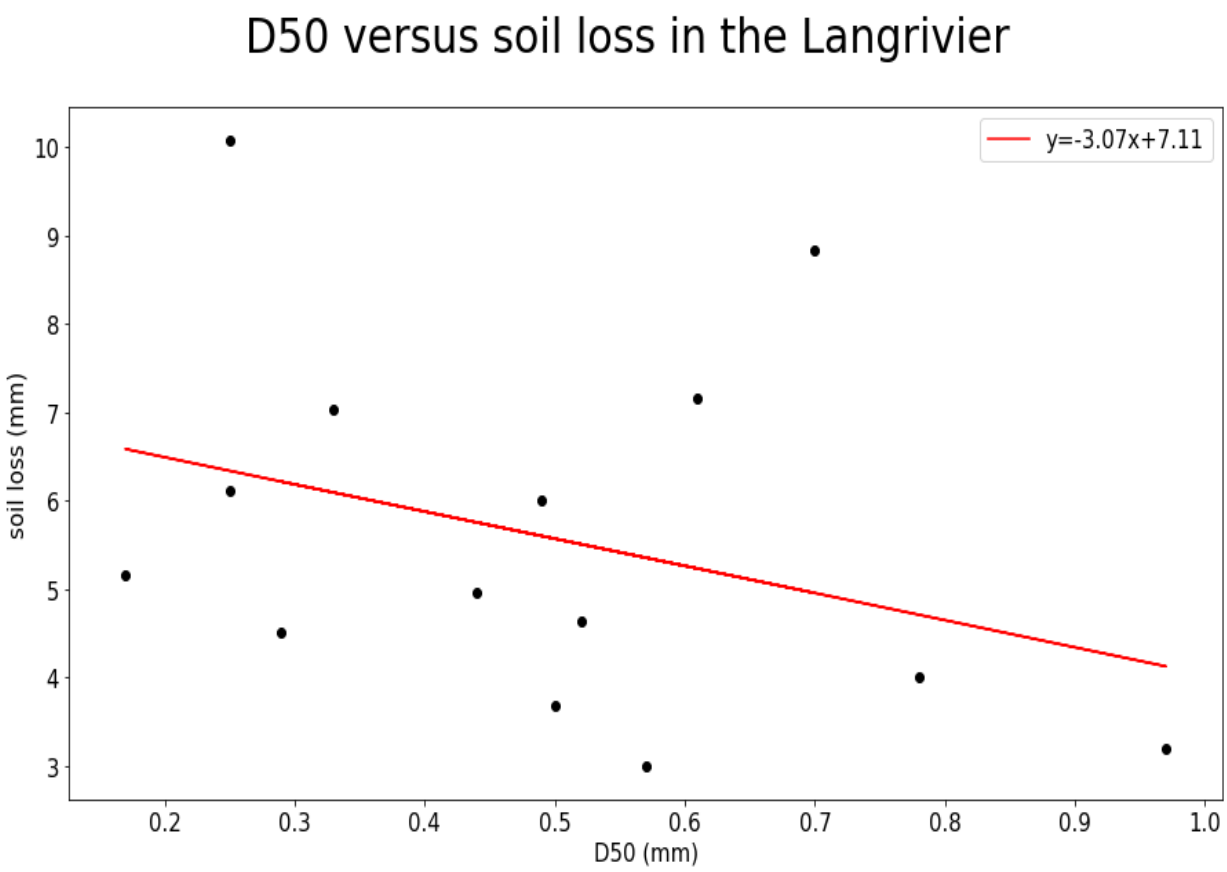

Figure 5.14. Regression analysis using median grain sizes as a predictor of soil loss in Langrivier. The graph shows that a weak negative relationship exists, $R^2 = 0.1$.

5.7.2.4. Topographic influences and its influence on soil loss.

5.7.2.4.1. Influence of slope on soil loss.

In Langrivier, data on slope derived from the 10 m SUDEM varied from 6° to angles of 36°, having a range of 30° with a mean and standard deviation of 21.5° and 8° respectively. Results were slightly different in the Tierkloof catchment. Here, the minimum and maximum slope angles were 6 ° to 27 ° respectively, with a mean of 16 ° and a standard deviation of 7°. The correlation between slope and soil were different between the two catchments. For Langrivier (*Rs* = 0.6, *p* = 0.02) a strong positive correlation was found, whereas in Tierkloof (*Rs* = - 0.03,

p = 0.9) low negative relationship. Figure 5.15 shows an increase in soil loss with slope in Langrivier, r^2= 0.2. Table 5.5 and Table 5.6 shows the results of soil loss and slope.

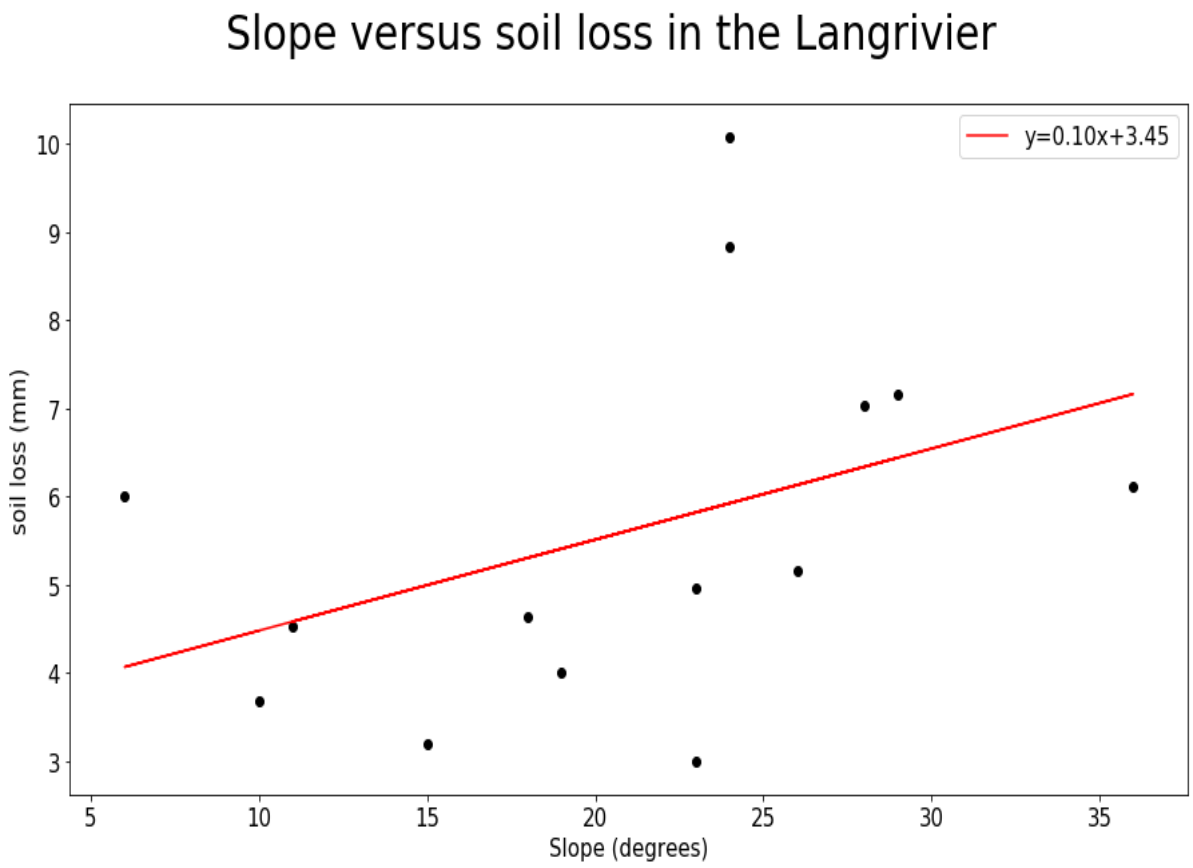

Figure 5.15. Regression analysis using slope as a predictor of soil loss in Langrivier. The graph shows a weak positive relationship exists, $R^2 = 0.2$.

5.7.2.4.2. Influence of elevation on soil loss.

Summary statistics on remote sensing derived elevation data show that the lowest plot in the Langrivier catchment is at 390 *m*, while in Tierkloof the lowest plot is situated at 302 *m*. The maximum plot elevation in Langrivier is 635 *m*, having a range of 245 *m* with a mean of 495 *m*, standard error of 22 *m* and a standard deviation of 82 *m*, whereas Tierkloof plots only reach an elevation of 576 *m*, having a range of 274 *m*, with a mean of 443 *m*, standard error of 21 *m* and a standard deviation of 104 *m*. The correlation (Table 5.5 and Figure 5.11, 5.12) matrix

and trend analysis (Table 5.6) show that there is a very weak positive relationship between elevation and sediment flux in both Langrivier and Tierkloof.

5.7.2.4.3. Influence of flow accumulation on soil loss.

In Langrivier, flow accumulation at the sampled plots, as derived from a 10 m SUDEM, varied from 2.3 m^2 to as high as 50.20 m^2, with a mean of 13.55 m^2, standard error of 4.07 m^2 and standard deviation of 15.22 m^2. In Tierkloof the results for the sample plots varied from as low as 3.00 m^2 to as high as 70.10 m^2, with a mean of 26.75 m^2, standard error of 6.40 m^2 and a standard deviation of 23.06 m^2. As seen in Figure 5.11 the correlation matrix shows a weak negative correlation between surface sediment flux and flow accumulation in Langrivier (*Rs* = - 0.34, *p* = 0.6), while there was a weak but positive relationship in Tierkloof (*Rs* = 0.13, *p* = 0.6). Figure 5.16 show the negative trend in Langrivier.

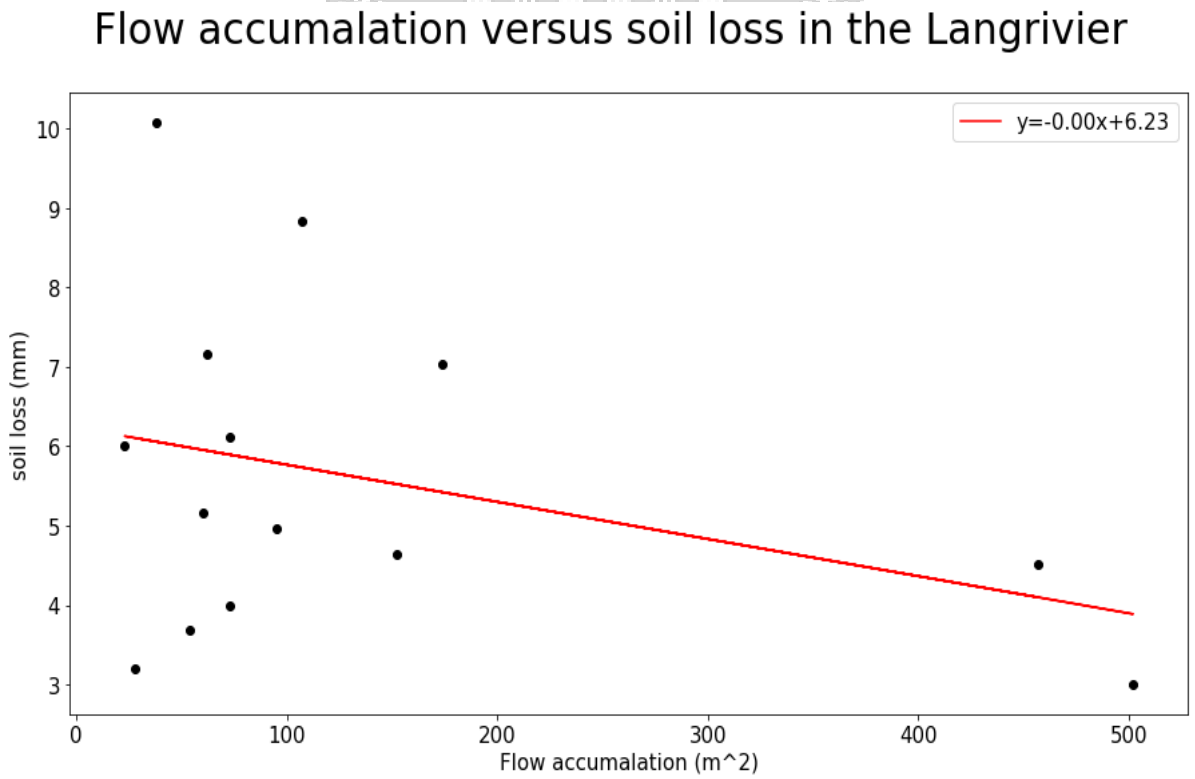

Figure 5.16. Regression analysis using flow accumulation as a predictor of soil loss in Langrivier. The graph shows a weak negative relationship exists, $R^2 = 0.1$.

5.7.2.4.4. Influence of LS USPED on soil loss.

The summary statistics on remote sensing derived LS USPED data show that the minimum value recorded for the sampled plots in Langrivier was 3 and a maximum of 20, with a mean of 12.1 and a standard deviation of 5.3 (Table 5.4). There was a small positive correlation between soil loss from Langrivier plots and LS USPED as seen in Figure 5.17 and Table 5.4. The results indicate that as the LS USPED factor increases, sediment flux increases. This relationship between soil loss and LS USPED was reported by several authors including Sharma. (2010). Similarly, this finding demonstrates the influence of slope and vegetation i.e. generally given a threshold slope, the soil surface with little protection from vegetation would experience more erosion in comparison to the same surface with a higher density of vegetation cover. In contrast, the relationship was negative in Tierkloof. In Tierkloof the minimum and maximum LS USPED estimated was 3 and 16 respectively, and a mean and standard deviation of 10.2 and 4.1 (Table 5.5).

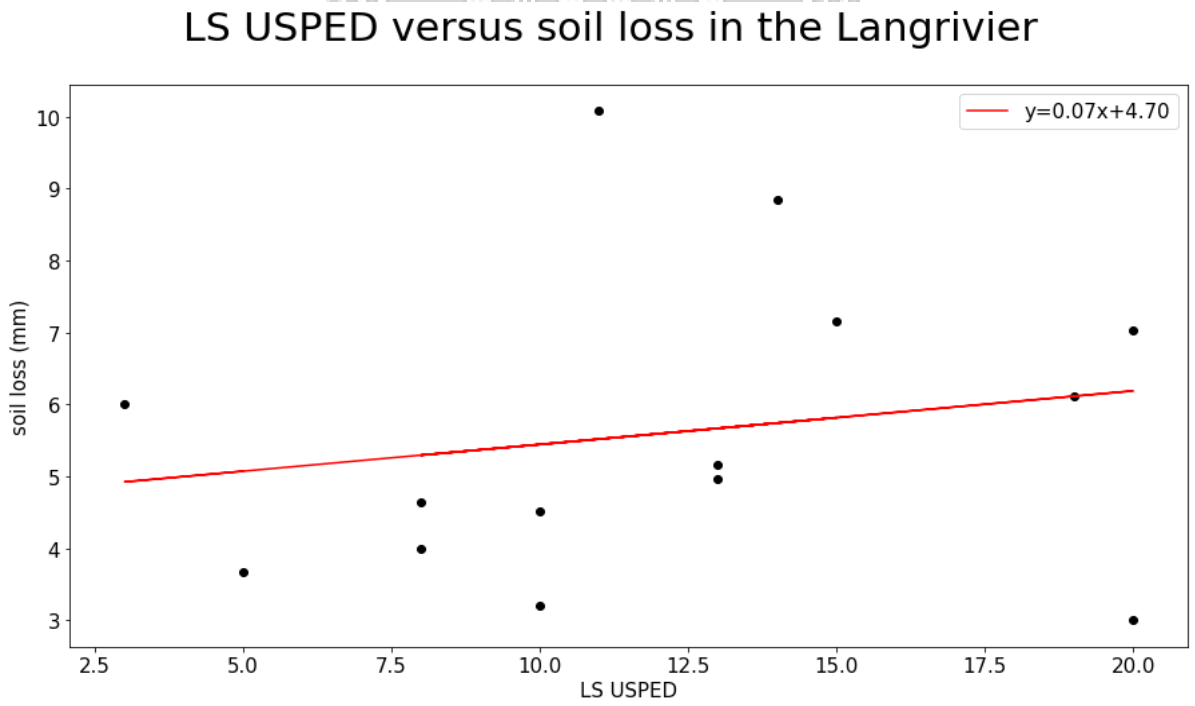

Figure 5.17. Regression analysis using LS USPED (Unit Stream Power Erosion and Deposition) as a predictor of soil loss in Langrivier. The graph shows a weak positive relationship exists, $R^2 = 0.2$.

5.7.3. Exported sediment and suspended sediment concentration.

5.7.3.2. Suspended sediment concentration.

The results obtained from hourly grab samples and discharge measurements are illustrated in Figure 5.18 and Figure 5.19. Stream discharge estimates for the duration of the sampled event in Langrivier varied from as low as 1119600 *l/hr* to as high as 4863600 *l/hr* with a mean of 226285 *l/hr* and a standard deviation of 1001965. The total hourly sediment concentration varied from 0.001 g/l to 0.012 g/l with a mean of 0.0044 g/l and a standard deviation of 0.004561. In Tierkloof stream discharge estimates varied from 361440 *l/hr* to 1824840 *l/hr* with a mean of 778695 *l/hr* and standard deviation of 386815.8, while the total hourly sediment concentration varied from as low as 0.01 g/l to 0.026 g/l with a mean of 0.0096 g/l and a standard deviation of 0.011675.

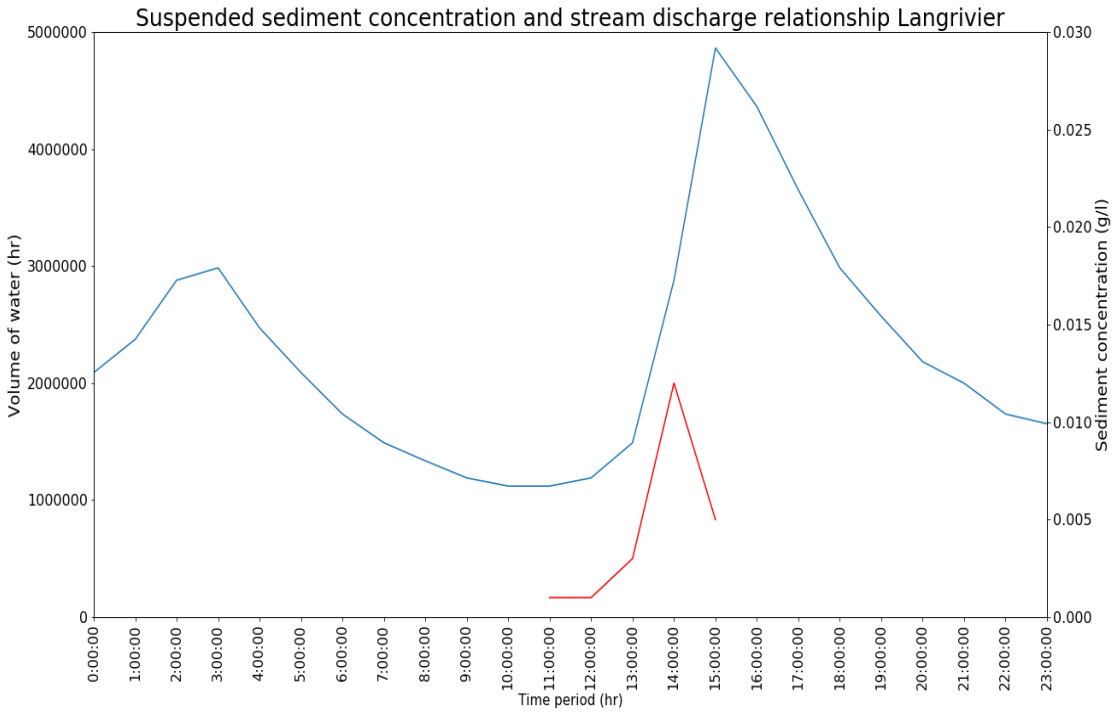

Figure 5.18. Sediment-discharge relationship. In Langrivier sediment concentration increases rapidly with stream discharge. The maximum concentration was 0.012 g/l.

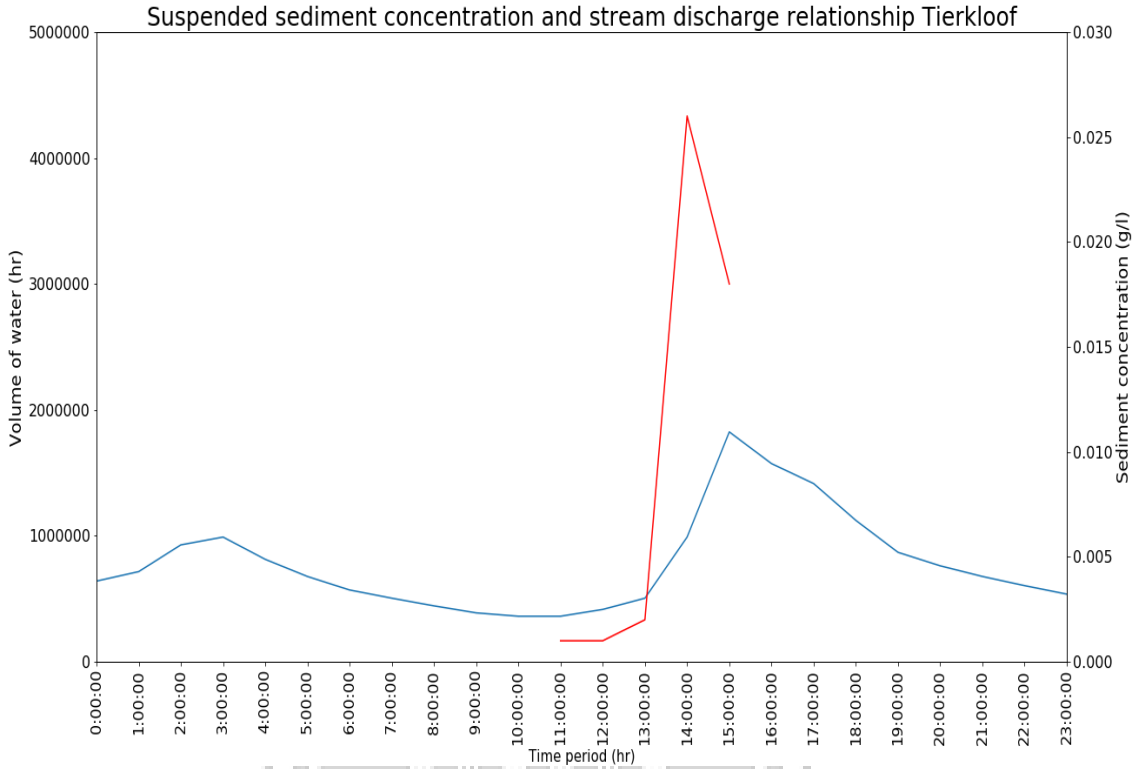

Figure 5.19. Sediment-discharge relationship. In Tierkloof shows a gradual increase in stream discharge with a relatively steep increase in sediment concentration. The maximum concentration was 0.026 g/l.

Generally, the graph seems to show that the concentration of sediment increases with discharge volumes, but with slightly different trends and magnitude. Additionally, there exists a lag difference between peak sediment concentration and peak flow. For example, peak sediment discharge occurred at 14:00, while peak stream discharge occurred at 15:00 where sediment concentration starts to decrease in both catchments. However, the drop-in concentration is much more rapid in Langrivier than the gradual drop in Tierkloof. At 14:00 Langrivier had a total flow volume of 2878920 *l/hr* with a sediment concentration of 0.012 g/l, whereas in Tierkloof the flow volume at this time was 990000 *l/hr* with a sediment concentration of 0.026 g/l. At 15:00, flow increased to 4863600 *l/hr* and 1824840 *l/hr*, while sediment load decreased to 0.005 *g/l* and 0.018 g/l in Langrivier and Tierkloof respectively. Peak sediment discharge was higher in Langrivier compared to Tierkloof. In Langrivier, peak sediment discharge was 34547.04 *g/hr* with and average sediment discharge over the sample period of 13128.84 *g/hr*.

For Tierkloof, peak sediment discharge was 32847.12 *g/hr* with an average sediment discharge of 12074.69 *g/hr*. However, once normalized by catchment area total sediment discharge for the duration of the storm event was higher with a value of 389.51 *g/ha* in Tierkloof, compared to 255.42 *g/ha* in Langrivier.

The relationship was significant when fitting a second order polynomial regression curve, which shows a non-linear relationship between sediment concentration and stream discharge within the two catchments. The results of the polynomial graphs were $y = -0.0001x^2 + 0.1927x - 52.712$ ($R^2 = 0.9138$) for Langrivier and $y = -0.0002x^2 + 0.1367x - 13.129$ ($R^2 = 0.9713$) in Tierkloof. The results of the Spearman correlation tests revealed statistically significant sediment-discharge relationships. To describe the strength of association between stream discharge and sediment concentrations, the test indicated that there exists a statistically significant positive correlation at a significance level of $p = .05$ in Langrivier, $Rs = 0.9$ at $p = 0.37$ and Tierkloof, $Rs = 0.9$ at $p = 0.37$. In addition, multi-collinearity exists for stream discharge between the two catchments, which was statistically significant $Rs = 1$ at $p = 0.01$. However, this was not the case for sediment discharge, $Rs = 0.8$ at $p = 0.104$.

5.7.3.1. Sediment export

The results obtained from suspended sediment samplers for the Langrivier and Tierkloof catchments represents a quantitative relative indicator of the mass of suspended sediment exported over a 6-month period in the two catchments. It should be noted that the amount retained in the samplers over this period may be the combined input of eroded material from the catchment surface and in-channel supply. However, due to the nature of bed morphology, mostly boulders and very coarse sediment, it is assumed that there was minimal contribution from instream sediment supply. When normalized by catchment area, results indicated that the sampled sediment export normalized by catchment area from the Langrivier was 0.21 *g/ha* and in Tierkloof 0.36 *g/ha*. When rock cover was excluded from calculations of catchment area, results indicate that Tierkloof exported nearly double the amount of sediment per unit area in Langrivier of the 6-month period. In Langrivier, the area normalised export caught by the samplers was 0.36 *g/ha* over 6-months, while in Tierkloof it was 0.62 *g/ha*.

Table 5.5. Summary of outcome of correlation analysis on variables measured.

Variables	Langrivier		Tierkloof		Catchment vs Catchment
	Result	**Comment**	**Result**	**Comment**	
TERRAIN					
Elevation + soil loss	*Rs = 0.16, p = 0.6*	Weak positive relationship, statistically insignificant	*Rs = 0.02, p = 0.9*	Very weak positive relationship, statistically insignificant	Soil loss increase with elevation in Langrivier, but results are insignificant.
Slope + soil loss	***Rs = 0.6, p = 0.02***	Strong positive relationship, statistically significant	*Rs = - 0.03, p = 0.9*	Very weak (or no) negative correlation, statistically insignificant	Soil loss increases with slope in both Langrivier, and Tierkloof but more significant in Langrivier.
Aspect + soil loss	*Rs = 0.3, p = 0.2*	Moderate positive relationship, but statistically insignificant	*Rs = 0.1, p = 0.7*	Weak positive relationship, statistically insignificant	Aspect influences soil loss in both catchments, but results are insignificant
Flow accumulation + soil loss	***Rs = -0.2, p = 0.6***	Weak negative relationship, but statistically insignificant	*Rs = 0.04, p = 0.9*	Very weak relationship, but statistically insignificant	Opposite trend, negative in Langrivier and positive in Tierkloof, but results insignificant
LS USPED + soil loss	***Rs = 0.31, p = 0.1***	Weak positive relationship	*Rs = 0.04, p = 0.9*	Very weak positive relationship	Similar trend, but more dominant in Langrivier
SOIL					
Medium grainsize + soil loss	**Rs = - 0.4, p = 0.2**	Moderate negative relationship, but statistically insignificant	*Rs = -0.2, p = 0.7*	Weak negative relationship, but statistically insignificant	Same trend in each catchment, with greater influence in Langrivier, but results insignificant
VEGETATION					
NDVI + in-situ cover	***Rs = 0.8 p = 0.01***	Strong positive relationship, statistically significant	*Rs = 0.09, p = 0.8*	Very weak positive correlation, statistically insignificant	NDVI is a good predictor of in situ cover in Langrivier, but not in Tierkloof
NDVI + soil loss	***Rs = 0.2, p = 0.8***	Weak positive relationship, statistically insignificant	*Rs = -0.2, p = 0.5*	Weak negative relationship, statistically insignificant	Opposite trend between Langrivier and Tierkloof, both weak and insignificant
Stem density + soil loss	*Rs = 0.1, p = 0.8*	Weak positive relationship, statistically insignificant	*Rs = -0.2 p = 0.5*	Weak negative relationship, statistically insignificant	Opposite trend between Langrivier and Tierkloof, both weak and insignificant

Table 5.6. Summary of outcome of trend analysis on variable measured

Variable	Langrivier		Tierkloof		Catchment vs Catchment
	Result	Comment	Result	Comment	
TERRAIN					
Elevation + soil loss	r^2 = 0.02 y = 0.0024x + 3.0191	No relation	r^2 = 0.01 y = -0.0035x + 7.719	No relation	Elevation is an insignificant predictor of soil loss in both catchments
Slope + soil loss	**r^2 = 0.2** **y = 0.10x + 3.45**	Positive relation	r^2 = 0.041 y = -0.1006x + 7.805	No relation	Slopes in Langrivier catchment contribute to soil loss but remains insignificant in Tierkloof
Aspect + soil loss	r^2 = 0.042 y = 0.0045x + 3.2706	No relation	r^2 = 0.045 y = 0.0218x + 0.9983	No relation	Aspect is an insignificant predictor of soil loss in both catchments
Flow accumulation + soil loss	**r^2 = 0.1** **y = -0.0035x + 6.23**	Positive relation	r^2 = 0.02 y = 0.002x + 5.6331	No relation	Flow accumulation contribute to soil loss but remains insignificant in Tierkloof
LS USPED + soil loss	**r^2 = 0.2** **y = 0.07x + 4.70**	Positive relation	r^2 = 0.05 y = -0.1787x + 7.9714	No relation	LS UPED contributes to soil loss but remains insignificant in Tierkloof
SOIL					
Medium grainsize + soil loss	**r^2 = 0.1** **y = -3.07x + 7.11**	Positive relation	r^2 = 0.03 y = -6.0616x + 9.71	No relation	Medium grainsize contribute to soil loss but remains insignificant in Tierkloof
VEGETATION					
NDVI + in-situ cover	**r^2 = 0.6** **y = -2.3037x + 5.3305**	Positive relation	r^2 = 0.1 y = 92.872x + 8.3101	Positive relation	In-situ cover predicted NDVI estimates in both catchments.
NDVI + soil loss	**r^2 = 0.003** **y = 2.1809x + 3.6517**	No relation	r^2 = 0.04 y = -12.684x + 9.1524	No relation	NDVI is an insignificant predictor of soil loss in both catchments
Stem density + soil loss	r^2 = 0.02 y = -3.1982x + 4.4528	No relation	r^2 = 0.05 y = -3.0605x + 6.8861	No relation	Stem density is an insignificant predictor of soil loss in both catchments

5.8. Discussion

5.8.1. Impact of rainfall.

The rainfall pattern experienced during 2016 was typical of Mediterranean-type mountainous environments, with 80% of the rain concentrated during the winter months between March and October (Scott, 1995). However, the 2016 period was a relatively dry year compared to previous years as reported by others. Wicht et al., (1967) analysed historical data of the Langrivier catchment and found a mean annual rainfall of 1838 *mm/yr*. over a 10-year period for the same rain gauge in Langrivier. In 2016 the total rainfall amount in Langrivier was 971.8 *mm* and 708.3 *mm* in Tierkloof.

The total amount of rainfall received during 2016 was significantly different between the two study catchments, where 37% more rain occurred in Langrivier in comparison to Tierkloof. However, results indicate that there were more days with rain in Tierkloof (154 wet days) relative to Langrivier (124 wet days). This equates to a total number of 30 days with low magnitude rainfall in Tierkloof. This means that Langrivier experience large amounts of rainfall in a short period of time, while this was more variable and of lower magnitude in Tierkloof. The results found in this study indicates a similar pattern. Although both catchments were dominated by low magnitude rainfall (< 5 mm), higher magnitude (> 10 mm) rainfall were more frequent in the Langrivier catchment.

Increases in rainfall towards the south-east end of the valley has been reported by others, and may be related to orographic influences as reported by numerous researchers within the same study area (Wicht et al., 1967, Scott, 1993). In the Jonkershoek valley, the steep orographic rainfall gradient, which increases towards the southeast end of the valley results in higher rainfall not only in a horizontal south-east direction but also increases vertically with altitude from the base of the valley up toward the mountain tops. Langrivier is situated further east in the valley than Tierkloof, which may explain some of the variability and higher magnitudes in rainfall received for this catchment (Wicht et al., 1969).

Several scientific papers related to rainfall and erosion have shown that rainfall erosivity increases significantly during these months (Nunes et al., 2011). It is reasoned that the energy available to perform geomorphic work was highly concentrated during this period. The studies of Moussaoui et al. (2014), Arnaez et al. (2007) and Romkens et al. (2001) all indicate that the concentration of rainfall influences rainfall intensities and thus increasing the probability of erosion. This somewhat contrasts the findings of this study, which found that more soil was eroded in total in Tierkloof even though larger intensities were observed in Langrivier catchment, indicating the role of other factors. In this study, rainfall intensities rarely exceeded 10 *mm/day*, with more than 50% of rainfall being < 5 *mm/day* during the study period. Catchment response and how they transform rainfall input into geomorphic work determines the magnitude of sediment being exported and surface erosion, and influenced by catchment characteristics.

5.8.2. Influence of streamflow characteristics.

In 2015, the entire study area experienced a wildfire. Additionally, the Tierkloof catchment was undergoing a plantation round, which left surfaces bare and tilled. Several studies have indicated an increase in overland flow and streamflow post-fire and after disturbances (Lana-Renault et al., 2011, Shakesby, 2011, Scott, 1993). These activities are responsible for observed increases in streamflow and soil losses across the globe. For example, Scott. (1993) showed that two timber plantation catchments in the study area experienced large and significant increases in stormflows and soil loss post-fire. The magnitude of increase was different for different plantations, such that observed increases varied from 242% and 319% for storm response ratio, 201% and 92% for quick flow volume, while peak discharge was 290% and 1110% for pine and eucalyptus plantation catchments respectively (Scott, 1993, Scott et al., 2008). In the same study, the comparison fynbos catchment, also Langrivier, showed little change in stormflow response post fire (Scott, 1993).

There was a significant difference in total streamflow volumes between Langrivier and Tierkloof during the study period. Tierkloof streamflow estimates was 65% higher than Langrivier, which equates to 575.1 *mm* more water flowing through the catchment relative to Langrivier. The hydrographs presented in Figure 5.6 and Figure 5.7, and the statistical results

show that the average streamflow was greater in the Tierkloof catchment: 3.92 *mm/day* runoff in Tierkloof compared to 2.39 *mm/day* in Langrivier. These findings are supported by the run-off ratio estimated for 2016 in the two catchments. Run-off ratios were estimated for the winter period as well as for the extreme storm event that occurred on 26 July 2016. Results show that ratios were consistently higher in Tierkloof: 198% during winter and 88% during the big storm event compared to 88% and 43% in Langrivier respectively.

The runoff ratio greater than 1 for Tierkloof has a few potential explanations: the rainfall gauge data used is likely not representative of rainfall across the entire catchment area and/or groundwater inputs from a regional aquifer (beyond the surface flow catchment area) also feed the stream. However, the rainfall gauges used in the two catchments are at similar positions within their respective catchments and the geologic composition of the two areas is similar, so the ratios calculated are considered comparable across the catchments, particularly for the storm response when groundwater forms a smaller proportion of the total. This finding shows a significant difference between the two catchments in how rain is translated to run-off, with Tierkloof having a much greater proportional runoff response, which has implications for erosion and sediment export.

The difference between streamflow responses may be due to introduction of water repellent soils caused by wildfire, drainage density, catchment morphology and hillslope channel connectivity (Nearing et al., 2005). Versfeld (2010) indicated in his study that thinning and burning in a fynbos catchment had no significant effect on the relationship between increasing rainfall and overland flow. The finding of this study indicates that both burning and clearing of vegetation cover can have a significant impact on run-of and streamflow, which ultimate influences soil loss and movement in the catchment. The lower run-off and streamflow response in the Langrivier may be due to the quick rejuvenation of fynbos vegetation (Dalwai, 2014). Numerous researchers show increase in storm run-off and peak discharge after disturbance of vegetation. As reported by others, as vegetation cover re-established overtime and allows for increased infiltration and reduced run-off and streamflow response. In this study, the landcover map shows that 40 to 49 % Tierkloof was bare (to low) cover. This means that the rainfall to run-off ratio is small and coupled with steep slope increase flow velocity and thus surface water erosion.

5.8.3. Factors influencing soil loss in the two catchments.

The estimated average soil loss over the sampling period for the two catchments were ~8.20 *mm* for Tierkloof and ~5.6 *mm* for Langrivier. At the time of sampling, the catchment was being prepared for plantations of exotic pine species. This was done by excavating 3 m x 3 m compartments for planting. Surfaces between the seedlings are then left bare until vegetation establishes over time. Fields left bare during critical periods of erosive rains increases probability of soil loss. Nunes et al. (2011) showed that relative to indigenous vegetation, afforestation caused the most severe run-off and erosion. In their study, soil transported by run-off peaks during autumn/winter coincided with the highest and erosive rainfall. Looking at the geomorphic impact of afforestation on soil erosion in Southeast Spain, Romero-Diaz et al. (2010) showed contrasting results between an afforested catchment and a natural scrubland. In the scrubland catchment surface run-off and erosion was reduced because surface wash was negligible with no concentrated flow evident, while the afforested catchment increased soil losses by 1 to 2 orders of magnitude.

In addition, the study area experienced a wildfire one year prior to this study. It is known that species like *Pinus sp*. and *Eucalyptus sp* have a high content of resins and essences that fuel combustion and the spreading of fire, which is in agreement with the results found in this study and by Scott. (1993) in the same study area showing that a catchment planted with *Pinus sp* produced higher volumes of soil when compared to the catchments still carrying indigenous vegetation such as Langrivier. Several studies have been carried on the impact of invasive species include increased fire intensities and consequent soil erosion (Chamier et al., 2012). Post-fire studies have also indicated the significant different in the hydrological and erosional response in catchments with contrasting vegetation cover i.e. comparison between alien species relative to indigenous vegetation. Several studies show that the hydrological and erosional response between areas covered with alien species produce significantly higher hydrological and erosional response compared to areas with indigenous vegetation. Due to highly flammable substances associated with alien vegetation because fire spread in pines and eucalyptus mean that more total area is burned compared to fynbos. Additionally, the substances increase fire intensity resulting in physical and chemical transformation of the soil surface, lessens organic material and consumes more cover relative to fynbos, which results in higher run-off and

erosion. Fynbos is fire-adapted and therefore a certain number of fires are naturally expected and required for the regeneration of vegetation. Although not in absolute terms, the results in this study were similar to that found by Scott. (1993) and Romero-Diaz et al. (2010), where Langrivier is maintained with the natural vegetation produced lower soil losses.

Surface erosion at the catchment scale is influenced by the inherent catchment characteristics such as vegetation cover, slope and soil properties as shown by several researchers (Defersha et al., 2011, Vásquez-Méndez et al. 2010, Peterson, 2005). In this study although there was relatively low statistical significance between surface erosion and controlling factors, important information can be extrapolated from the results. Several studies have reported on the role of vegetation cover and soil erosion. These studies showed that erosion reduced as vegetation re-established over time. Our finding is in agreement with others showing a negative correlation between vegetation cover and sediment flux across plots in the two catchments (Zou et al., 2015, Vásquez-Méndez et al., 2010, Nearing et al., 2007 Scott, 1993). In addition, we found that stem density increases with vegetation cover and that there exists a negative relationship between sediment flux and stem density. These finding are in agreement with Istanbulluoglu et al. (2004) and Madi et al. (2013). Istanbulluoglu et al. (2004) indicated that cover plays and important role in regulating erosion, while Madi et al. (2013) argues the role of stem density causes additional roughness to overland flow and therefore reduces the detachment of soil particles and sediment transport. Although while Madi et al. (2013) study was conducted using laboratory experiments, this study shows that stem density may also influence sediment flux.

The influence of terrain characteristic and soil properties was also highlighted in this study. Our study shows the importance of terrain indices such as slope, elevation, flow accumulation and LS USPED on sediment flux, but somewhat contrasting between the two catchments. For example, in Langrivier soil loss increased with slope however the opposite trend was found in Tierkloof. The results found in Langrivier is similar to Defersha et al. (2011). Defersha et al. (2011) assessed erosion mechanisms taking into account slope steepness and found that soil loss increases on slopes between 9° to 25°, and then decreases for slope > 20°. Results found in Langrivier indicate that the total sediment flux increased with slope until a threshold gradient is reached, and soil loss is reduced. However, the findings in Tierkloof may be more complex.

Le Roux et al. (2008) has stated that the erodibility of parent material and resultant soils are the main factors influencing erosion in South Africa. Median grain size showed similar patterns in both catchments. Although on average grain sizes found in plots situated in Tierkloof were slightly larger, sediment flux reduced with increasing grain sizes. This finding may be one of the causes for the contrasting findings for slopes and soil loss between the catchments. For example, more sand and less silt would require more prolonged moisture accumulation, weathering and translocation (favoured in lower slope parts of the landscape). More sand on steeper slopes would mean better infiltration, such that runoff rates and erosion risk may actually decrease for very steep slopes. The results produced in this study are therefore similar to that found by others, however the total sediment flux across slopes in Tierkloof were highly sporadic and of greater magnitude.

In addition, the wildfire that occurred in the study area may have contributed to the insignificant correlations between surface erosion and factors controlling its variability. Istanbulluoglu et al. (2004) showed that wildfire removes vegetation leaving the surface expose and alters the physical properties of soil by introducing a water repellent layer, which increases both overland flow and soil erosion. Here sediment yields are synchronized from different parts of the basin post-fire and exceed non-disturbed basins (Perreault et al., 2016, Shakesby, 2011, Istanbulluoglu et al., 2004). This is in agreement with the geospatial analyses showing that large parts of each catchment were still either bare or had low cover density even a year post-fire. In Langrivier 40% of the total area was in bare to low class, while in Tierkloof 48% of the area fell into these classes respectively.

5.8.4. Influence of river sediment flux and storm-based event on suspended sediment concentration.

The relative sediment discharge rates for the streams varied over time as a result of precipitation, discharge patterns and sediment source areas i.e. surface vs instream. The movement of water and sediment from catchments is determined by climate, geology, topography, soil and vegetation of the landscape. This is essentially why rivers from different catchments have different flow and sediment regimes (Poff, 1997). The sediment-discharge relationship between Langrivier and Tierkloof differed for an extreme event during the study

period. The relationship is clearly hysteretic for Langrivier, with *Qs* peaking before *Q*, but there is less clear peak separation for Tierkloof – this is important insight, as it tells us something about sediment exhaustion and storage effects in the two catchments, which can be related to land cover or to topography. The relationship seen in Figure 5.20 and Figure 5.21 clearly show that more sediment was found in suspension in Tierkloof. Here we assuming the in-stream sediment supply is negligible in both channels due to their boulder rock morphology and step pool sequence, hence all sediment was delivered from surface erosion. Interestingly, there was a sudden drop in sediment concentration during peak flow for Langrivier, while in Tierkloof the drop was gradual. This may be due to a steady supply of sediment over time in Tierkloof. Nearing et al. (2005) assessed the sediment yields in the Kendell (grasses) and Lucky (shrubs) catchments in south eastern Arizona, USA, and showed that the Lucky catchment transported more sediment due to well-incised channels, which transported material more efficiently. In Kendell bulk of the material was deposited before the outlet. The geospatial modelling done in this study revealed interesting results in terms of drainage network. While the channel in Langrivier show a straight forward linear pattern marked by steep v-shaped slopes, the drainage in Tierkloof was complex and often disconnected. These characteristics may have resulted in deposition just before the stream channel, thus limiting the amount of sediment transported to the stream channel.

The data retained from suspended sediment samplers provided an estimate of mass transport considering the full range of flow conditions over the sampling period, providing a continuous record of suspended sediment flux. In this study, the relative amount of sediment exported over the 6-month study period normalized by catchment area (either with or without rock cover) show that Tierkloof consistently exported more sediment per unit area relative to Langrivier. These differences may be due to source areas and the connectivity between hillslope and channels. Surface erosion estimates also showed that more sediment was being removed in Tierkloof, which likely contributed to the difference in sediment load. However, the relationship between precipitation and streamflow gave the impression that there may be less connectivity between hillslopes and channel in Tierkloof than Langrivier. In contrast, the relationship between precipitation and streamflow in Langrivier indication some sort of connectivity between hillslope and channel, therefore expecting more water and sediment interaction. The lower sediment output in Langrivier may then be the result of supply limited

surface material or the transport capacity of overland flow. In addition, water feeding Langrivier flow might be shallow subsurface flow rather than surface runoff.

Surface water erosion is controlled by numerous factors such as rainfall, topography, soil physical properties and vegetation cover. Due to the high variability of individual factors, assessing erosion and catchment sediment yields becomes extremely difficult. Effective soil and water conservation strategies require quantitative information on soil erosion and factors controlling its variability at the catchment scale. This section presents the results obtained using field measurements for the Langrivier and Tierkloof catchments.

CHAPTER 6: NUMERICAL MODELLING OF SOIL EROSION UNDER CURRENT CATCHMENT CHARACTERISITICS.

6.1. Introduction

Disturbances such as land cover changes can have a significant impact on basin connectivity and therefore sediment dynamics. Various available models were reviewed in order to choose the one that fits better with the scope of the current project, to simulate the potential impact of land-use change on sediment yields at the catchment scale. For detailed descriptions of various geomorphological models and their applicability in the assessment of erosional responses, readers are referred to Meadows, 2014 and Coulthard et al., 2016. In this study, a numerical modelling experiment was conducted, using CAESAR-Lisflood (Coulthard et al., 2016), to assess the likely erosional response and catchment yields in response to land cover change in the Langrivier and Tierkloof catchments.

CAESAR-Lisflood is capable of simulating erosion/deposition in river catchments and reaches in response to a rainfall event or series of events. The model is a raster-based landscape evolution model using a hydrological model to generate spatially distributed run-off (i.e. rainfall-runoff module), which is routed using a 2-D inertia hydraulic model for flow routing (conservation of mass and partial conservation of momentum). The integration of the new 2-D hydrodynamic code means that the physics of flow propagation is maintained enhancing flow process representation and therefore improves calculation of flow properties (velocity and depth). Flow depths and velocities (discharge) feeds into sediment transport equations (driven by shear stress) used for sediment erosion/deposition and morphological change (i.e. geomorphological module).

The model therefore allows improved understanding how landscapes evolve under various conditions with a high level of detail and realism. Based on the research produced by Meadow (2014), CAESAR-Lisflood includes the most sophisticated representation of flow hydraulics due to the new hydraulic module, detailed module of fluvial erosion/deposition that accounts for multiple grain size distributions and suspended sediment load, and the most comprehensive

representation of catchment hydrology. Additionally, research has shown that the model is able to demonstrate the complex and non-linear behaviour of fluvial and geomorphic systems (Van De Wiel et al., 2007, Meadows, 2014, Pasculli et al., 2015, Seoane et al., 2015, Coulthard et al 2016). This section highlights the main features of the model as used in this study and model configuration.

6.2. Methods

6.2.1. CAESAR-Lisflood landscape evolution model

The CAESAR-Lisflood model is based on the cellular automaton concept, which consists of a regular grid of cells representing the landscape, each in one of a finite number of states and dimensions (Pasculli et al., 2015). These states are defined by several parameters or initial conditions including precipitation, elevation and grainsize distribution (Coulthard et al., 2012). By defining the catchment of interest, an initial state (at $t = 0$) for each cell is assigned. For example, the cell may consist of an area of the landscape (size given as grid resolution e.g. 10 m x 10 m) representing bare slopes, vegetated slopes or a heterogeneously spread across the area. At every model time step, a new state for each cell is generated according to a set of rules or mathematical function that aim to replicate the physical processes that dynamically adjust the landscape according to erosion and deposition, i.e. water and sediment fluxes, and dependant on factors controlling process variability (Hancock, 2009, Coulthard et al., 2013). For example, surface water flow is routed across the mesh of model cells creating shear stresses that control the movement of sediment, thus modifying the cells bed elevations (Van de Wiel et al., 2007, Coulthard et al., 2013, Seoane et al., 2015).

In the model, these functions or processes are grouped into hydrology, hydraulic routing, fluvial erosion and deposition, and hillslope processes (Van de Wiel et al., 2007, Hancock, 2009, Hancock et al., 2015). The basic model structure can be seen in Figure 6.1, however several advances have been made to improve the physical basis of the model. For example, the integration of the new hydrodynamic 2D flow model based on the Lisflood FP code of Bates et al. (2010) conserves mass and partial momentum. This means that the physics of flow

propagation is maintained, which enhances flow process representation such as flow depths and velocities, producing reliable discharge estimates that are fed into sediment transport equations to drive (by shear stress) sediment movement (Coulthard et al., 2013).

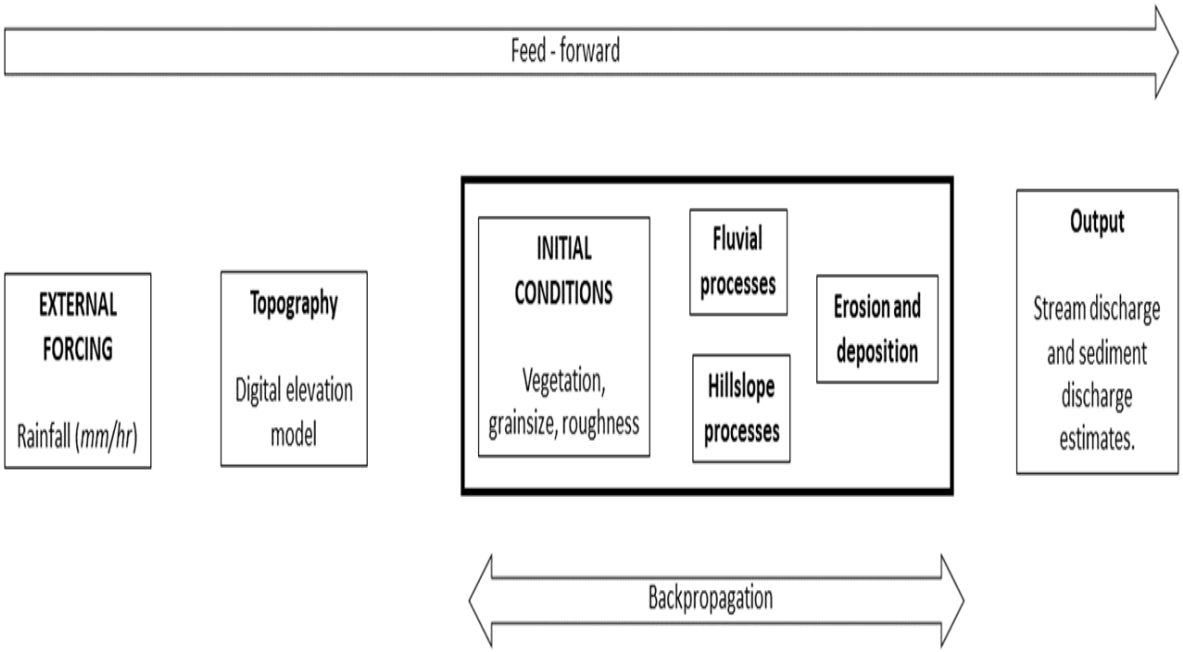

Figure 6.1. CAESAR-Lisflood basic model structure (adapted from Van de Wiel et al., 2007). The catchment of interest is defined (i.e. initial condition) and subjected to some forcing (i.e. rainfall), which alters (i.e. erosion and deposition) the output state of the landscape.

6.2.3. Hydrological and hydraulic modelling

A full description of CAESAR-Lisflood is given in Coulthard et al. (2013) and others (Van De Wiel., 2007, Hancock et al., 2009, Pasculli et al., 2015). In catchment mode, the C-L model operations commence by calculating the water discharge of each individual cell, Q_{tot}, using rainfall (*mm*) estimates as input with an hourly (*hr*) temporal resolution. The calculation of Q_{tot} for a given rainfall is calculated based on an adaption of TOPMODEL, and depends on the local rainfall rate r ($m\ h^{-1}$) specified by input rainfall estimates (Coulthard et al., 2016).

When local rainfall rate r ($m\,h^{-1}$) specified by an input rainfall file is greater than 0, total surface and subsurface discharge (Q_{tot}) is calculated as (Coulthard et al., 2013);

$$Q_{tot} = \frac{m}{T} log\left(\frac{(r - j_t) + j_t\, exp\left(\frac{rT}{m}\right)}{r}\right)$$

$$j_t = \left(\frac{r}{\left(\frac{r - j_{t-1}}{j_{t-1}} \exp\left(\left(\frac{(0-r)T}{m}\right)\right) + 1\right)}\right) \quad (6.1)$$

Where T is time since started (seconds), r is local rainfall rate ($m\,h^{-1}$), m is a user-defined parameter used in TOPMODEL that effectively controls the rise and fall of the soil moisture store (0.005 – 0.02), and j_t is the soil moisture deficit at time-step *t*. The soil moisture deficit (j_t) is calculated as a function of the deficit in the previous timestep (j_{t-1}), rainfall, and the *m* parameter (Coulthard et al., 2013, Coulthard et al., 2016, Hancock et al., 2015, Pasculli et al., 2015). The model calculates erosion, volume water and sediment at hourly timesteps and set to run for the entire 2016 year. However, when there is no precipitation in a time-step ($r=0$), then discharge is calculated as (Coulthard et al., 2013);

$$Q_{tot} = \frac{m}{T} log\left(1 + \left(\frac{j_t T}{m}\right)\right)$$

$$j_t = \frac{j_{t-1}}{1 + \left(\frac{j_{t-1} - T}{m}\right)} \quad (6.2)$$

The equations (6.1 and 6.2) above calculate a total surface and subsurface discharge (Q_{tot}) for a given rainfall event.

Before run-off can be routed across the landscape using the hydraulic model, Q_{tot} is separated using a simple run-off threshold, which represents a balance of: soil hydraulic conductivity an internal parameter calculated from particle size information (K given in ms^{-1}), and thus the

amount of water that infiltrates the soil: the slope (S given in *m/m*); and the grid cell size ($Dx\ given\ in\ m$) (Coulthard et al., 2013, Hancock et al., 2015, Pasculli et al., 2015).

$$Run\text{-}off\ threshold = KS\ (Dx)^2 \tag{6.3}$$

If Q_{tot} exceeds this threshold there will be surface run-off in the model. The volume of water above the threshold is treated as run-off and the amount below treated as subsurface flow (Coulthard et al., 2013, Hancock et al., 2015, Pasculli et al., 2015). In this study the portion treated as surface flow is of interest and is discussed further. Any value set above a user-defined minimum value (Q_{min}) is treated as surface run-off. For detailed explanation on sub-surface flow movement readers are referred to Van De Wiel (2007).

The volume of water above this threshold is treated as overland flow and is routed using the LISFLOOD-FP hydrodynamic flow model developed by Bates et al., (2010) (Coulthard et al., 2013). If overland flow occurs, surface water is routed across cells using;

$$q_{t+\nabla t} = \frac{q_t - g h_t \nabla t \frac{\partial (h_t + z)}{\partial x}}{(1 + g h_t \Delta t n^2 q_t / {h_t}^{10/3})} \tag{6.4}$$

Where Δt is the length of the time step (s), t and $t + \Delta t$ is the present time step, $t + \Delta t$ is the next time step, q is flow per unit width ($m^2 s^{-1}$), h flow depth (m), g is the gravitational force (ms^{-2}), z bed elevation (m), x grid cell size (m), $\frac{\partial (ht+z)}{\partial x}$ water surface slope and n is manning's roughness coefficient (Coulthard et al., 2013). After discharge has been established for a cell, the water depth is updated;

$$\frac{\nabla \mathrm{h}_{i,j}}{\Delta t} = \frac{Qx_{i-1,j} - Qx_{i,j} + Qy_{i,j-1} - Qy_{i,j}}{\Delta x^2} \tag{6.5}$$

Where i, j are coordinates. The length of a time step is controlled by cell size and water depth;

$$\Delta t_{max} = \alpha \frac{\Delta x}{\sqrt{gh}} \quad (6.6)$$

α is the Courant number, a coefficient ranging from 0.3 to 0.7. To control the stability of the model and account for cell size for this study, a value of 0.4 was used in both catchment simulations.

6.2.4. Sediment layers and sediment transport

Morphological changes result from the entrainment, transport and deposition of sediment across the landscape. After the hydraulic model determines flow depths and inundation locations for the catchment, fluvial erosion and deposition is calculated (Coulthard et al., 2013, Van De Wiel et al., 2007).

6.2.4.1. Sediment transport

CAESAR-Lisflood provides two options to calculate sediment transport. The amount of material eroded by fluvial action from cell to cell can be determined using the Einstein-Brown (1950) or Wilcock and Crowe (2003) transport equations (Pasculli et al., 2015). Wilcock and Crowe (2003) is based on a combination of field and laboratory data for coarser bed gravels and sand mixtures thus more relevant to rivers, so once the flow gets into a channel, transport processes in the channel would be well represented. Wilcock and Crowe (2003) formulation is covered in brief as it was used in this study. Readers are referred to Van De Wiel et al. (2007) and (Coulthard et al., 2013) for further details on the two sediment transport equations.

Sediment is transported using a mixed-sized formula, which calculates transport rates (q_i) ($m^3 s^{-1}$), for each sediment fraction, i (Wilcock and Crowe, 2003):

$$q_{i=} \frac{F_i \ U_*^3 W_i^*}{(S-1)_g} \quad (6.7)$$

F_i denotes the fractional volume of the $i-th$ sediment size class in the active layer, U_* is the shear velocity ($U_* = [\tau / \rho]^{0.5}$), s is the ratio of sediment to water density, g is gravity (ms^{-2}), and w_i^* is a function relating the fractional transport rate to total transport rate. Estimation of w_i^* is derived from calculating τ_{rm} and represents the critical shear stress for the mean size of the bed sediment (Meadows, 2014). τ_{rm} is a function that is approximated and relates the Shields parameter for the mean bed material size (τ_{rm}^*) to the percentage of sand on the bed surface (F_s), for details of calculation see Meadows. (2014). Although developed for sand/gravel mixtures only, it can be used as a proxy to include finer non-cohesive sediment such as silt (expansion of w_i^*) (Pasculli et al., 2015).

Transport rates can then be converted into a volume (V_i), by multiplying with the time step of the iteration:

$$V_i = q_i dt \tag{6.8}$$

In equation 6.8, *i* is the grainsize fraction; V is volume (m^3); q is the transport rate ($m^3 s^{-1}$) and d*t* is the time step (seconds) (Meadows, 2014). The d*t* parameter is specified by the user and controls the maximum elevation change at every model time step and is calculated using equation 6.9:

$$dt = \frac{\Delta Z_{max}\, c_w^2}{q_{max}} \tag{6.9}$$

The model uses variable length time steps for each iteration, such that the maximum calculated rate of entrainment, q_{max} results in a maximum allowed elevation change, ΔZ_{max} (default ΔZ_{max} = 0.1 L_h, where L_h is the thickness of the sediment layers) (Pasculli et al., 2015):

6.2.4.2. Bedload and suspended sediment transport

Eroded sediment is transported either as bedload or as suspended load depending on the grain sizes being entrained (Van De Wiel et al., 2007). Bedload is distributed proportional to the local bed slope using the equation below;

$$V_{i,k} = \frac{S_k}{\sum S} V_i \tag{6.10}$$

Where i is the sediment fraction, k is the direction of the neighbour, V is the volume of sediment (m) and S is slope. Only those neighbours where S_k>0 (lower bed elevations) are considered. Suspended load is routed according to flow velocities and is expressed using the equation below;

$$V_{i,k} = \frac{U_k}{\sum U} V_i \tag{6.11}$$

Where U is the flow velocity ($m^3 m^{-1}$) and all neighbouring cells where the bed elevation is lower than the water elevation in the current cell are considered.

Deposition of sediment differs between bedload and suspended load (Van De Wiel et al., 2007). For bedload, at every iteration all bedload material that is transported is deposited in the receiving cells where it can be re-entrained in the next iteration;

$$V_{i,dep} = V_i \tag{6.12}$$

For suspended sediment load, sediment is deposited as a result of fall velocities V_i ($m\, m^{-1}$) and sediment concentration, K_i for each sediment fraction

$$V_{i,dep} = {}_{K_i} V_i C_w^2 d_t \tag{6.13}$$

In this study, the grain size used for suspended sediment was 0.0000625 m, and the relative fraction of this sediment class was determined by the particle size analysis.

6.2.5. Representation of sediment layers

The model allows for sediment spatial heterogeneity by keeping track of up to 9 different grainsize fractions. Grain sizes are represented from 0.004 to 1.024 m in whole phi classes (-2 ϕ to -10 ϕ) (Van De Wiel et al., 2007). Since this information varies both horizontally and vertically, CAESAR-Lisflood stores subsurface sediment data using a systematic series of layers comprising an active layer representing the streambed and land surface, multiple buried layers called strata, a base layer as well as an immovable bedrock layer (Hancock et al., 2009, Coulthard et al., 2013). Furthermore, the surface layer has an additional layer representing protective surface vegetation, Figure 6.2 provides a schematic representation of this profile. This allows the selective erosion, deposition and transport of the user defined grain fractions resulting in spatially variable grainsize distributions across the landscape. (Van De Wiel et al., 2007)

Layers

1. Active layer - a layer exposed to topographic change and has a variable thickness. The thickness varies from 25% to 150% of the strata's thickness - 5 to 30 cm using the default value).

2. Strata layer - layers situated in the upper part of the buried regolith, with variable thicknesses (L_h, default is 20cm) and the positions are fixed relative to the bedrock layer. It stores multiple buried layers, where up to 20 strata can be stored at any cell on the grid.

3. Base layer - is the lower part of the buried regolith. It has a variable thickness, which depends on how many strata overlay it.

4. Bedrock - is a layer where erosion cannot happen.

5.

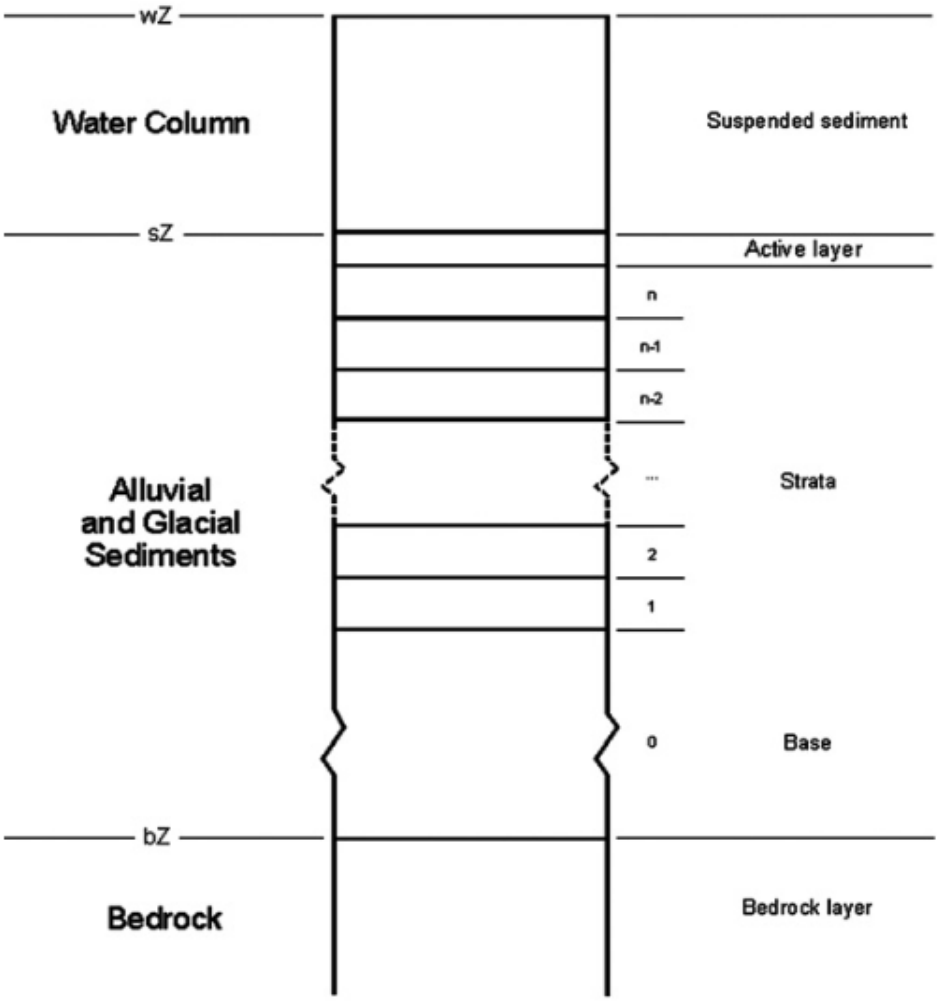

Figure 6.2. Shows the sediment layers in CAESAR-Lisflood (Van De Wiel et al., 2007).

Erosion removes sediment causing the active layer to decrease. When the thickness, L_h of the active layer becomes less than a threshold value, $L_h > 0$ the upper stratum is incorporated into the active layer forming a new thicker active layer. Conversely, deposition adds material causing the active layer to grow. When the thickness of the active layer becomes greater than a set value, $L_h = 1.5$ a new stratum is created, leaving a new thinner active layer. For deposition the lowest layer may be incorporated in the base layer when too many layers have been created for the cell (>20 strata), Figure 6.3 provides a schematic of erosion and deposition (Van De Wiel et al., 2007).

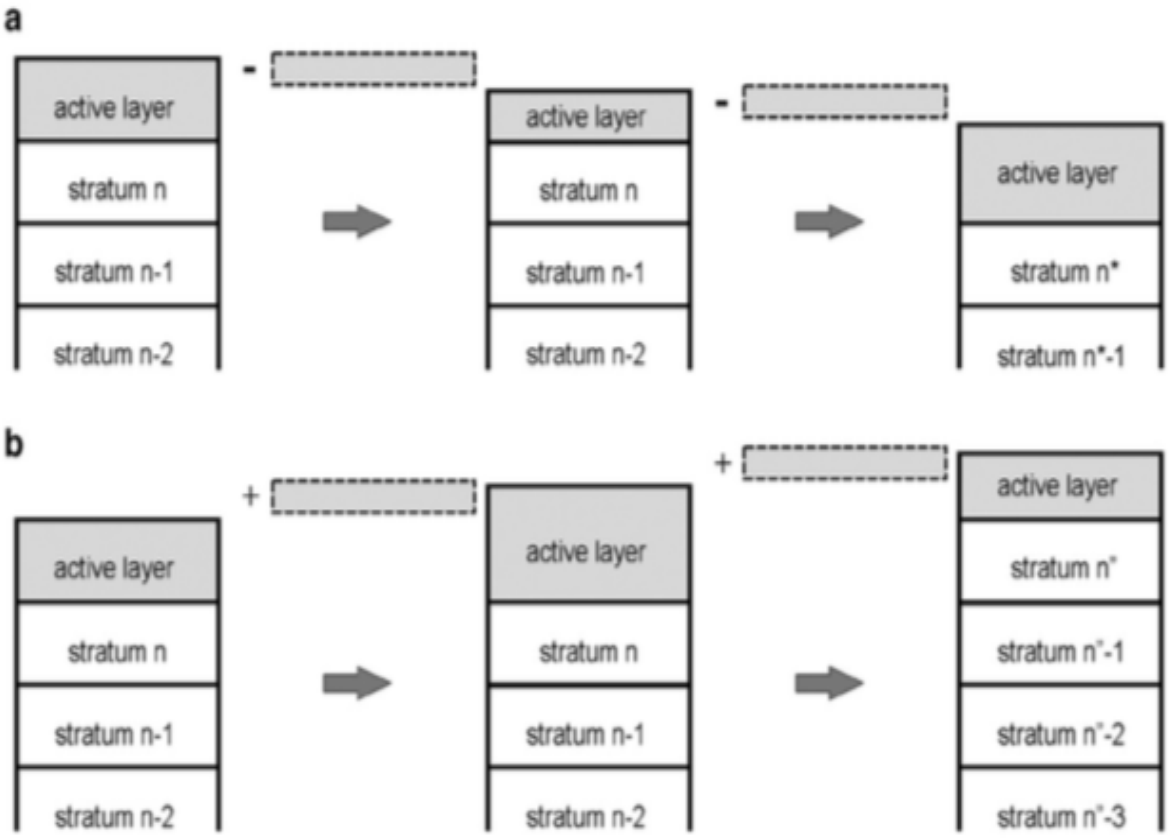

Figure 6.3. Evolution of the active layer during erosion (a) and deposition (b) iteration, where n denotes the initial number of strata. n^{*} *and* n'' shows the new number of layers that are buried, either as erosion or deposition: n^{*}= n-1 and n''+1 (Van De Wiel et al., 2007).

Where a cell is eroded, the material is progressively exposed from the lower layers through;

$$E_i = \left(\frac{F_i^{x+1}}{\sum F_{i-n}^{x+1}}\right)\left(A - \sum F_{i-n}^{x}\right) \quad (6.14)$$

When material is deposited to the active layer, material is removed from this layer and added to the layer below (Pasculli et al., 2015);

$$E_i = \left(\frac{F_i^{x}}{\sum F_{i-n}^{x}}\right)\left(\sum F_{i-n}^{x} - A\right) \quad (6.15)$$

E_i denotes the amount of material removed from the top layer (x) and added to the next layer down ($x + 1$) of grainsize fraction i. A represents the correct thickness of the active layer ($2D_{90}$ or $4D_{90}$) (Pasculli et al., 2015).

6.2.6. Hillslope processes

Hillslope processes are important in terms of overland flow velocities and sediment transport capacity. CAESAR-Lisflood simulates slope processes and includes a function for diffusive soil creep function, which is calculated as a function of slope, slope failure threshold (angle in degrees above which landslides occur) and soil erosion rate (an adaptation of USLE where soil erosion is a function of the slope length, slope and a series of coefficients). For further details readers are referred to (Coulthard et al., 2013, Van De Wiel et al., 2007)

6.2.2. Model input parameters

The primary data required by the model are rainfall, soil particle size distribution and a digital elevation model (DEM). The 10 m resampled SUDEM was used as representative of the terrain in the two catchments. Hourly rainfall data (mm/hr) was acquired for 2016 from SAEON for stations in each catchment. Rainfall data from the two stations (T13B and L14B) provided the external forcing and considered representative of each catchment.

Soil particle size data was estimated from field samples as described in chapter 5. To compare outputs from model grid cells (10m x 10m = 100 m^2) matching the locations of erosion plots (25m x 25m = 25 m^2) in the field CAESAR-Lisflood saves an ascii file of elevation differences i.e. the difference is calculated by subtracting elevation at the end of simulation from initial elevation values. To compare plot estimates with model estimates, the average soil loss from pin plot and corresponding array of 9 10x10m cells was assessed. This allows to determine the relative amount of material eroded from a surface at a particular location. We explore the relative difference in simulated erosion with actual surface erosion.

An average potential evaporation of 0.0038 (m/day) was used as determined by Schulze (2009). The potential evaporation rate was only used in simulations in L2 and T2 runs for vegetated catchments. In the model it was only possible to specify a single rate of evaporation throughout the year. Streamflow data was derived from weir stations in each catchment for the 2016 period. These stations are situated at the outlet of each catchment. Streamflow data consisted of hourly streamflow in m^3/s. This contrasts the stream output from the model which is given as the average flow in m^3/hr. In this study, all streamflow data (modelled and observed) was converted to *mm/day* for comparison to the observed rainfall. The input-out difference for the model was determined using the average annual streamflow in each catchment for the 2016 period.

6.2.7. Model calibration

6.2.7.1. Calibration of 'm' parameter with field-based rainfall and streamflow data

As an initial step, it was important to ensure that the hydrology of the catchment was representative of field conditions. From the calibration test, a suitable 'm' value was tested for the modelled period under the current conditions. In this study, the 'm' parameter was used as a proxy for the influence of vegetation cover on sediment yields (Coulthard et al., 2013, Van De Wiel et al., 2007). The 'm' parameter controls the rise and fall of the soil moisture store, which influences the modelled hydrograph ultimately affecting basin hydrology (Coulthard et al., 2016). Higher values of *m* indicate more water storage and slow run-off, and hence lower and more delayed flow peaks after rainfall events, while lower values of '*m'* indicate less storage and fast run-off, and hence larger flow peaks occurring more quickly after rainfall. For example, Coulthard et al. (2016) indicated that values of 0.01 and 0.02 have been used to represent natural scrublands and forest/woodlands respectively, whereas 0.005 has been used to represent sparsely vegetated or bare areas. Coulthard et al. (2016) successfully used 'm' values of 0.02 and 0.005 to compare the difference between bare and vegetated catchment.

To determine the correct *'m'* value for each catchment, a sensitivity analysis of this parameter was carried out. In this study, we tested a range of 'm' values from 0 – 0.1, with guidance form

the literature due to time constraints to test all values. From this analysis each catchment was modelled using different 'm' values. A value of 0.004 in Langrivier (i.e. L1) and 0.003 in Tierkloof (i.e. T1) showed the best correlation to field estimates and these values were then used as current cover baseline simulations. Although this may be an over-simplification, it is interesting to see that the 'm' values used matched the hydrological response of field data. From this we can assume that at the time of field sampling the catchment was relatively bare of vegetation, which is in agreement with the geospatial modelling exercise indicating that more than half the catchments were bare and therefore susceptible to erosion.

6.2.7.2. Model configuration

The modelling exercise in this study assesses the influence of land cover change on sediment yields at the catchment scale. The control simulations (L1 and T1) were compared with simulations where vegetation was introduced uniformly over each catchment (L2 and T2). For comparison, an 'm' value of 0.02 as determined by Coulthard et al. (2016) was used and seen as representative of a well-vegetated catchment. Each simulation was run for the entire 2016 period (366 days, 8784 hours).

Each scenario was assessed through comparison between hydrographs (actual and modelled) and the relative sediment discharge from the catchment after the simulated period as well as the grain size distributions. In the model, discharge represents the average discharge per model time step (m^3/s), while sediment discharge (m^3/hr) is the total discharge in that time step. The final output from the model was converted to daily estimates to keep it consistent with field data timesteps.

6.2.8. Model performance and evaluation

To determine the relationship between model estimates with observed values, the spearman rank correlation coefficient was used. Furthermore, model evaluation forms an important part of the model development process and assist finding the most suitable model and model set-up to represent a specific catchment area. In addition, this shows how well the model will perform

in future assessments. There are many criteria available to evaluate model's performance. In this study four indicators were used to evaluate model performance: Root Mean Square Error (RMSE), Mean Absolute Error (MAE) and the Relative Bias (RE).

The Root Mean Square Error (RMSE) shows the differences (residuals) between the values predicted with observed values from the catchments being modelled. The desired value approach zero, for a perfect model and occurs when the simulated value is less than half the standard deviation of the measured data (Moraisi et al, 2007).

$$\text{RMSE} = \sqrt{\frac{\sum_{i=1}^{n}(X_{O,i} - X_{p,\ i})^2}{n}} \tag{6.17}$$

Where$(X_{O,i})$ is the observed streamflow value and $(X_{p,\ i})$ is the streamflow value predicted in CAESAR-Lisflood.

Mean Absolute Error (MAE) determines the absolute value of the difference between observed and simulated values, which highlights the error to be expected from the simulated estimates. MAE between observed and predicted values was determined by;

$$\text{MAE} = \frac{1}{n}\ x\ \sum_{i=1}^{n} |O_i - P_i| \tag{6.18}$$

Where $|O_i - P_i|$ is the absolute errors of the observed (O) and predicted (P) values.

The Relative Bias (RB) or systematic bias determines whether the model being used is positively or negatively biased on average and determines average deviation of modelled values from the true value (Moraisi et al, 2007, Walther et al., 2005). The RB is determined by;

$$\text{RB} = \frac{\sum_{i=1}^{n}(O_i - P_i)}{\sum_{i=1}^{n} O_i} \quad (6.19)$$

Where O_i is the observed value, while P_i is the predicted value.

The Nash-Sutcliffe efficiency (NSE) is a normalized statistic that determines the relative magnitude of the residual variance compared to the measured data variance. Nash-Sutcliffe efficiency indicates how well the plot of observed versus simulated data fits the 1:1-line AgriMetSoft (2019).

$$\text{NSE} = 1 - \frac{\sum_{i=1}^{n}(OBS_i - SIM_i)^2}{\sum_{i=1}^{n}(OBS_i - OBSbar)^2} \quad (6.20)$$

Where OBS_i is the observation value and SIM_i is the forecast value and OBSbar is average of observation values. NSE = 1, corresponds to a perfect match of the model to the observed data. NSE = 0, indicates that the model predictions are as accurate as the mean of the observed data, Inf < NSE < 0, indicates that the observed mean is a better predictor than the model AgriMetSoft (2019).

6.2.9. Uncertainty analysis and model limitations

Bras et al. (2003) indicates that it is not possible, from a philosophical perspective, to verify a geomorphological model (only the code can be verified): "verification is impossible given that reality is imperfectly known. We can strive for some level of confirmation of model behaviour, and this confirmation must generally be of a statistical, distributional, nature." See the paper for further clarification. In simple terms, there can never be any certainty that a geomorphological model accurately represents suitable initial conditions for any simulation, because it is impossible to have a priori knowledge of the conditions that lead to that initial condition – the morphodynamic spin up issue is a good example of this. We try to create model environments that are physically representative of what is observed (statistically similar in form and characteristics), and then experiment to test the effects of changing one variable on an

outcome of interest, accepting that it is not possible to reproduce an actual observed outcome in exact detail.

Due to the limited time and data for model calibration, there exist various uncertainties and simplifying assumptions related to the modelling exercise. One of the major limitations of the study, is the spatial and temporal variation of various environmental parameters used in during model set-up. For example, the modelled catchments were built having uniform sediment, vegetation, roughness over the whole area (i.e. no riparian vegetation buffering, etc). In reality, these factors are far from constant in space, and changes over time. The 'm' parameter used in this study to represent vegetation is an oversimplification of reality and neglects factors such as vegetation type, evaporation, etc. Although the model allows for the influence of evaporation, in the model this is represented as a single that remains constant over both spatial and temporal scales.

6.3. Results

6.3.1. Calibration of the m-parameter (controlling the rise and fall of the hydrograph)

Table 6.1. CAESAR-Lisflood parameters used in Langrivier and Tierkloof to simulate how changes in land cover influences basin hydrology and sediment yields.

Parameters	**Langrivier**	**Tierkloof**
Grainsize distribution (m)	0.0000625, 0.000125, 0.00025, 0.0005, 0.001, 0.002	0.0000625, 0.000125, 0.00025, 0.0005, 0.001, 0.002
Grainsize proportions (as a fraction of 1)	0.057, 0.109, 0.144, 0.124, 0.148, 0.418	0.057, 0.109, 0.144, 0.124, 0.148, 0.418
Sediment transport rule	Wilcock and Crowe	Wilcock and Crowe
Maximum erode limit	0.01	0.01
Active layer thickness	0.1	0.1
m value (soil moisture store parameter)	0.004 (L1), 0.02 (L2)	0.003 (L1), 0.02 (L2)
Input-output differences (m^3/hr)	0.071	0.027
Evaporation (m/d)	0.0038	0.0038
Manning's n	0.05	0.05

The resulting output from L1 and T1 provide the control simulations against which changes in land use (L2, T2) are compared. Simulation L1 and T1 were calibrated against field data to define parameters and initial conditions of the catchment at the time of field sampling. A range of trial simulations were carried out and the most suitable parameters were selected and are representative of L1 and T1. The parameters used in simulations for L1 and L2 catchment can be seen in Table 6.1. In the table, the input-output (m^3/hr) difference controls the model operations. For example, when discharge coming out of the model is equal to the amount of water being added to the model, a steady-state flow is assumed. The time step of the flow model

is detached form the erosion model allowing to extend the time step to be determined by erosion (https://sourceforge.net/p/CAESAR-Lisflood/wiki/). Although the hydrology i.e. total streamflow was in agreement with field estimates, it should be noted that the outcome of each model run was done to test the relative differences of erosion and sediment yields between the two catchments, and makes no attempt to provide absolute values.

6.3.2. Modelled streamflow

Table 6.2 Summary statistics of daily observed and modelled stream discharge in the Langrivier and Tierkloof catchments. Qd represents observed discharge given as unit runoff, Qm represents modelled discharge given as unit runoff, while 1 and 2 indicates non-vegetated and vegetated catchment respectively.

Statistic	Langrivier observed, Qd (mm/day)	Langrivier modelled L1, Qm (mm/day)	Langrivier modelled L2, Qm (mm/day)	Tierkloof observed Qd (mm/day)	Tierkloof modelled T1, Qm (mm/day)	Tierkloof modelled T2, Qm (mm/day)
mean	2.39	2.41	1.73	3.96	1.48	0.97
standard deviation	4.07	6.26	3.54	6.74	4.34	2.29
min	0.43	0	0	0.71	0	0
25%	0.64	0	0	1.05	0	0
50%	1.00	0.22	0	1.66	0	0
75%	2.40	1.90	2.26	3.98	0.81	0.95
max	42.09	49.14	25.26	69.79	36.10	19.37

Results of the observed rainfall and streamflow data used during model simulation can be seen in Figure 5.6 and Figure 5.7. while Table 6.2 brings together summary statistics of observed and modelled streamflow characteristics during 2016, and discussed here for comparison. The hydrological response under the current conditions of L1 and T1 can be seen in Figure 6.4 and Figure 6.5 respectively, which shows that each catchment experienced high daily and seasonal variability of streamflow in both model output and weir estimates. In Langrivier, the observed total discharge in 2016 was 873.91 *mm*, while model discharge in L1 showed a slightly higher total discharge of 883.76 *mm*. Total discharge estimates from L2 was reduced by 28% relative to observed data producing a total discharge of 633.23 *mm* for the year. However, in Tierkloof the results found were significantly different. Here, the total observed discharge was 1449.99 *mm*, while model estimates was 551.02 *mm* and 354.43 *mm* for T1 and T2 simulations. The results of T2 was 75% lower than observed and 34% lower than modelled T1. The reduction in streamflow during L2 and T2 shows the influence of vegetation cover.

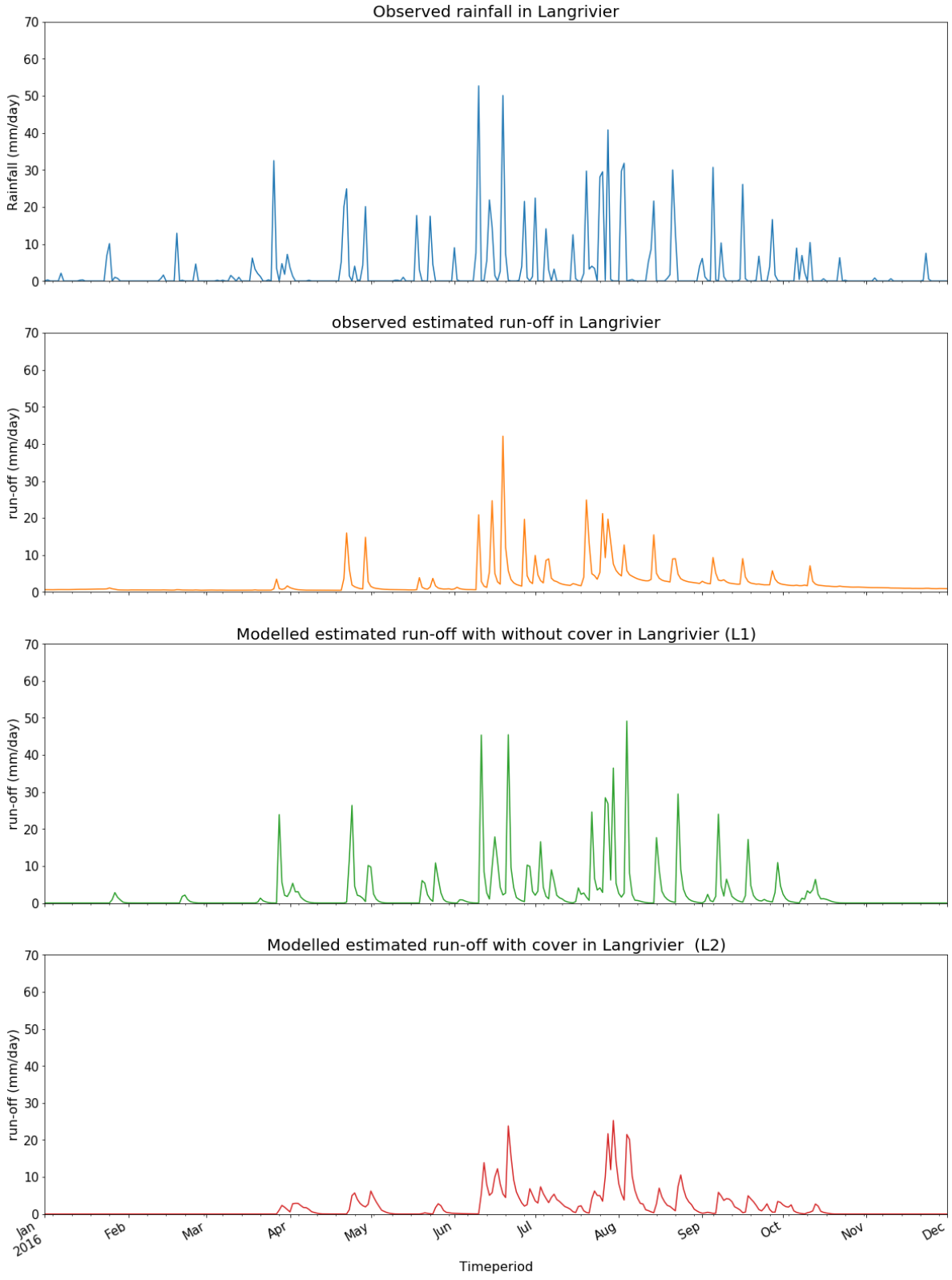

Figure 6.4. Actual run-off (*mm/day*) blue and modelled run-off (*mm/day*) for Langrivier 2016. Average observed run-off was 2.39 *mm/day* and modelled observed run-off was 2.41 *mm/day* in L1 simulation.

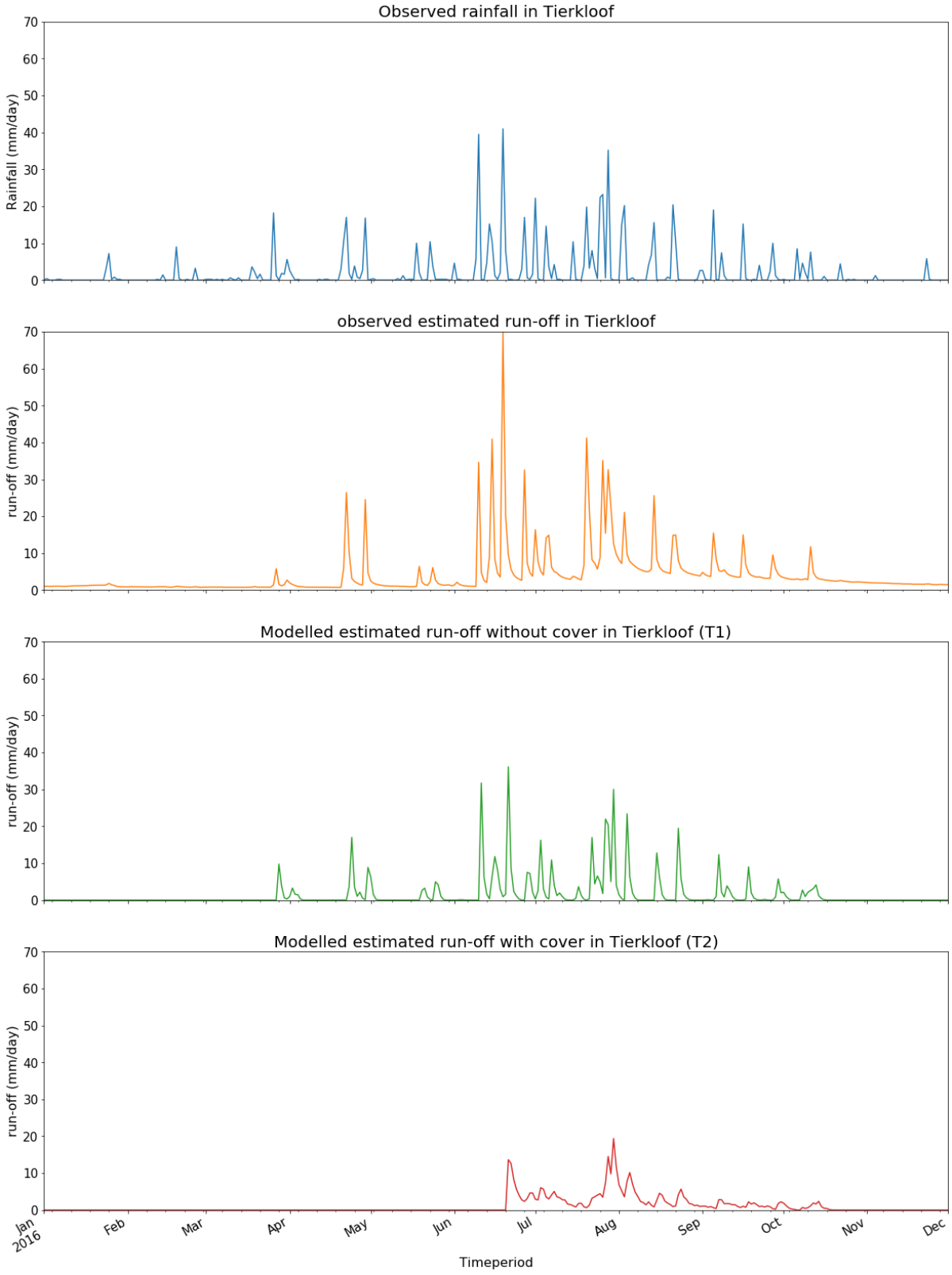

Figure 6.5. Actual run-off (*mm/day*) blue and modelled run-off (*mm/day*) for Tierkloof 2016. Average observed run-off was 3.96 *mm/day* and modelled observed run-off was 1.48 *mm/day* in T1 simulation.

During 2016 Langrivier experienced an average stream discharge of 2.39 *mm/day* when transformed to unit runoff, with a maximum and minimum of 42.09 *mm/day* and 0.43 *mm/day* respectively. The L1 simulation achieved a similar predicted average discharge, with average runoff of 2.41 *mm/day*, but modelled peak flows were higher and low flows were lower than observed, with the modelled flow having a maximum of 49.14 *mm/day* and a minimum of 0. In Tierkloof the observed average stream discharge for the duration of the study period was 3.96 *mm/day* with a maximum and minimum of 69.79 *mm/day* and 0.71 *mm/day* respectively. For T1 simulation, the model estimated discharge to be on average 1.48 *mm/day*, with a minimum of 0 and a maximum of 36.10 *mm/day*. Tierkloof model overestimated some flow peaks but not others and the max peak flows was lower.

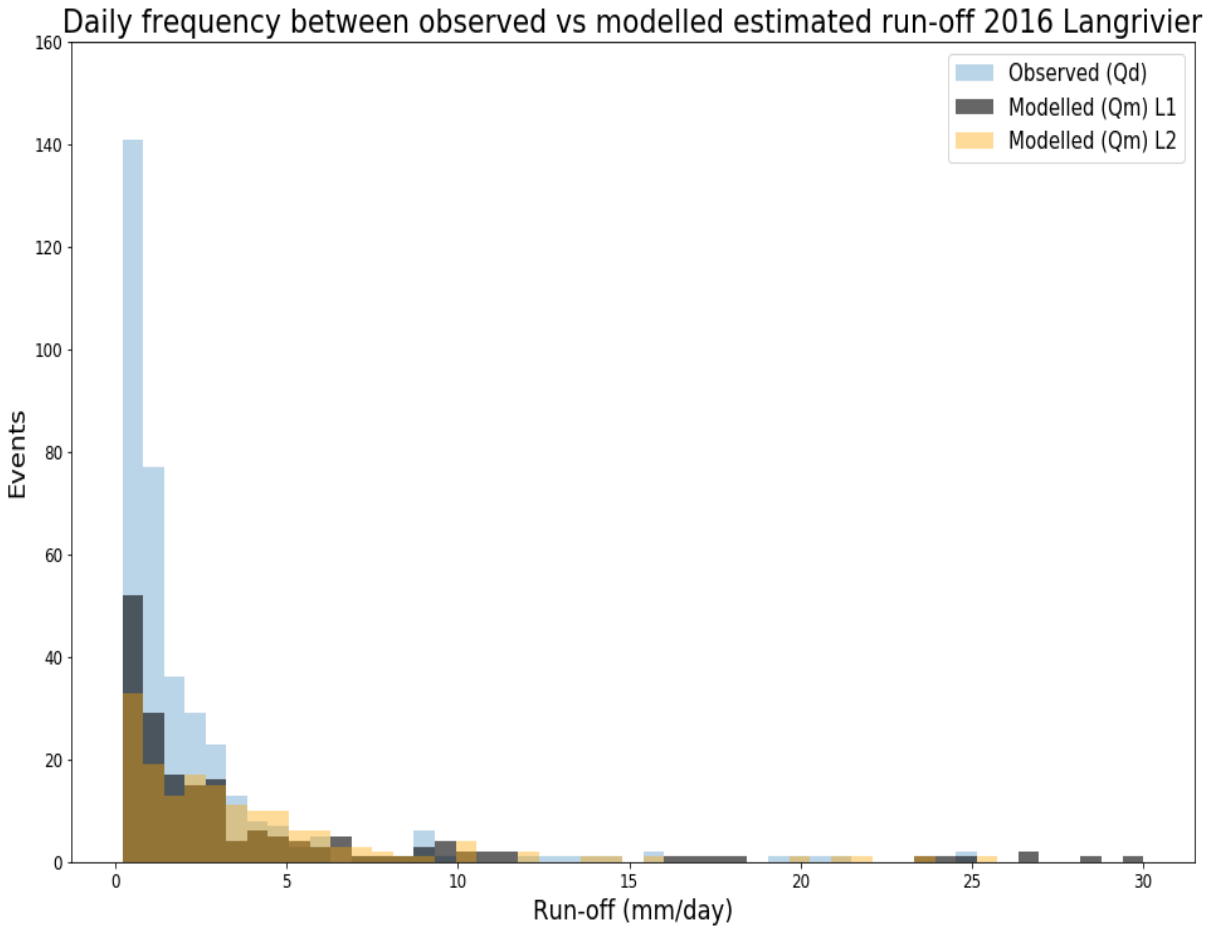

Figure 6.6. Frequency and magnitude of daily observed and simulated stream discharge in Langrivier catchment. Flows < 5 mm/day was common during observed data and simulation. Simulated data estimated lower frequencies than observed.

Figure 6.6 and Figure 6.7 shows the frequency and magnitude of daily observed and simulated stream discharge. It is evident from model estimates that the Langrivier and Tierkloof were dominated by different magnitudes of flow. The results show that L1 was dominated by runoff rates ranging from > 0 *mm/day* to 5 *mm/day*, while T1 was dominated by no flow conditions. The number of days with runoff < 5 *mm/day* estimated from the model was 260 in L1 and 103 in T1, while observed data indicated that these daily flow rates occurred for approximately 332 and 297 days during the study period. Similarly, days with runoff between 5 *mm/day* to 10 *mm/day* was significantly underestimated in T1, which was observed on 44 days compared to 15 estimated by the model, which is a difference of 65%. For the same flow magnitude, L1 simulation underestimated observed runoff days in the range by 3%.

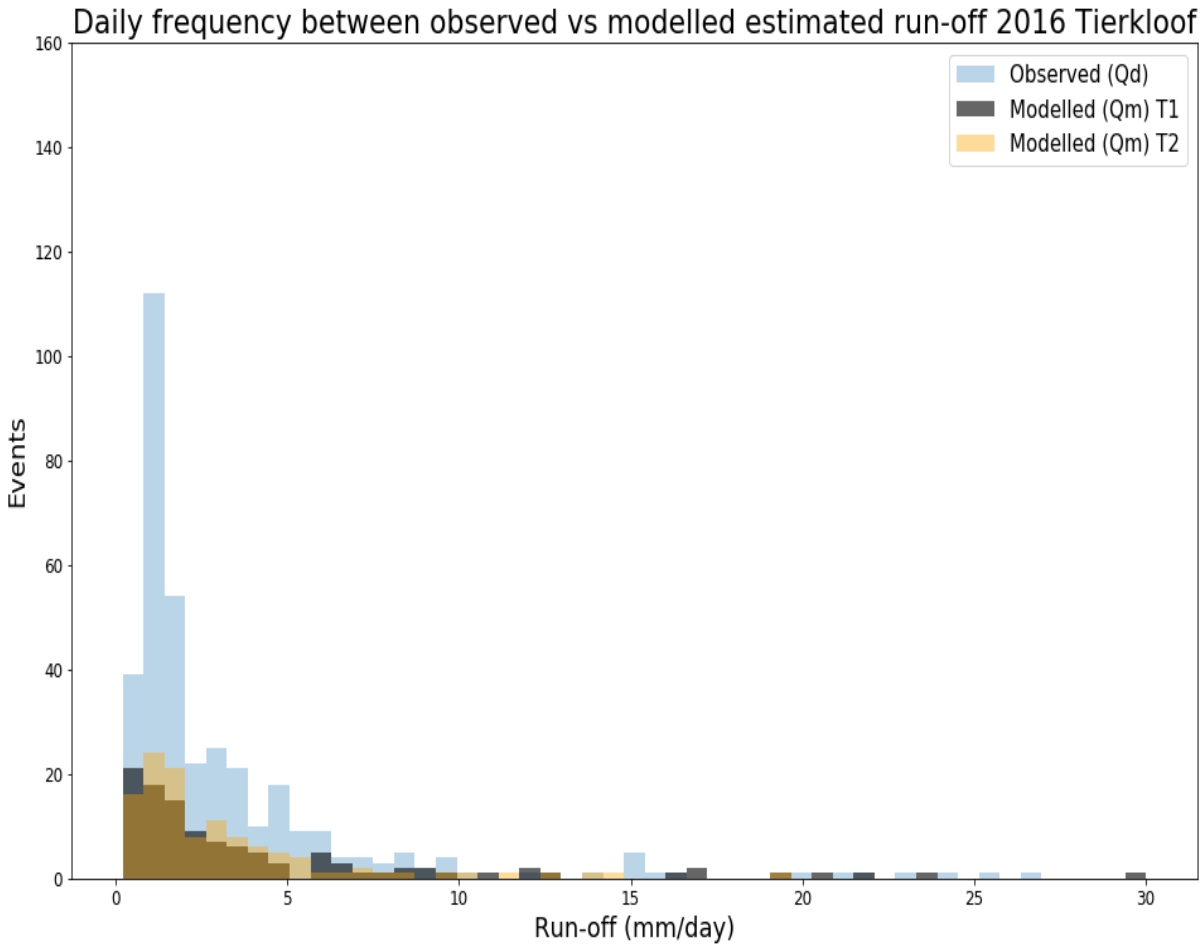

Figure 6.7. Frequency and magnitude of daily observed and simulated stream discharge in Tierkloof catchment. Flows < 5 *mm/day* was common during observed data and simulation. Simulated data estimated lower frequencies than observed.

Similar to the observed data, higher magnitude flows were less common during simulation of L1 and T1. However, the data shows that runoff > 10 *mm/day* was overestimated in L1 and underestimated in T1. In Langrivier, observed flows between 10 *mm/day* to 20 mm/d*ay* occurred 9 times, flows between 20 *mm/day* to 30 *mm/day* occurred 4 times and flows greater than 30 *mm/day* occurred 1 time. The L1 simulation estimated values of 10, 7 and 4 for flows between 10 *mm/day* to 20 *mm/day*, 20 *mm/day* to 30 *mm/day* and greater than 30 *mm/day* respectively. For the same flow magnitudes in Tierkloof the observed frequency of occurrences was 11, 7 and 7 while the model estimated occurrences of 8, 4, and 2 respectively.

The 'm' value was then adjusted to a value of 0.02 for both catchments to simulate increased vegetation cover. The difference in hydrological response of the two modelled catchments given the two 'm'-value scenarios (0.02 and 0.004 or 0.003) can be seen in Figure 6.4 and Figure 6.5. Table 6.2 provides summary statistics of stream discharge estimated by the model under vegetated conditions. It is evident from the results that stream discharge was significantly reduced under these conditions. The estimated average stream discharge for L2 once vegetation cover over the entire catchment was established was 1.73 *mm/day* having a maximum of 25.26 *mm/day* and a minimum of 0. Average estimated discharge in T2 was 0.97 *mm/day*, with a maximum and minimum discharge of 19.37 *mm/day* and 0.

It is evident from model estimates that the Langrivier and Tierkloof were dominated by different magnitudes of flow. The magnitude and frequency of daily simulated discharge for L2 and T2 can be seen in Figure 6.6 and Figure 6.7. From the results it is evident that the occurrence of no flow increased from L1 and T1 simulation, indicating the influence of vegetation. Although L2 was still dominated by flows greater than zero to flow less than 2 mm/day, no flows increased from 62 in L1 to 159 in L2. However, in T2 no flows only increased slightly from 234 in T1 to 247 in T2. These results are different to L1, T1 and observed data showing that during the 2016 study period there was always some level of discharge moving through the catchment.

Results indicate that the dominant daily flows during L2 simulation were runoff rates of between > 0 *mm/day* and 5 *mm/day*, while T2 was dominated by no flow conditions. These

flow conditions in L2 were reduced by 24% relative to L1. Runoff generation between 5 *mm/day* and 10 *mm/day* occurred 24 times and 12 times under L2 and T2 conditions respectively. Here, these flows show and increase from L1 and a decrease in T2 from T1. Runoff generation between 10 *mm/day* and 20 *mm/day* show a similar trend in L2 and T2, which occurred 9 times and 6 times respectively. The results were different for runoff rates between 20 *mm/day* and 30 *mm/day*, showing reduced number in both L2 and T2 relatively to L1 and T1. However, the reduction was only slight in L2. For flows greater than 30 *mm/day*, results show that this dropped from 4 and 2 in L1 and L1, to 0 in both L2 and T2 respectively.

Table 6.3. Show the evaluation criteria used to assess observed and predicted streamflow (L1, T1 current condition catchments).

Evaluation	**Langrivier**	**Tierkloof**
Mean Absolute Error (MAE)	0.09	0.03
Root Mean Square Error (RMSE)	0.3	0.1
Relative Bias (RB)	0.1	0
Nash-Sutcliffe (NSE)	-2.262	-0.884

To test the strength of the correlation, the spearman rank correlation coefficient was used. There was a strong positive statistically significant correlation between modelled streamflow and actual streamflow for both catchments: $Rs = 0.6$, $p = .01$ in Langrivier, as well as in Tierkloof, $Rs = 0.5$, $p = .01$.

The predicted and observed estimates were compared using RMSE, for which a value of zero would indicate a perfect fit. The results show that there was a better fit around the mean estimates from Tierkloof compared to Langrivier, where the RMSE was, 0.1 and 0.3 for Tierkloof and Langrivier respectively. Additional statistics can be seen in Table 6.3. NSE indicate that the observed mean is a better predictor than the model.

6.3.3. Modelled surface erosion and sediment yields

6.3.3.1. Modelled surface erosion

Table 6.4.Summary statistics of the relative soil loss (*mm*) from model grid cells matching the locations of surface erosion plots in the field. Plots are L1 (Langrivier no cover), L2 (Langrivier cover), T1 (Tierkloof no cover) and T2 (Tierkloof cover).

Statistics	Observed Langrivier	L1	L2	Observed Tierkloof	T1	T2
count	14	14	14	13	13	13
mean	5.6	1.49	0.41	8.21	4.87	0.73
standard deviation	2.09	0.76	0.4	4.27	7.1	1.5
min	3.00	0.27	0.027	2.64	0.24	0.08
25%	4.13	0.76	0.141	4.04	1.78	0.135
50%	5.06	1.74	0.18	9.00	1.97	0.243
75%	6.81	2.07	0.74	10.84	2.37	0.59
max	10.08	2.59	1.29	15.76	25.24	5.67

A descriptive summary of the relative differences in simulated and observed soil loss experienced in the two catchments can be seen in Table 6.4. Figure 6.6 and Figure 6.7 shows the relative differences between observed and simulated soil loss in Langrivier and Tierkloof respectively. Based on visual inspection of the graphs model estimates show a similar distribution to actual soil loss however, with different magnitudes. For example, in Langrivier it is evident that the magnitude of soil loss was higher in the lower and upper position plots relative to the middle-positioned plots. In contrast, in Tierkloof the most sever soil loss occurred in the middle-positioned plots. In terms of the magnitude of modelled soil loss, both model simulations consistently overestimated actual soil loss expect two sites in Tierkloof.

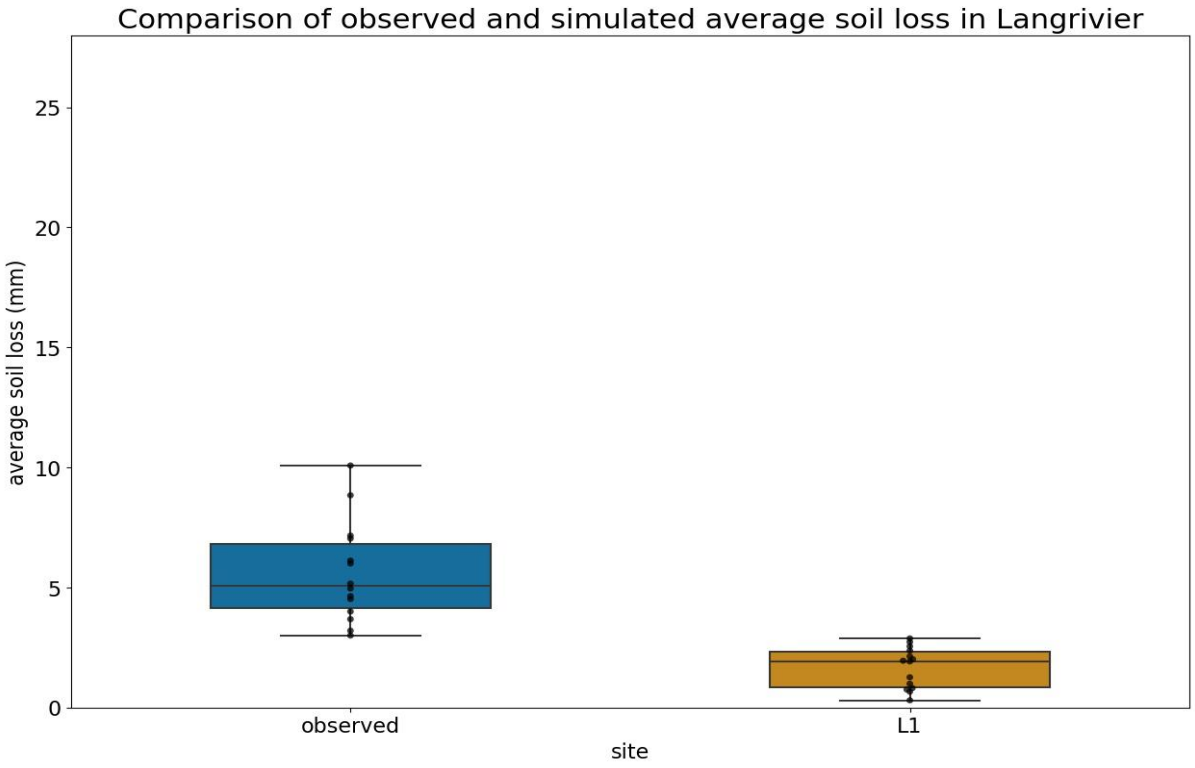

Figure 6.8. Comparison of observed and simulated sediment from erosion plots in the Langrivier. The observed average soil loss was ~5.6 *mm* and the simulated soil loss ~1.49 *mm*.

For both catchments, the simulation generally overestimated soil across the plots, with two exceptions in Tierkloof (Figure 6.7). In L1 the minimum and maximum soil loss from Langrivier plots was 0.27 *mm* (3.24 tons/ha) per plot, and 2.59 *mm* (31.08 tons/ha) per plot, respectively, and an average loss across all plots of 1.49 *mm* (17.88 tons/ha) per plot, whereas the observed average soil loss was 5.6 *mm* (67.2 tons/ha) per plot, with a minimum and maximum losses of 3.00 *mm* (36 tons/ha) and 10.08 *mm* (120.96 tons/ha) per plot. In Tierkloof the average simulated soil loss simulated for the plots was 4.87 *mm* (58.44 tons/ha) in T1, while the average observed loss across all plots was 8.20 *mm* (98.4 tons/ha). The maximum and minimum observed loss for the duration of the study period was 15.79 *mm* (188.88 tons/ha) and 2.64 *mm* (31.68 tons/ha) respectively, and 0.24 *mm* (2.88 tons/ha) and 25.24 *mm* (302.88 tons/ha) for simulated average soil loss in T1 simulation. Correlation analysis showed a positive relationship between simulated and field estimates. The results obtained in L1 and T1 were Rs = 0.2 and Rs = 0.7 respectively.

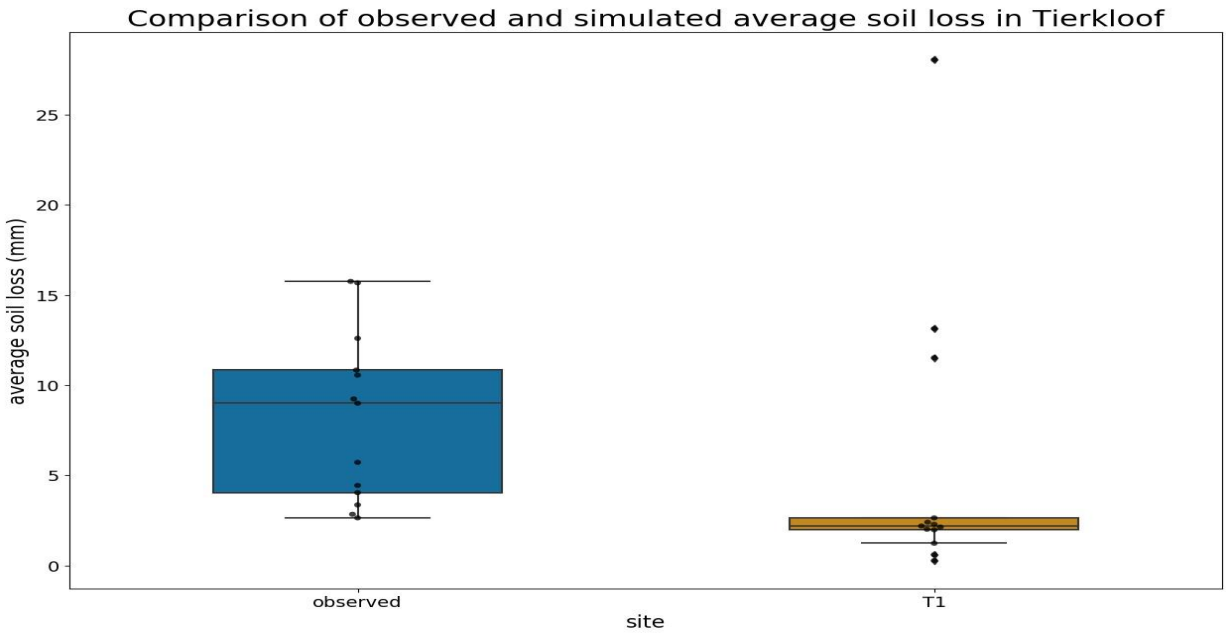

Figure 6.9. Comparison of observed and simulated sediment from erosion plots in the Tierkloof. The observed average soil loss was ~8.20 *mm* and the simulated soil loss ~4.87 *mm*.

6.3.3.2. Modelled sediment yields

Table 6.5.Summary statistics of the daily simulated sediment output in *mm*. Plots are L1, L2, T1 and T2, representing catchments with and without cover during simulation.

Statistics	**L1**	**L2**	**T1**	**T2**
mean	7.85	4.17	2.90	1.57
Standard deviation	24.48	8.51	8.98	3.56
min	0	0	0	0
25%	0	0	0	0
50%	0.38	0	0	0
75%	5.25	5.80	1.88	1.84
max	204.78	64.79	76.43	29.11

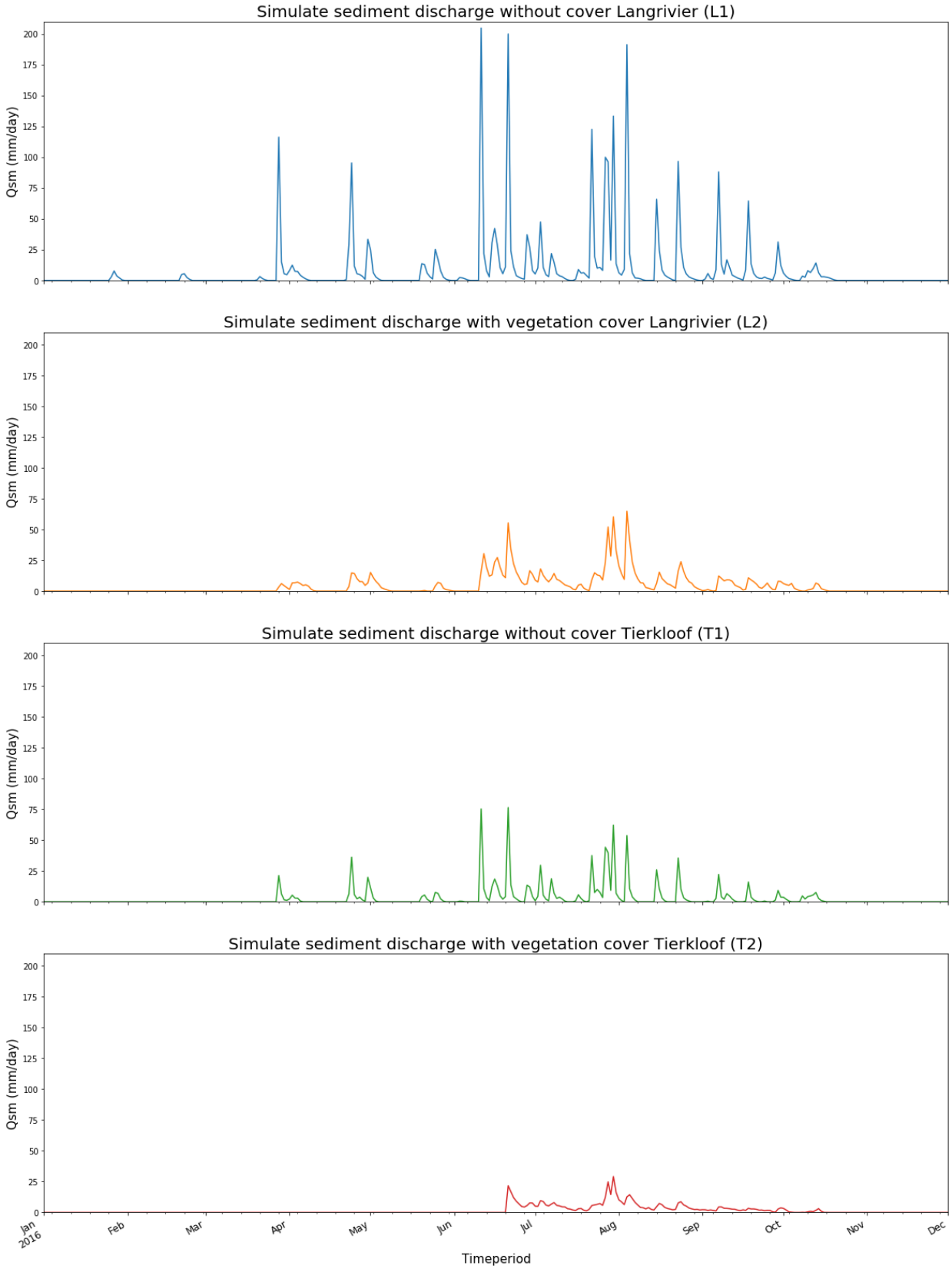

Figure 6.10. Comparison of the daily relative difference in sediment output (*mm*) from simulations, showing the influence of vegetation on sediment output.

Modelled sediment yields can be seen in Table 6.4, while Figure 6.8 shows the daily sediment discharged for vegetation cover versus no vegetation cover in the Langrivier and Tierkloof catchment. The total simulated sediment yields were significantly different between the two catchments.

In Langrivier, the average simulated sediment yield for L1 was 7.85 *mm*, with a minimum and maximum of 0 and 204.78 *mm* respectively. In the L2 simulation, the mean sediment yield was 4.17 *mm*, having a maximum 64.79 *mm* of and a minimum 0. When modelled estimates were normalized by catchment area, the total sediment yield in Langrivier was 11.85 *mm* without vegetation cover (L1) and 5.94 *mm* with vegetation cover. When rock cover was removed, normalized totals were 17.64 *mm* without vegetation cover and 9.37 *mm* with vegetation cover. This indicates that there was a 47% in sediment leaving the catchment once vegetation was fully established.

In Tierkloof, the average simulated sediment yield for T1 was 2.90 *mm*, with a minimum and maximum of 0 and 76.43 *mm* respectively. In the T2 simulation, the mean sediment yield was 1.57 *mm*, having a maximum 29.11 *mm* of and a minimum 0. In Tierkloof, total simulated yields were 6.85 *mm* without vegetation cover and 3.69 *mm* with cover. When rock cover was removed, normalized totals were 9.70 *mm* without vegetation cover and 5.21 *mm* with vegetation cover. The reduction in total sediment yield as a result of vegetation was 46 %, which was 1% lower than Langrivier.

6.4. Discussion

During the baseline simulations (L1 and T1) each catchment was designated unique ‘m’ values, which was seen as representative of the conditions at the time of field sampling. As mentioned in earlier sections, small ‘m’ values lead to higher, flashier peaks, representative of non-vegetated catchments (Coulthard et al., 2016). In these simulations a smaller ‘m’ value was used in Tierkloof (0.003) compared to Langrivier (0.004). These results are supported by observed streamflow estimates, showing that Tierkloof produced flashier peak flows relative to Langrivier despite receiving less rainfall during the study period.

In Vasquez-Mendez et al. (2010) it was shown that surface water run-off was influenced by vegetation type and that in some cases vegetation displayed similar run-off to that of bare surfaces under natural conditions. For example, run-off was assessed under Opuntia sp, O. imbricata and bare surfaces in a natural scrubland environment. Their result show that the Opuntia sp produced less run-off than bare surfaces and O. imbricata, while the latter displayed similar run-off to that of the bare ground. They concluded that vegetation characteristics (morphological i.e. vegetation patch area, total height, trunk height, canopy cover and ground cover) had an overriding effect.

This was the case in Tierkloof, where run-off ratios were significantly higher than what was found in Langrivier. These finding are different to that of Versfeld (2010), showing that burning and thinning had no significant effect on overland flow before and after treatments i.e. plantation, fire etc. His study assessed the influence of run-off over four relatively small (0.8 ha) plots in a Fynbos catchment without consideration of different vegetation types. However, in this study it was found that run-off ratios were of lower magnitude in Langrivier a Fynbos catchment relative to Tierkloof a pine plantation catchment.

Additionally, results of the geospatial analysis provide some insight into the stronger streamflow response experienced in Tierkloof. The maps produced for this catchment show more area mapped as bare surfaces and a significant contiguous bare area connected to the streamline not buffered by riparian vegetation. It is also possible that the pines played a role

despite not showing significant differences in cover classes and soil types. Chamier et al. (2012) indicated that many invasive species tend to increase biomass and fire intensity and consequent erosion. The Langrivier still carries the natural Fynbos vegetation, while Tierkloof is currently under pine plantations. When plantations occur, surfaces are often disturbed using heavy machinery and left exposed, which is more severe in peak erosive periods, causing major changes to surface hydrology (Garcia-Ruiz et al., 2013).

Furthermore, the catchments were recently disturbed by a severe wildfire. Wildfire causes both physical and chemical changes to the soil making the surface vulnerable to erosion (Perreault et al., 2016, Shakesby, 2011). This leads to a different hydrological behaviour than an unaffected surface. The main cause of change is due to the formation of a water repellent layer, which reduces infiltration and increases overland flow (Shakesby, 2011). Repellency occurs during combustion of the organic material as a result of high temperatures. The magnitude of impact depends on vegetation type, where species with high resin content are likely to be more affect as seen in the study conducted by Scott. (1993). The nature of vegetation in Tierkloof may have resulted in a fire that was more server or different and made the soils more hydrophobic or left fewer stems, etc on the ground. Although, Repellency was not assessed in this study, but several authors have reported its effects years later, while some reported that its effects are most severe within the first-year post-fire (Florsheim et al., 2015, Lamb et al., 2011, Shakesby, 2011, Scott, 1993).

Istanbulluoglu et al. (2004) modelled the interaction between forest vegetation, disturbances both natural fires and anthropogenic activities. The occurrence of water repellency in their model was spatially uniform and present only in areas experiencing some fraction of de-vegetated surfaces. They found that the effects of fire reduced the timing between overland flow erosion events. Over time the roots from growing vegetation breaks down the repellent layer, which forms preferential pathways that facilitates infiltration and to some extent restores surfaces to pre-fire conditions (Istanbulluoglu et al., 2004). The results of this study may be seen as analogous to that of Istanbulluoglu et al. (2004) study, showing a significant reduction in streamflow and sediment yields once vegetation was established over the catchments during model simulation and clearly show the influence of vegetation on basin hydrology in the model, decreasing mean and peak flows, which is in agreement with findings elsewhere (Garcia-Ruiz

et al., 2013, Coulthard et al., 2016). However, model estimates contradict field estimates, which shows that on average, streamflow was greater in Tierkloof compared to Langrivier.

Surface erosion estimates for the selected plot locations from erosion pin field measurements and model grid cell predictions were in agreement in a relative sense in both catchments, where Tierkloof showed more surface erosion. These findings are in agreement with studies in the same catchment area. For example, Scott (1993) found that, although there was a distinct within difference in sediment yield between burnt (7.4 $t\ ha^{-1}$) and unburnt (0.1 $t\ ha^{-1}$) fynbos catchment (i.e. Langrivier), this change was small when compared to timber plantation areas (e.g. Tierkloof) in which soil losses between slash piles averaged around 52 $t\ ha^{-1}$. Higher soil losses experienced in Tierkloof may be due to severity of fire, vegetation characteristics and land management practices. These factors may have caused a reduction in infiltration due to water repellent soil or disturbances to surface for plantations, which ultimately increase run-off ratios and thus erosion in Tierkloof. The results may be further exacerbated to the surfaces in this catchment have limited protection from raindrop impact due to the preparation of land for plantation of pines.

Sediment yield estimates at the catchment outlet were quite different. Field estimates from the suspended sediment samples showed that more sediment was exported from Tierkloof, whereas the models predicted that Langrivier should export more material for both scenarios (L1 and L2). Although, several studies indicated that soil loss measured at a plot scale within catchment may be dramatically different from sediment yields exported by the same catchment, where soil losses of 20 $t\ ha^{-1}$ on a hillslope plot could correspond with a sediment yield of 10 $t\ ha^{-1}$ at the catchment outlet, as a result of deposition internally along the flow paths (Le Roux et al., 2014, Scott, 1993). Therefore, sediment yields may be a poor indicator of erosion taking place within the catchment (Nearing et al., 2005). Nearing et al. (2005) compared hillslope soil losses and catchment sediment yields of two small catchments with different land cover types. They showed that the shrub catchment eroded more than the grass catchment. The main reason for difference in yields was catchment morphology. For example, more sediment was being deposited in the grass catchment due the presence of a swale at the bottom of the catchment trapping material before reaching the outlet. However, the field measurements found in Langrivier had less streamflow, lower surface erosion from field and modelling plots, less bare

ground, more riparian vegetation buffering, no pine planting disturbances and potentially less severe fires than Tierkloof due to pines. These influences may be responsible for the lower export and sediment yields found experienced in the catchment.

CHAPTER 7: UNDERSTANDING POST-FIRE EROSION DYNAMICS IN THE TWO CATCHMENTS

Accelerated soil erosion and its subsequent delivery to streams and reservoirs is one of the main causes of ecosystem and water quality degradation. This is particularly true in areas where disturbances (e.g. wildfire and land cover change) are increasing, and where such changes affect vital soil and water resources. How landscapes respond to disturbances such as wildfire and land cover change is critical for long-term sustainability of these resources.

Numerous studies carried have been conducted on the impact wildfire and land cover change has on hydrological (i.e. infiltration, overland flow) and geomorphic (i.e. erosion, transport and deposition) processes occurring at various scales of the affected landscape (Lamb et al., 2011, Shakesby, 2011, Fernqvist et al., 2003, Doer et al., 2009). General consensus demonstrates that soil loss from steep hillslopes to stream channels increases following disturbances. In addition, these disturbances impact soil structural and chemical properties that may alter hillslope erosion rates, thereby leading to high post-fire soil erosion risk. Prescribed burns or wildfire removes the protective layer i.e. vegetation cover, leaving the surface susceptible to detachment. Several authors have reported on the long-term impact of fire, where some has reported the impact several years post-fire (Shakesby, 2011). However, the major effects occur and seen immediately post-fire until vegetation re-establishes over time.

Re-establishment of vegetation depends on the species. For example, Fynbos is a fire adapted species and generally re-establishes in a shorter period of time compared to other vegetation species (Dalwai, 2014). In this study, a comparison of post-fire soil erosion between two catchments, Fynbos and Pines was carried out. From historical evidence, as well as description of the two study sites by several research scientist working in the study area over the past few years, the main disturbances affecting the landscape are related to land-use and wildfire, and land cover change related wildfires. Several studies related to the hydrological consequences have been carried out in the Langrivier, with little dated information on soil loss and export from the two these catchments.

Potential erosion risk maps based on terrain and vegetation indices was produced and compared to provide a catchment scale evaluation of current erosion risk between two catchments with contrasting vegetation cover. It was observed that there is a gradual shift in the percentage erosion risk classes between the two catchments and that these classes where relatively similar in comparison to one another. Classes range from low to very high, with a smaller percentage (19% in Langrivier and 23% in Tierkloof) in both catchments being high to very high. These areas generally occur in the catchment having steep slopes, relatively long slope lengths and little protection from vegetation cover (Sharma, 2010). No studies have been conducted in the study area that may be compared to the risk map produced here. However, these finding seem somewhat contradictory to what has been established by others in the study area using field-based estimates. The study was conducted a year post-fire, and at the time of sample the surfaces in Tierkloof were being tilled for first round plantation of pines. However, our spatial assessment shows that these catchments produced relatively similar erosion risk. When viewing proportion of land affected relative to catchment size, areas affected by medium and high erosion risk was larger in Tierkloof than Langrivier. These findings were supported by the filed data collected in the two study sites.

Spatial distribution maps were supported by field soil loss estimates. Soil loss from each plot within each catchment was highly variables. In general, soil loss differed within catchment. In Langrivier, the highest losses occurred midway downslope of the catchment (when facing north) and the mid-top section on either side of the river channel (left, right facing north). In contrast, the highest losses in Tierkloof came from the mid-section (facing north) in the catchment. Nevertheless, these findings generally coincide with the positions of low-high classes on the erosion risk map.

It is evident from the results that the average soil loss estimated for the two catchments were different. Our finding also shows that on average soil loss was greater in the pine catchment (Tierkloof) relative to the Fynbos catchment (Langrivier). This finding support those showing the influence of vegetation in regulating surface hydrological processes and soil erosion processes at the plot and catchment level (Scott, 1993, Nearing et al., 2007). For example, in the same study area evidence from Scott. (1993) show that a catchment afforested with pines produced significantly more sediment when compared to a naturally maintained Fynbos

catchment post-fire. These differences were found in this study, where normalized catchment average soil losses were found to be 68.32 *tons/ha* and 100.15 *tons/ha* in Langrivier and Tierkloof catchment respectively. This means that over the duration of this study, the Tierkloof catchment soil losses was 32% higher than losses estimated for Langrivier. However, the it should be noted that the estimates found in the fynbos catchment (Langrivier) was greater than previously reported by Scott (1993). They have also indicated that the one of the main reasons for these differences were related to the effect of wildfires. Additionally, run-off ratios were greater in Tierkloof post-fire.

These findings those made by Versfeld. (2010) showing that treatments such as thinning of plants and fire had no significant influence on overland flow. He indicated that, his findings were done on relatively small plots and cannot be extrapolated to larger areas, have steeper slopes and incorrect management practices. Similarly, a study conducted in Walnut Gulch Experimental watershed by Wainwright et al. (2000) on hillslope erosion rates from a shrub and grassland environment indicates higher estimates from the shrub catchment. Based on rainfall simulations, the structure and density of the grassed catchment relative to the shrub catchment was less affected and obstructs overland flow.

However, at the plot level contrasting results were obtained between vegetation as ground cover and stem density across the two catchments. Evidence from the Tierkloof catchment aligns with research indicating in influence of vegetation on soil loss (Nearing et al., 2007). The main effect of vegetation are interception and cohesive soil binding strength, which protects the soil surface from detachment. In Langrivier the relationship between cover and soil loss was the opposite. However, in this catchment an increase in stem density reduced soil loss at the plot scale. Although under a different setting, Madi et al. (2013) under rainfall simulations indicated that the mean flow velocity deceased with an increase in stem density. Here, stems decreased the velocity of overland flow by between 14.11% and 27.45% relative to soil having no stems and that the concentration of sediment in overland flow was significantly reduced as a result of stem density. Based on regression analysis, stem density may have influenced soil loss from plots in Langrivier as a result of hydraulic roughness caused reducing flow velocity.

Soil loss in Langrivier was largely controlled by topographic characteristic such as elevation, aspect, flow accumulation (convergence/divergence), Length-slope factor of USPED and slope gradient. Here slope gradient was the overriding factor in regulating soil loss. This contrast findings found by Le Roux et al. (2008), showing that vegetation cover may play a more significant role in reducing erosion at the larger scale. Our findings are similar to Defersha et al. (2011) under laboratory conditions showing increases in erosion with increasing slope gradient. Their study reported a threshold value where soil erosion either increases or decreases. It was found that erosion tended to increase between 9° to 25°, and then decrease above > 20°. The findings from Langrivier under natural conditions show that steeper slopes, generally greater that > 20° showed substantial amounts of soil loss. This difference may be relation other external factors such as wildfire and the physical transformation of the soil properties caused by the fire was not considered in their study. Generally, finer sediment is detached from the surface with the first few rainfall events. The average grainsizes found in the two study sites were between 0.5 mm to 0.6 mm and can be classified as a sandy soil. Results indicate a negative correlation between average grainsize across the two catchments i.e. It was soil loss reduced as grainsizes increased.

Modelling results indicated that changes in vegetation cover could lead to significant changes in catchment hydrology and total sediment yields in the two catchments. Similar finding was reported by Coulthard et al. (2016) modelling basin connectivity as a result of land use change. They illustrated that land use change reflected rapidly in basin hydrology and total sediment loads. Our findings support these findings with results from our study. It is evident from this study that once vegetation re-establishes over time, basin hydrology and sediment yields are significantly reduced to pre-disturbance levels, which have been reported by field estimates across many landscapes as well (Zhou et al., 2008, Vásquez-Méndez et al. 2010).

Although the magnitudes of soil loss were off and the pattern of which locations were higher and lower than one another was not very reliable, the model predicted more average grid cell erosion in Tierkloof than in Langrivier over the plot locations which is consistent with the field data. Coulthard et al. (2012) predicted soil erosion from a 900 m^2 plot using Caesar and stated that once calibrated the model can successfully be applied to small scale assessments. In this study the latest version of CAESAR-Lisflood model was used to model to simulate how

changes in land cover potentially affects soil loss at various scales between the two catchments and conclude based on our findings that the model was not able to simulate the relative soil loss from plot to catchment scales. The reason could be that the model had uniform vegetation cover over the whole area, which was not a true representation of field conditions. The model was therefore responding to slope and landscape position factors to differentiate different locations, not vegetation.

In contrast, total simulated sediment loads different to what was found from field-based estimates of sediment export. The model indicated that more sediment was being exported from the Langrivier catchment relative to Tierkloof. Nearing et al. (2005) assessed the spatial patterns of hillslope erosion and sediment yields in a semi-arid catchment considering influences of vegetation, slope, rocks, and landscape morphology. They showed that sediment yields were related to catchment morphology and channel incision. While the average erosion rates were greater in the shrub catchment, most of the soil eroded in the shrub watershed was exported from the watershed outlet by way of a well-incised channel system. They concluded that measurement of sediment yield from a catchment may be a poor indicator of erosion taking place within the watershed.

Several researches have reported on the high spatial variability of soil erosion in affected areas (Le Roux et al., 2008). The spatial distribution is often related to many environmental and anthropogenic factors that interact such that a particular area can either be inherently vulnerable to erosion or susceptible to potential erosion based on particular activities such as afforestation. Similarly, the effect of wildfire further enhances erosion from pre-fire levels and has been reported in many countries across the globe. Adopting a multi-layer approach to understand post-fire catchment erosion dynamics is critical to gain deeper insight into catchment sediment dynamics and to improve management of affected environments. Our study shows the spatial and temporal complexity of process interaction of various environment factors to erosional response as indicated by Garcia-Ruiz et al. (2010) and others.

CHAPTER 8: CONCLUSIONS AND RECOMMENDATIONS

8.1. Conclusion

Soil loss and catchment sediment yields was assessed using the combined effort of field work, laboratory experiments and numerical modelling. Geospatial modelling results indicate that each catchment was susceptible to varying degrees of water erosion. Areas with steeper slopes, longer slope lengths and lack vegetation cover are highly susceptible to erosion. Erosion plot estimates reveal that on average, soil loss in Tierkloof was greater. Here, the average soil loss was 8.20 *mm* (100.15 *tons/ha*) compared to 5.6 *mm* (68.32 *tons/ha*). The difference in post-fire soil loss between the two catchments may be due to different vegetation cover, management and fire severity. Higher soil losses have been reported to be more sever post-fire in areas carrying invasive tree species, similar to pine plantation in Tierkloof, relative to natural landcover types, such as the fynbos catchment in Langrivier (Scott, 1993). While there were no significant controls found in Tierkloof, in Langrivier slope gradient, LS USPED, medium grainsize and flow accumulation played an important in soil loss, with the dominant factor being slope gradient. This contradicts larger scale findings of Le Roux et al. (2008), indicating that slope gradient has limited influence on soil loss in South Africa. The findings found in Tierkloof may be due to the long-term effect of fire and current land use and cover changes. It is reasoned that the impact of these disturbances may have obscured the influence of other controls within the catchment.

Nevertheless, this led to greater loss from slopes and more material being delivered to the stream channel. In-situ sediment exported from the catchments during the study was higher in Tierkloof as indicated by the suspended sediment sampler results. Normalized by catchment area, sediment caught in the samples in Langrivier was the equivalent of 0.21 *g/ha* and in Tierkloof 0.36 *g/ha*, while when rock cover was excluded from the total catchment area during normalisation, the resulting value in Langrivier was 0.36 *g/ha*, and in Tierkloof 0.62 *g/ha* over 6-months study period. Furthermore, the average sediment concentration estimates from the storm event was greater in Tierkloof. Once normalized by catchment area total sediment concentration for the duration of the storm event was higher with a value of 389.51 *g/ha* in Tierkloof, compared to 255.42 *g/ha* in Langrivier. However, sediment peaks (*Qs*) before peak

discharge (*Qd*) in Langrivier, which may be related to hillslope-channel connectivity and land-cover. The relationship is clearly hysteretic for Langrivier. There was less clear peak separation for Tierkloof, indicating a steady but constant supply of sediment during the storm event.

Simulations show contrasting results when compared to field data. Although, the overall estimates produced by the model in terms of plot soil loss was similar to field data – more sediment was eroded from Tierkloof surface both in-situ and simulated relative to Langrivier, the patterns and magnitude of modelled soil loss was inaccurate. For example, simulated catchment averages produced were 20.31 *tons/ha* (observed = 68.32 *tons/ha*) Langrivier and 66.10 *tons/ha* (observed = 100.15 *tons/ha*) Tierkloof. Similarly, it was found that modelled sediment yield estimates were not representative of field estimates, indicating that larger amounts of sediment were exported in Langrivier during simulation. However, it is evident from field data that, despite receiving less rainfall Tierkloof had more streamflow and exported more sediment during the study period. This may be due to the underrepresentation of certain processes that were not captured by the model. For example, simulated streamflow estimates of Tierkloof was significantly underestimated in terms of total flow over the duration of the study. As a result, the model exported lower amounts of sediment over the 6-month period in Tierkloof, which contradicts field-based estimates. In addition, the model set-up used in this study was based on an oversimplified representation of actual field conditions, to assess the impact of wildfire and thus landcover change on the overall erosional and catchment sediment yields between the two catchments. It is evident from simulations L2 and T2, that the establishment of vegetation over the catchment influenced the hydrological and erosional responses within the two catchments. With future work dedicated to improve model set-up and performance, this study shows that the combined effort of field data and modelling may assist in gaining a better understand on the extent and magnitude of erosion dynamics at the catchment scale.

The findings in this study support the views set forth by Garcia-Ruiz et al. (2011) and Grenfell. (2015), where adopting a multiscale approach and efforts that combine both field work and numerical modelling provides the greatest potential for full explanation of erosion and river dynamics. Further refinements to model representation show potential for future studies in the

study area and topic. This serves as an important step for future assessments in similar mountain environments across the globe.

8.2. Limitations and recommendations

8.2.1. Field-based limitations

- The fact that Tierkloof streamflow (*mm*) is greater than rainfall (*mm*) shows that the rainfall gauge is not a full representation of the precipitation over the catchment as a whole.

8.2.2. Model based limitations

The model produced here is a very rough and less certain approximation of conditions in the field. In addition, the model was very simple in its consideration of spatial and temporal differences of environmental variable representation over the catchment during the study period. Below, the following limitations were noted:

- Manning's n to represent the impacts of the different vegetation covers was not used in this study. In this study, the default value for this parameter was used and kept constant throughout the simulation period.

- The same evaporation rate for both the vegetation types (pines and fynbos?) assessed in this study. The model software constrains the user in terms of how evaporation is represented (i.e. only ask for a single daily rate as an input).

- The model uses uniform sediment properties over the catchments.

- The model uses uniform vegetation cover over the catchments.

- The model uses uniform rainfall characteristics over the catchments.

This was a simple set-up trial in the scope of this project – further work and model experimentation should be done. Future work should focus on incorporating the factors highlighted above. Additionally, to improve model performance a further step would be to do a sensitivity analysis and find appropriate changed values for evaporation and manning's n in further modelling work. It should be noted that soil erosion and factors controlling its variability vary both spatially and temporally. Although not used in this study, the model allows for variation of the factors and should be considered.

References

AgriMetSoft (2019). Online Calculators. Available on: https://agrimetsoft.com/calculators/Nash%20Sutcliffe%20model%20Efficiency%20coefficient.

Akbari, A., Azimi, R., Ramli, N.I., Ramli, B. (2014). Influence of Slope Aspects and Depth on Soil Properties in a Cultivated Ecosystem. Electronic Journal of Geotechnical Engineering. 19. 8601-8608.

Arellano-Pérez, S, Castedo-Dorado, F, López-Sánchez, C.A, González-Ferreiro, E, Yang, Z, Díaz-Varela, R.A, Álvarez-González, J.G, Vega, J, Ruiz-González, A. (2018). Potential of Sentinel-2A Data to Model Surface and Canopy Fuel Characteristics in Relation to Crown Fire Hazard. Remote Sensing, 10, 1645.

Arnaez, J., T. Lasanta, T., P. Ruiz-Flano, P., Ortigosa, L. (2007) Factors affecting runoff and erosion under simulated rainfall in Mediterranean vineyards. Soil & Tillage Research 93, 324–334.

Bagio, B, Bertol, IIdegardis Bertol, Wolschick, N.H, Schneider, D, and Nascimento dos Santos, M.A. (2016). Water erosion in different slope lengths on bare soil. Revista Brasileira de Ciencia do Solo, 41: e0160132.

Barati, S, Rayegani, B, Saati M, Sharifi, A, Nasri, M. (2011). Comparison the accuracies of different spectral indices for estimation of vegetation cover fraction in sparse vegetated areas. The Egyptian Journal of Remote Sensing and Space Sciences, 14, 49–56.

Bates, P.D., Horritt, M.S., Fewtrell, T.J. (2010). A simple inertial formulation of the shallow water equation for efficient two-dimensional flood inundation modelling. J. Hydrol. 387, 33–45.

Boardman J, Hoffman T, Holmes P, Wiggs G. (2012). Soil erosion and land degradation in southern Africa. In, Holmes P, Meadows M. (eds.) Southern Africa Geomorphology: re cent trends and new directions. SUN Media, Bloemfontein, pp 327-338.

Boardman, J., David F.M.D. (2016). The use of erosion pins in geomorphology, Geomorphological Techniques, Chap. 3, Sec. 5.3 (2016).

Boardman, J., Mortlock, F.D., Foster, I. D. L. (2015). A 13-year record of erosion on badland sites in the Karoo, South Africa. Earth Surface Processes and Landforms. 40 (14), pp. 19641981. 01979337.

Bodí, M.B., et al. (2012). Spatial and temporal variations of water repellency and probability of its occurrence in calcareous Mediterranean rangeland soils affected by fires. Catena, doi: 10.1016/j.catena.2012.04.002.

Boix-Fayos, C, Martínez-Mena, M, Arnau-Rosalén, E, Calvo-Cases, A, Castillo, V, Albaladejo, J. (2006). Measuring soil erosion by field plots: Understanding the sources of variation. Earth-Science Reviews 78: 267–285.

Bras, R., Tucker, G., Teles, V. (2003). Six Myths About Mathematical Modeling in Geomorphology. Washington DC American Geophysical Union Geophysical Monograph Series. 135. 18. 10.1029/135GM06.

Busari, A., Li, C. (2014). A hydraulic roughness model for submerged flexible vegetation with uncertainty estimation. Journal of Hydro-environment Research. 9. 10.1016/j.jher.2014.06.005.

Centeri, C, Jakab, G, Szabó, S, Farsang, A, Barta, K, Szalai, Z, Bíró, Z. (2014). Comparison of particle size analysing laboratory methods. Environmental Engineering and Management Journal, Vol.14, No. 5, 1125-1135.

Chakrapani, Govind. (2005). Factors controlling variations in river sediment loads. Current Science. 88.

Chapman A. (2007). The Jonkershoek Research Catchments: History and Impacts on Commercial Forestry in South Africa. Department of Forest and Wood Science, Stellenbosch University, Stellenbosch, South Africa. 21 September 2007.

Chuai, X., Huang, X., Wang, W., Bao, G. (2013). NDVI, Temperature and Precipitation Changes and Their Relationships with Different Vegetation Types during 1998–2007 in Inner Mongolia, China. International Journal of Climatology. 33. 1696-1706. 10.1002/joc.3543.

Compton JS, Herbert CT, Hoffman MT, Schneider RR, Stuut J-B. (2010). A tenfold increase in the Orange River mean Holocene mud flux: implications for soil erosion in South Africa. The Holocene 20: 115-122.

Coulthard, T. J., Neal, J. C., Bates, P. D., Ramirez, J., De Almeida, G. a. M., Hancock, G. R. (2013). Integrating the LISFLOOD-FP 2D hydrodynamic model with the CAESAR model: implications for modelling landscape evolution. Earth Surface Processes and Landforms, 38, 1897-1906.

Coulthard, T.J, Skinner, C.J. (2016). The sensitivity of landscape evolution models to spatial and temporal rainfall resolution, Earth Surf. Dynam, 4, 757–771, 2016.

Coulthard, T.J, Van de Wiel, M.J., (2013). Climate, tectonics or morphology: what signals can we see in drainage basin sediment yields? Earth Surface Dynamics, 1, 13-27.

Coulthard, T.J., Van De Wiel, M.J. (2016). Modelling long term basin scale sediment connectivity, driven by spatial land use changes. Geomorphology.

Coulthard, T.T, Hancock, G.R., Lowry, J.B.C. (2012). Modelling soil erosion with a downscaled landscape evolution model. Earth Surf. Process. Landforms (2012).

Hans, D (2015). Spatial variation of soil physical properties and soil water characteristics of the Langrivier catchment in Jonkershoek Nature Reserve. Honours thesis, University of the Western Cape, South Africa.

Versfeld, D. B (1981) Overland Flow on Small Plots at the Jonkershoek Forestry Research Station, South African Forestry Journal, 119:1, 35-40, DOI: 10.1080/00382167.1981.9630222

Dalwai, R. (2014). Biogeochemical niche construction in the forest-fynbos mosaic of Jonkershoek Nature Reserve, South Africa. University of Cape Town.

Datta, P.S., Schack-Kirchner, H. (2010). Erosion Relevant Topographical Parameters Derived from Different DEMs—A Comparative Study from the Indian Lesser Himalayas. Remote Sensing, 2, 1941-1961.

De Luis, M., Gonzalez-Hidalgo, J., Longares, L. (2010). Is rainfall erosivity increasing in the Mediterranean Iberian Peninsula?. Land Degradation & Development. 21. 139 - 144. 10.1002/ldr.918.

de Vente, J., Poesen, J., Arabkhedri, M., Verstraeten, G. (2007). The sediment delivery problem revisited. Progress in Physical Geography. 31. 155-178. 10.1177/0309133307076485.

DeBano, L.F. (1981). Water repellent Soils: a state-of-the-art. United States Department of Agriculture.

Defersha, M.B., Quraishi, S., Melesse, A. (2011). The effect of slope steepness and antecedent moisture content on interrill erosion, run-off and sediment size distribution in the highlands of Ethiopia. Hydrology and Earth System Sciences, 15, 2367-2375.

Díaz, A., Serrato, F., Ruiz-Sinoga, J. (2010). The Geomorphic Impact of Afforestations on Soil Erosion in Southeast Spain. Land Degradation & Development. 21. 188 - 195. 10.1002/ldr.946.

Doerr, S.H., Shakesby, R.A., Dekker, L.W., Ritsema, C.J. (2009). Occurrence, predictions and hydrological effects of water repellency amongst major soil and land-use types in a humid temperate climate. European Journal of Soil Science, 57, 741-754.

Doerr, S.H., Shakesby, R.A., Walsh, R.P.D. (2000). Soil water repellency: its causes, characteristics and hydro-geomorphological significance. Earth-Science Reviews, 51, 33-65.

Fagbohun, B.J, Anifowose, A, Odeyemi, A.C, Aladejana, O.O, Aladeboyeje, A.I. (2016). GIS-based estimation of soil erosion rates and identification of critical areas in Anambra sub-basin, Nigeria. Model. Earth Syst. Environ, 2:159.

Feng, Q., Zhao, W., Wang, J., Zhang, X., Zhao, M., Zhong, L., Liu, Y., Fang, X. (2016). Effects of Different Land-Use Types on Soil Erosion Under Natural Rainfall in the Loess Plateau, China. Pedosphere. 26. 243-256. 10.1016/S1002-0160(15)60039-X.

Fernqvist J. Florberger I., (2003). Fire and post-fire soil erosion in the Western Cape, South Africa: Field observations and management practices. Journal of Hydrology. 25 (3), pp 231-232.

Ferro, V, Mirabile, S. (2009). Comparing particle size distribution analysis by sedimentation and laser diffraction method. Ag. Eng – Riv di Ing. Agr. 2, 35-43.

Florsheim, J.L, Chin, A, O'Hirok, L.S, Storesund, R. (2015). Short-term post-wildfire dry-ravel processes in a chaparral fluvial system. Geomorphology.

Ganasri, B.P, Ramesh, H. (2016). Assessment of soil erosion by RUSLE model using remote sensing and GIS - A case study of Nethravathi Basin. Geoscience Frontiers 7 (2016) 953-961.

Garcia-Quijano, J.F., Peters, J., Cockx, L., van Wyk, G., Rosanov, A., Deckmyn, G., Ceulemans, R., Ward, S.M., Holden, N.M., van Orshoven, J., Muys, B. (2007) Carbon sequestration and environmental effects of afforestation with Pinus radiata D. Don in the Western Cape, South Africa. Climatic Change. 83. 323-355. 10.1007/s10584-006-9204-5.

García-Ruiz, J.M., Nadal-Romero, E., Lana-Renault, N., Beguería. (2013). Erosion in Mediterranean Landscapes: changes and future challenges. Geomorphology. 198. 10.1016/geomorph.2013.05.023.

García-Ruiz, José M. (2010). The effects of land uses on soil erosion in Spain: A review. CATENA. 81. 1-11. 10.1016/j.catena.2010.01.001.

Gelagay, H.S, Minale, A.S. (2016). Soil loss estimation using GIS and Remote sensing techniques: A case of Koga watershed, North-western Ethiopia. International Soil and Water Conservation Research 4 (2016) 126–136.

Ghimire, S.K, Higaki, D, Bhattarai, T.P. (2013). Estimation of Soil Erosion Rates and Eroded Sediment in a Degraded Catchment of the Siwalik Hills, Nepal. Land, 2, 370-39.

Grenfell., M.C. (2015). Modelling Geomorphic Systems: Fluvial. British Society for Geomorphology, Geomorphological Techniques, Chap. 5, Sec. 6.4.

Hancock, G.R., Evans, K.G. (2010). Gully, channel and hillslope erosion – an assessment for a traditionally managed catchment. Earth surface processes and landforms 35, 1468–1479 (2010).

Hancock, G.R, Lowry, J., Coulthard, T.J. (2015). Catchment reconstruction — erosional stability at millennial time scales using landscape evolution models. Geomorphology 231 (2015) 15–27.

Hancock, G.R. (2009). A catchment scale assessment of increased rainfall and storm intensity on erosion and sediment transport for Northern Australia. Geoderma 152 (2009) 350–360

Hortan, R.E. (1945). Erosional development of streams and their drainage basins. Hydrophysical approach to quantitative morphology, Geol Soc Amer Ball, 1945, 56 (3): 275 – 370.

HRABALÍKOVÁ, M., JANEČEK, M. (2015). Comparison of Different Approaches to LS Factor Calculations Based on a Measured Soil Loss under Simulated Rainfall. Soil and Water Res.

Huddle, J.A., Awada, T., Martin, D.L., Zhou, X., Pegg, S.E. (2011). Do invasive riparian woody plants affect hydrology and ecosystem processes. Great Plains Research, 21, 49-71.

Istanbulluoglu, E., Tarboton, D.G., Pack, T.R. (2004). Modeling of the interactions between forest vegetation, disturbances, and sediment yields. JOURNAL OF GEOPHYSICAL RESEARCH, VOL. 109.

Jazouli, A.E, Barakat, A, Ghafiri, A, Moutaki, S.E, Ettaqy, A, and Khellouk, R. (2017). Soil erosion modeled with USLE, GIS, and remote sensing: a case study of Ikkour watershed in Middle Atlas (Morocco). Geoscience Letters, 4: 25.

Jomaa, S., Barry, D.A., Heng, B.C.P., Brovelli, A., Sander, G.C., Parlange, J.Y. (2012). Rock fragment coverage on soil erosion and hydrological response: Laboratory flume experiments and modeling, WATER RESOURCES RESEARCH, VOL. 48, W05535, doi:10.1029/2011WR011255, 2012.

Junakova, N, Klescova, Z, Gergelova, M, Holub, M. (2014). The Influence of Topographical Factor Calculation on the Estimation of Water Erosion Intensity Using Geographical Information Systems.

Kleinhans, M.G. (2010). Sorting out river channel patterns. Progress in Physical Geography, 34(3) 287–326.

Lamb, M.P., Scheingross, J.S., Amidon, W.H., Swanson, E., Limaye, A., 2011. A model for fire induced sediment yield by dry ravel in steep landscapes. Journal of Geophysical Research: Earth Surface VOL. 116, F03006, doi:10.1029/2010JF001878, 2011.

Lana-Renault, N., J. Latron., Karssenberg, D., Serrano-Muela., Regüés, D., M.F.P. Bierkens, M.F.P. (2011). Differences in stream flow in relation to changes in land cover: A comparative study in two Sub-Mediterranean Mountain catchments. Journal of Hydrology 411, 366–378.

Le Roux, J.J, Morgenthal, T.L, Malherbe, J, Pretorius, D.J, and Sumner, PD. (2008). Water erosion prediction at a national scale for South Africa.

Le Roux, J.J, Newby, T.S, and Sumner, P.D. (2007). Monitoring soil erosion in South Africa at a regional scale: review and recommendations. South African Journal of Science 103.

Macfarlane, D., Kotze, D., Ellery, W., Walters, D., Koopman, V., Goodman, P., Goge, M. (2009). A technique for rapidly assessing wetland health. WRC Report TT 340/09.

Madi H, Mouzai, L, Bouhadef, M. (2013). Plants Cover Effects on Overland Flow and on Soil Erosion under Simulated Rainfall Intensity. World Academy of Science, Engineering and

Technology International Journal of Environmental, Chemical, Ecological, Geological and Geophysical Engineering Vol:7, No:8, 2013.

Malkinson, D., Wittenberg, L. (2011). Post-fire induced soil water repellency- modeling the short- and long-term processes. Geomorphology, 125, 186-192. Doi: 10.1016/j.geomorph.2010.09.014.

Martins, S.G., Avanzi, J.C., Silva, M.L.N, Curi, N., Norton, L.D., Fonseca, S. (2010). Rainfall erosivity and rainfall return period in the experimental watershed of Aracruz, in the coastal plain of Espirito Santo, Brazil. Revista Brasileira de Ciencia do Solo. 34. 10.1590/S0100-06832010000300042.

Mbali, G (2016). Improving estimation of precipitation and prediction of river flows in the Jonkershoek mountain catchment. MSc dissertation, University of the Western Cape, South Africa.

Mataix-Solera, J., Arcenegui V., Guerrero C., Mayoral A.M., Morales J., González J., García-Orenes F., Gómez I. (2007). Water repellency under different plant species in a calcareous forest soil in asemiarid Mediterranean environment. HYDROLOGICAL PROCESSES, 21, 2300-2309. DOI 10.1002/hyp.6750.

Meadows, Tim. (2014). Forecasting long-term sediment yield from the upper North Fork Toutle River, Mount St. Helens, USA.

Midgley J.J., Scott D.F. (1994). The use of stable isotopes of water (D and 18O) in hydrological studies in the Jonkershoek valley. Water SA 20:2.

Mitsova, H. (1995). Modelling topographic potential for erosion and deposition using GIS.

Montgomery, D.R. (2007). Soil erosion and agricultural sustainability. PNAS August 14, 2007 vol. 104 no. 33.

Moriasi D.N., Arnold J.G., Van Liew M.W., Bingner R.L., Harmel R.D., and Veith T.L. (2007). Model evaluation guidelines for systematic quantification of accuracy in catchment simulations. American Society of Agricultural and Biological Engineers 50(3): 885−900.

Moses, G (2008). The established of the long-term rainfall trends in the annual rainfall patterns in the Jonkershoek valley, Western Cape, South Africa. MSc dissertation, University of the Western Cape, South Africa.

Moussouni, A., Mouzai L. and Bouhadef M. (2012). Laboratory experiments: Influence of rainfall characteristics on runoff and water erosion, Waset, 68. 1540-1543.

Nearing, M., Kimoto, A., Nichols, M. (2005). Spatial patterns of soil erosion and deposition in two small, semiarid watersheds. J. Geophys. Res.. 110. 10.1029/2005JF000290.

Nearing, M., Nichols, M., Stone, J.J., Renard, K.G., Simanton, J.R. (2008). Correction to "Sediment yields from unit-source semiarid watersheds at Walnut Gulch". Water Resources Research. 43. 10.1029/2008WR006907.

Nunes, A.N., de Almeida, A.C., Celeste O.A. Coelho, C.O.A. (2011). Impact of land use and cover type on runoff and soil erosion in a marginal area of Portugal. Applied Geography 31, 687-699.

Oliveira, A.H, da Silva, M.A, Naves Silva, M.L, Curi, N, Neto, G.K, and França de Freitas, D.A. (2013). Development of Topographic Factor Modeling for Application in Soil Erosion Models. Soil Processes and Current Trends in Quality Assessment, Chapter 4.

Pasculli, A., Audisio, C., 2015. Cellular automata modelling of fluvial evolution: real and parametric numerical results comparison along River Pellice (NW Italy). Environmental Modelling and Assessment, vol. 20 (5), pp. 425-441. ISSN: 14202026; doi: 10.1007/s10666-015-9444-8; WOS: 000360554900002; SCOPUS id: 2-s2.0-84940588890.

Paterson, G, Turner, D, Wiese, L, van Zijl, G, Clarke, C, van Tol., (2015). Spatial soil information in South Africa: Situational analysis, limitations and challenges. South African Journal of Science. Vol. 111. No. 5/6.

Perreault, L., Yager, E., Aalto, R. (2016). Effects of gradient, distance, curvature and aspect on steep burned and unburned hillslope soil erosion and deposition: Effects of terrain on burned and unburned hillslope soil transport. Earth Surface Processes and Landforms. 42. 10.1002/esp.4067.

Phillips J. M., Russel M. A., Walling D.E (2000). Time-integrated sampling of fluvial suspended sediment: a simple methodology for small catchments. Hydrol. Process. 14, 2589-2602 (2000), 15.

Poff, N.L, Allan, B.B, James, R.K., Prestegaard, K.L, Richter, B.D, Sparks, R.E, and Stromberg, J.C. (1997). The Natural Flow Regime. Bioscience, Vol 437 No. 11.

Prasannakumar, V, Vijith, H, Abinod, S, Geetha, N. (2012). Estimation of soil erosion risk within a small mountainous sub-watershed in Kerala, India, using Revised Universal Soil Loss Equation (RUSLE) and geo-information technology. Geoscience frontiers 3(2) (2012) 209-215.

Qing-quan, L, Li, C, Jia-chun. (2001). Influences of slope gradient on soil erosion. Applied Mathematics and Mechanics, 22, 5.

Renner, F.G. (1936). Conditions influencing erosion of the boise river watershed. V S Dep Agri Tech bull, 1936, 528.

Romkens, M.J.M., K. Helming, K. Prasad, S.N. (2001). Soil erosion under different rainfall intensities, surface roughness, and soil water regimes. Catena 46, 103–123.

Romkens, M.J.M., K. Helming, K. Prasad, S.N. (2001). Soil erosion under different rainfall intensities, surface roughness, and soil water regimes. Catena 46, 103–123.

Schachtschneider, K., Chamier, J., Le Maitre, D., Ashton, P., van Wilgen, B. (2012). Impacts of invasive alien plants on water quality, with particular emphasis on South Africa. Water S.A. 38. 345-356. 10.4314/wsa.v38i2.19.

Schulze R.E. (1995). Hydrology and Agrohydrology: A text to accompany the ACRU 3.00 . Agrohydrological Modelling System.

Scott, D.F, Prinsloo, F.W. (2008). Longer-term effects of pine and eucalypt plantations on streamflow. Water Resources Research, vol. 44.

Scott, D.F. (1993). The hydrological response of fire in South African mountain catchments. Journal of hydrology, 150, 409-432.

Seoane, M., Rodriguez, J.F., Saco, M.S., Rojas, S.S. (2015). A geomorphological modelling approach for landscape evolution analysis of the Macquarie marshes, Australia. E-proceedings of the 36th IAHR World Congress, 28 June – 3 July, 2015, The Hague, the Netherlands.

Shakesby, R.A. (2011) Post-wildfire soil erosion in the Mediterranean: Review and future research directions. Earth Science Reviews, 105, 71-100.

Sharma, A. (2010). Integrating terrain and vegetation indices for identifying potential soil erosion risk area. Geo-spatial Information Science.

Sharp, R.P., (1982). Landscape evolution (A Review). Proc. Natl. Acad. Sci. USA, Vol. 79, pp. 4477-4486.

Shi, Z, Wena, A, Zhang, X, Yan, D. (2011). Comparison of the soil losses from 7Be measurements and the monitoring data by erosion pins and runoff plots in the Three Gorges Reservoir region, China, Applied Radiation and Isotopes 69 (2011) 1343–1348.

Showman, S.J. (2012). The impact of soil moisture content and particle size variations on heat flow in laboratory simulated wildfires. Masters dissertation, University of Iowa.

Silva, R., De Maria, I. (2011). Erosion in no-tillage system: Influence of ramp length and seeding direction. Revista Brasileira de Engenharia Agrícola e Ambiental. 15. 554-561. 10.1590/S1415-43662011000600003.

Smith, T., Owens, P. (2014). Flume- and field-based evaluation of a time-integrated suspended sediment sampler for the analysis of sediment properties. Earth Surface Processes and Landforms. 39. 10.1002/esp.3528.

Syvitski, J, Milliman, J.D. (2007). Geology, Geography, and Humans Battle for Dominance over the Delivery of Fluvial Sediment to the Coastal Ocean. The Journal of Geology, 2007, volume 115, p. 1–19.

Syvitski, J., Milliman, J. (2007). Geology, Geography, and Humans Battle for Dominance over the Delivery of Fluvial Sediment to the Coastal Ocean. Journal of Geology. 115. 10.1086/509246.

Syvitski, J., Peckham, S., Mueller, R., Mulder, T. (2003). Predicting the terrestrial flux of sediment to the global ocean: A planetary perspective. Sedimentary Geology. 162. 5-24. 10.1016/S0037-0738(03)00232-X.

Tennant W.J., Hewitson B.C. (2002). Intra-seasonal rainfall characteristics and their importance to the seasonal prediction problem. International Journal of Climatology 22: 1033-1048.

Van De Wiel, M. J., Coulthard, T. J., Macklin, M. G., Lewin, J. (2007). Embedding reach-scale fluvial dynamics within the CAESAR cellular automaton landscape evolution model. Geomorphology, 90, 283-301.

Van De Wiel, M.J., Coulthard, T.J., Macklin, M.G., Lewin, J. (2010). Modelling the response of river systems to environmental change: Progress, problems and prospects for palaeo-environmental reconstructions, Earth-Science Reviews 104 (2011) 167–185.

Van Dijk, A.I.J.M., Bruijnzeel, L.A.,Rosewell, C.J., (2002). Rainfall intensity – kinetic energy relationships: a critical literature appraisal. Journal of Hydrology 261: 1-23.

van Wilgen, B.W., Richardson, D.M., Kruger, F.J. and van Hensbergen, H.J. (2012) Fire in south African mountain Fynbos: Ecosystem, community and species. (Accessed: 22 August 2016).

Van Wyk D.B. (1987). Some effects of afforestation on streamflow in the Western Cape Province, South Africa. Water SA 13: 1.

Vásquez-Méndez, R, Eusebio Ventura-Ramo, E, Oleschko, k, Luis Hernández-Sandoval, L.H, Jean-Francois Parrot, J.F, Nearing, M.A. (2010). Soil erosion and runoff in different vegetation patches from semiarid Central Mexico. Catena 80, 162–169.

von Bennewitz, E., Aladro, J. (2017). The effects of rainfall intensity and rock fragment cover on soil hydrological responses in Central Chile. Journal of Soil Science and Plant Nutrition, 2017, 17 (3), 781-793.

Waghmare, B., Suryawanshi, M. (2017). Mapping Soil Erosion Risk: Using Remote Sensing and Gis. IOSR Journal of Applied Geology and Geophysics. 05. 01-05. 10.9790/0990-0503020105.

Wainwright, J., Parsons, A., Abrahams, A. (2000). Plot-scale studies of vegetation, overland flow and erosion interactions: Case studies from Arizona and New Mexico. Hydrological Processes. 14. 2921-2943. 10.1002/1099-1085(200011/12)14:16/17<2921: AID-HYP127>3.0.CO;2-7.

Walling, D.E., Webb, B.W. (1982). Sediment availability and the prediction of storm-period sediment yields. Recent Development in the Explanation and Prediction of Erosion and Sediment Yield (Proceedings of the Exeter Symposium. July 1982). IAHS Publ. no. 137.

Walther, B., Joslin, M. (2005). The concepts of bias, precision and accuracy, and their use in testing the performance of species richness estimators, with a literature review of estimator performance. Ecography. 28. 815 - 829. 10.1111/j.2005.0906-7590.04112.x.

Wicht C.L. (1940). A preliminary account of rainfall in Jonkershoek. Transactions of the Royal Society of South Africa 28 (2): 161-173.

Wicht C.L. (1941). Diurnal fluctuations in the Jonkershoek streams due to evaporation and transpiration. Journal of the South African Forestry Association 7: 34-39.

Wicht C.L., Meyburgh J.C., and Bousted P.G. 1969. Rainfall at the Jonkershoek forest hydrological research station. University of Stellenbosch (44) series A.

Wischmeier W.H., Smith D.D. (1965): Predicting Rainfall – Erosion Losses from Cropland East of the Rocky Mountains: Guide for Selection of Practices for Soil and Water Conservation. Washington, D.C., USDA, Agricultural Research Service.

Wohl, E., Bledsoe, B.P., Jacobson, R.B., Leroy Poff, N., Rathburn, S.L., Walters, D.M and Wilcox, A.C. (2015). The Natural Sediment Regime in Rivers: Broadening the Foundation for Ecosystem Management. Published by Oxford University Press on behalf of the American Institute of Biological Sciences.

Yuksel, A, Gundogan, R, Abdullah E. Akay, A.E. (2008). Using the Remote Sensing and GIS Technology for Erosion Risk Mapping of Kartalkaya Dam Watershed in Kahramanmaras, Turkey. Sensors 2008, 8.

Zavala, L.M., Jordán, A., Bellinfante, N., Gil, J. (2010). Relationship between rock fragment cover and soil hydrological response in a Mediterranean environment. Soil Science & Plant Nutrition, 56:1, 95-104, DOI: 10.1111/j.1747-0765.2009. 00429.x.

Zhang, H, Wei, J, Yang, Q, Baartman, J, Gai, L, Xiaomei Yang, X, Li, S, Jiantao Yu, J, Ritsema, C.J, Violette Geissen, V. (2017). An improved method for calculating slope length (λ) and the LS parameters of the Revised Universal Soil Loss Equation for large watersheds. Geoderma, 308: 36–45.

Zhongming, W, Lees, B.G, Feng, J, Wanning, L, Shi Haijing, S. Stratified vegetation cover index: A new way to assess vegetation impact on soil erosion. Catena, 83: 87–93.

Zhou, P., Luukkanen, O., Tokola, T., Nieminen, J. (2008). Effect of Vegetation Cover on Soil Erosion in a Mountainous Watershed. CATENA. 75. 319-325. 10.1016/j.catena.2008.07.010.

Zingg, A.H. (1940). Degree and length of land slope as it affects soil loss in run-off. Agric Eng, 24, 59-64.